pmod wrc

Annual Report Jahresbericht 2013

Physikalisch-Meteorologisches Observatorium Davos und Weltstrahlungszentrum

Mission

Das PMOD/WRC

- dient als internationales Kalibrierzentrum für meteorologische Strahlungsmessinstrumente
- entwickelt Strahlungsmessinstrumente für den Einsatz am Boden und im Weltraum
- erforscht den Einfluss der Sonnenstrahlung auf das Erdklima.

Auftragerteilung

Das Physikalisch-Meteorologische Observatorium Davos (PMOD) beschäftigt sich seit seiner Gründung im Jahr 1907 mit Fragen des Einflusses der Sonnenstrahlung auf das Erdklima. Das Observatorium schloss sich 1926 dem Schweizerischen Forschungsinstitut für Hochgebirgsklima und Medizin Davos an und ist seither eine Abteilung dieser Stiftung. Auf Ersuchen der Weltmeteorologischen Organisation (WMO) beschloss der Bundesrat im Jahr 1970 die Finanzierung eines Kalibrierzentrums für Strahlungsmessung als Beitrag der Schweiz zum Weltwetterwacht-Programm der WMO. Nach diesem Beschluss wurde das PMOD beauftragt, das Weltstrahlungszentrum (World Radiation Center, WRC) zu errichten und zu betreiben.

Kerntätigkeiten

Das Weltstrahlungszentrum unterhält das Primärnormal für solare Bestrahlungsstärke bestehend aus einer Gruppe von hochpräzisen Absolut-Radiometern. Auf weitere Anfragen der WMO wurden 2004 das Kalibrierzentrum für Messinstrumente der atmosphärischen Langwellenstrahlung eingerichtet und 2008 das Kalibrierzentrum für spektrale Strahlungsmessungen zur Bestimmung der atmosphärischen Trübung. Seit 2007 wird auch das Europäische UV Kalibrierzentrum durch das Weltstrahlungszentrum betrieben. Das Weltstrahlungszentrum besteht heute aus vier Sektionen:

- Solare Radiometrie (WRC-SRS)
- Infrarot Radiometrie (WRC-IRS)
- Atmosphärische Trübungsmessungen (WRC-WORCC)
- UV Kalibrierzentrum (WRC-WCC-UV)

Die Kalibriertätigkeit ist in ein international anerkanntes Qualitätssystem eingebettet (ISO 17025) um eine zuverlässige und nachvollziehbare Einhaltung des Qualitätsstandards zu gewährleisten.

Das PMOD/WRC entwickelt und baut Radiometer, die zu den weltweit genauesten ihrer Art gehören und sowohl am Boden als auch im Weltraum eingesetzt werden. Diese Instrumente werden auch zum Kauf angeboten und kommen seit langem bei Meteorologischen Diensten weltweit zum Einsatz. Ein globales Netzwerk von Stationen zur Überwachung der atmosphärischen Trübung ist mit vom Institut entwickelten Präzisionsfilterradiometern ausgerüstet.

Im Weltraum und mittels Bodenmessungen gewonnene Daten werden in Forschungsprojekten zum Klimawandel und der Sonnenphysik analysiert. Diese Forschungstätigkeit ist in nationale, insbesondere mit der ETH Zürich, und internationale Zusammenarbeit eingebunden.

Das PMOD/WRC ist eine Abteilung der Stiftung
Schweizerisches Forschungsinstitut für
Hochgebirksklima und Medizin in Davos.

Physikalisch-Meteorologisches Observatorium Davos
und World Radiation Center (PMOD/WRC)
Dorfstrasse 33
7260 Davos Dorf
Schweiz

pmod wrc

Annual Report
Jahresbericht 2013

Annual Report 2013

Table of Contents

Jahresbericht 2013

Werner Schmutz

Infrastruktur

Der Umbau des Institutsgebäudes belastete den Betrieb des Observatoriums Davos über Jahre. Auch nach dem Wiedereinzug ins renovierte Institutsgebäude gingen diverse Renovations- und Anpassungsarbeiten weiter. Schlussendlich waren Mitte 2013 die Arbeiten im Wesentlichen abgeschlossen und das offizielle Ende der Renovation wurde am 28. August 2013 mit einer Einweihungszeremonie gefeiert. An der Feier waren Vertreter der Gemeinde Davos, des Kantons Graubünden, der Stiftung SFI und des Bundes anwesend. Der Bund wurde vertreten durch den ständigen Schweizer Delegierten an der Meteorologischen Weltorganisation, Dr. Christian Plüss, Direktor der MeteoSchweiz, der Kanton Graubünden durch den Amtsvorsteher Eugen Arpagaus, die Gemeinde Davos durch den Kleinen Landrat Reto Dürst und die Stiftung SFI durch deren Präsidenten Dr. Walter Ammann. Hauptredner war Dr. Ghassem R. Asrar, Direktor des World Climate Research Program der Meteorologischen Weltorganisation. Er betonte die Bedeutung des Weltstrahlungszentrums für das Verständnis des globalen Klimasystems. Es war sehr erfreulich, die vielen guten Wünsche zu hören und die volle Unterstützung der offiziellen Vertreter zu gewahren, die für die Finanzierung des Weltstrahlungszentrums verantwortlich sind. Die würdevolle Feier gab dem Observatorium Davos einen guten Start in eine engagierte Zukunft im neuen Gebäude.

Dienstleistungsbetrieb Weltstrahlungszentrum

Im Jahr 2012 war die Zahl der Kalibrieraufträge erstmals gegenüber dem Vorjahr zurückgegangen. Im letzten Jahr hat die Nachfrage nun wieder zugenommen und es ergibt sich dadurch, über die Jahre gesehen, ein Gesamtbild mit einer im Wesentlichen konstanten Auftragslage. Zwischen 2005 und 2010 hatten sich die Aufträge fast verdreifacht – über die letzten vier Jahre hat sich nun die Zahl der Kalibrierungen auf hohem Niveau stabilisiert. Diese Beurteilung ist sehr erfreulich, da sie bedeutet, dass die gegenwärtige Infrastruktur ausreicht, um die als Weltstrahlungszentrum geforderte Dienstleistung zu erbringen. Eine Fortsetzung des steilen Anstiegs, wie wir ihn im letzten Jahrzehnt erfahren hatten, brächte dagegen das Kalibrierzentrum bald an die Grenzen des Machbaren. Eine genauere Analyse der Zahl der Aufträge zeigt, dass vor allem die Dienstleistungen des UV Weltkalibrierzentrums stärker gefragt waren. Dies ist darauf zurückzuführen, dass diese Sektion bis vor zwei Jahren nur für den europäischen Raum zuständig war und erst seit Anfang des vergangenen Jahres offiziell von der Meteorologischen Weltorganisation beauftragt worden ist, weltweit als UV-Kalibrierzentrum tätig zu sein.

Entwicklung und Bau von Experimenten

Im vergangen Jahr wurden keine Präzisionsfilterradiometer verkauft, was angesichts des Verkaufserfolges dieses Instrumentes in früheren Jahren eher erstaunlich ist. Vermutlich ist der Grund auf die bald abgeschlossene Entwicklung des Präzisions-Spektroradiometers zurückzuführen, der die gleiche Beobachtungsinformation wie die Filterradiometer liefern wird, aber darüber hinaus mit seinem grossen spektralen Messbereich vom UV bis in den nahen Infrarotbereich weitere Anwendungen ermöglicht. Es ist gut möglich, dass Kunden, die prinzipiell am Filterradiometer interessiert wären, darauf warten, dass das Spektroradiometer kommerziell angeboten wird. Für die Institutsfinanzen bedeutet dies, dass die sonst üblichen zusätzlichen Einnahmen aus Instrumentenverkäufen viel kleiner als üblich ausfallen. Dies fällt umso mehr ins Gewicht, als letztes Jahr in den Bau der Null-Serie des Spektroradiometers wesentlich investiert wurde und daher die Ausgaben im Instrumentenbau ausserordentlich hoch waren. Das Resultat ist ein Verlust im Bereich Instrumentenbau und -verkauf, der aus unseren Reserven gedeckt werden musste. Die Meinung ist, dass diese Vor-Investition durch zukünftige Einnahmen aus dem Verkauf des Spektroradiometers wieder kompensiert werden wird.

Das PREMOS Experiment auf dem französischen Satelliten PICARD lief im vergangen Jahr problemlos und lieferte Daten der solaren Einstrahlung u.a. in der Periode von Juli 2013 bis Anfangs dieses Jahres, während der amerikanische Satellit SORCE mit seinen Radiometern wegen Batterie-Problemen nicht mehr messen konnte. Im Dezember haben die USA ein neues Radiometer-Experiment in den Umlauf gebracht. Die Messungen mit dem neuen Experiment kompensieren nun ihrerseits den Ausfall von PREMOS, das seit März dieses Jahres nicht mehr läuft, da die französische Weltraumorganisation CNES den Satelliten PICARD abgeschaltet hat. Die Kontinuität der Überwachung der solaren Einstrahlung auf die Erde ist zwar sicher gestellt, aber aus der Sicht des Observatoriums Davos ist es sehr schmerzlich, dass ein bestens funktionierendes Experiment aus finanziellen Gründen abgeschaltet worden ist.

CLARA ist das nächste vom PMOD/WRC gebaute Absolut-Radiometer, das die solare Einstrahlung aus dem Weltraum messen wird. Das Schweizer Experiment als Beitrag zum norwegischen Satelliten NORSAT-1 geschieht auf bilateraler Basis und liefert so einen wertvollen Beitrag zu den weltweiten Bemühungen, den wichtigsten natürlichen Einfluss aufs Erdklima, die solare Einstrahlung auf die Erde, zu überwachen.

Nebst Kalibrierung ist die Charakterisierung eines Radiometers ein essentieller Schritt, um ein Instrument vollständig zu verstehen. Am Weltstrahlungszentrum wurde letztes Jahr ein Heliostat installiert, der es ermöglicht, Sonnenlicht in die Labors zu bringen. Das Gerät ist erfolgreich getestet geworden und CLARA wird das erste Weltraumexperiment sein, das mit der neuen Einrichtung charakterisiert sein wird.

Wissenschaftsprojekte

Das wichtigste Wissenschafts-Projekt des Observatoriums ist das Klimaforschungsprojekt FUPSOL (Future and Past Solar Influence on the Terrestrial Climate). Es ist eine

Forschungs-Zusammenarbeit von vier Schweizer Instituten im Rahmen des SINERGIA Programms des Schweizerischen Nationalfonds. Die dreijährige Laufzeit ging Ende 2013 zu Ende. Im Rahmen dieses Projektes wurden drei Dissertationen geschrieben, die alle auf diversen publizierten oder eingereichten Artikeln in referierten Fachzeitschriften basieren. Dazu kommen zahlreiche weitere Veröffentlichungen der weiteren Partner. Insgesamt war das Forschungsprojekt ausserordentlich erfolgreich und produktiv. Viele der angegangenen Problemstellungen wurden beantwortet. Im Verlauf des Projektes kamen aber auch weitere neue Fragen zum Vorschein – wie es in ambitionierter Forschung normal ist. Konsequenterweise hat das Konsortium ein Folgeprojekt eingereicht, das vom Nationalfonds für weitere drei Jahre finanziert wird.

Bei den meisten PMOD/WRC Forschungsprojekten ist das Ziel, direkt oder indirekt, den natürlichen Faktor beim Klimawandel zu verstehen und so eine Basis zu schaffen, um die natürliche Komponente im zukünftigen Klimawandel abschätzen zu können. Die Resultate wurden in den Fachzeitschriften publiziert und es ist erfreulich zu sehen, dass die Artikel des Observatoriums von der Wissenschaftsgemeinschaft gut beachtet werden. Über die Jahre nahm die Zahl von Zitaten von Artikeln mit Autoren mit einer PMOD/WRC Zugehörigkeit stetig zu. Im 2013 ist nun die Zahl von 1000 Zitaten pro Jahr überschritten worden und spiegelt so den Erfolg und die Anerkennung der wissenschaftlichen Arbeiten am Observatorium Davos.

Organisation von Kongressen

Der Kongress Davos Atmosphere and Cryosphere Assembly, DACA-13, fand vom 8. bis 12. Juli 2013 im Davoser Kongresszentrum statt. Einladende waren die beiden internationalen Organisationen International Association of Meteorology and Atmospheric Sciences, IAMAS, und International Association of Cryospheric Sciences, IACS, die beide zur International Union of Geodesy and Geophysics, IUGG, gehören. Das Observatorium Davos war in der Organisation dieses Events von Beginn an involviert, nämlich schon im Juli 2009 am letzten vier-jährlichen Treffen dieser zwei Organisationen in Montreal, an der die Schweiz das Angebot machte, die nächste Tagung in Davos zu organisieren. Die Tagungsorganisation war ein gemeinsames Unternehmen mit der Gruppe von Professor Michael Lehning vom Davoser Schnee- und Lawinenforschungsinstitut, das von beiden Instituten einen grossen Aufwand forderte. Während des Kongresses war nicht nur die Administration gefordert, sondern es brauchte auch den Einsatz von Wissenschaftlern, um die rund 1000 Besucher aus aller Welt zu betreuen. Ich danke allen, die mit ihrem enthusiastischen Einsatz die erfolgreiche Durchführung der Tagung möglich machten. Dank gebührt auch dem schweizerischen Organisationskomitee, und im Speziellen der Projektmanagerin, Anja Schilling, die diesen besonderen Event möglich machten.

Personelles

Der Vertrag mit Frau Anja Schilling, die als Projektmanagerin von DACA-13 eingestellt war, lief einen Monat nach der Tagung aus. Das Organisationsteam schätzt sich glücklich, dass wir uns auf ihr professionelles Können und ihren unermüdlichen Einsatz bei der Kongressdurchführung verlassen konnten. Sie hat Wesentlich zum guten Gelingen dieses Kongresses beigetragen.

Frau Seraina Egartner, Sekretärin in der Administration, verliess das Observatorium nach rund einem Jahr, um sich neuen Aufgaben zuzuwenden. Wir danken ihr für ihren wertvollen Beitrag zum effizienten Betrieb der Administration. Ihre Stelle konnte mit Frau Alison Gustavsson besetzt werden und wir heissen unsere neue, engagierte Mitarbeiterin herzlich willkommen.

Dank

Allen Personen, die zur geglückten Renovation des Institutes beigetragen haben, sowie speziell meinen Mitarbeitern, die den Betrieb auch unter erschwerten Bedingungen aufrecht gehalten haben, möchte ich ganz herzlich meinen Dank aussprechen. Viele Menschen waren in den Umbau involviert und haben es ermöglicht, dass wir nun eine optimale Infrastruktur in einem attraktiven Gebäude zur Verfügung haben. Speziell möchte ich mich beim Projektleiter des Bundesamtes für Bauten und Logistik, Herrn Valentin Feubli, für seine grosse Geduld und souveräne Leitung bedanken. Der Umbau des Alten Schulhauses hat eine stattliche Summe gekostet und wir sind dem Bund zu grossem Dank verpflichtet, dass er grosszügig in die Zukunft des Weltstrahlungszentrums investiert hat. Ich danke dem Bund, dem Kanton und der Gemeinde Davos für ihre sehr positive Haltung gegenüber dem Observatorium Davos.

Die Mitglieder des Ausschusses des Stiftungsrates und der Aufsichtskommission des Weltstrahlungszentrums unterstützen stets die Interessen und Anliegen des PMOD/WRC. Der Übergang des langjährigen Präsidenten der Aufsichtskommission, Herrn Gerhard Müller, zu seiner Nachfolgerin Dr. Gabriela Seiz ist letztes Jahr reibungslos geglückt. Es ist sehr gut, dass wir uns nach wie vor auf die zuverlässige Unterstützung der Aufsichtskommission verlassen können und ich bedanke mich herzlich für deren wichtigen Beitrag zum erfolgreichen Betrieb des Observatoriums Davos.

Bild 1. Symbolische Schlüsselübergabe an der offiziellen Einweihung des renovierten Institutsgebäudes am 28. August 2014 durch den Projektleiter des Bundesamtes für Bauten und Logistik, Herr Valentin Feubli, an den Direktor des PMOD/WRC.

Davos Atmosphere and Cryosphere Assembly (DACA-13)

Luca Egli and Werner Schmutz

The joint scientific assembly DACA-13 of the International Association of Cryospheric Sciences (IACS) and the International Association of Meteorology and Atmospheric Sciences (IAMAS) was held on 8–12 July 2013 at the congress centre in Davos, Switzerland. The conference was attended by 989 participants from 52 countries on five continents.

The Swiss National Organising Committee of the DACA-13 joint assembly was chaired by Prof. Heini Wernli from ETHZ supported by two Davos scientific Institutes covering both themes of the conference: 1) cryospheric science was represented by the WSL – Institute for Snow and Avalanche Research (SLF) with Prof. Michael Lehning as the chair of the scientific programme committee, 2) atmospheric science was represented by Prof. Werner Schmutz from the PMOD/WRC acting as chair of the local organising committee (Figure 1).

The assembly covered numerous fields in cryospheric and atmospheric sciences resulting in 21 symposia featuring several sessions including more than 350 posters, which were on display to all participants during the assembly week. The concept of a permanent poster exhibition allowed presenters to showcase their scientific achievements to better advantage. At the end of each day, four distinguished scientists (Thomas Stocker, Valérie Masson-Delmonte, Ronald B. Smith and Georg Kaser) held well-attended key-note lectures in the main plenary room which was also open to the general public.

During the assembly, several committees and commissions held their annual business meetings, e.g. the IAMAS Executive Committee chaired by Dr. Hans Volkert (Figure 2, 4th from right) which discussed resolutions concerning geo-engineering and the International Radiation Commission (IRS). During the Opening Ceremony, the SLF and PMOD/WRC local institutes gave an overview of their areas of research and public services, while the first IAMAS Early Career Scientist Medal was awarded. During the closing ceremony, six further awards were presented to students with the best posters, sponsored by the Swiss Meteorological Society (SGM) and the Swiss Snow, Ice and Permafrost Society (SIP). The DACA-13 event was also sponsored by the Swiss Academy of Science, MeteoSwiss, the Federal Office of the Environment, the canton of Grisons, WMO and IUGG.

The pictures opposite give an impression of the opening ceremony (Figure 3), the assembly, and conference dinner which were both highly appreciated by the participants. Scientists from both communities used the opportunity to discuss interdisciplinary aspects in the Cryosphere and Atmosphere research fields against the backdrop of our alpine hometown in Davos. We look forward to seeing our colleagues as guests again.

Figure 1. Prof. Werner Schmutz giving an inaugural talk.

Figure 2. Presidents and Secretaries of the IAMAS and IACS associations, together with representatives of the Swiss National Organising Committee, gather for a group photo.

Figure 3. DACA-13 opening ceremony.

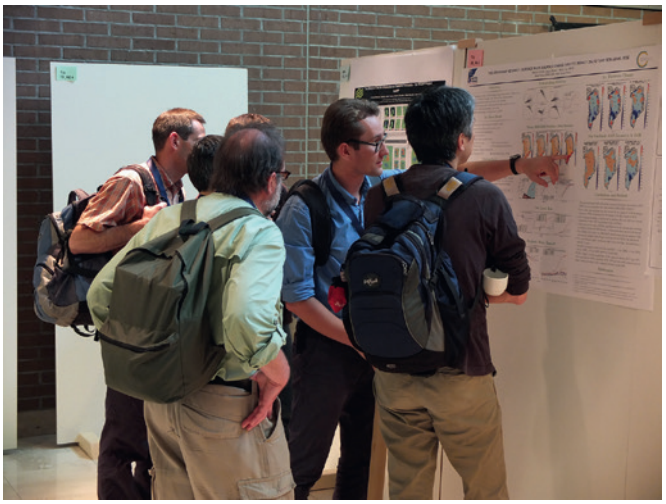

Impressions from DACA-13 at the Davos conference centre. Pictures courtesy of Diego Wasser and Marco Senft.

Introduction

Werner Schmutz

Renovation of the PMOD/WRC building has been an ongoing task for several years now. After the move back to the renovated building in August, modifications and some renovations continued. Basically, the work was finished by mid-2013, and the official end of the renovation was celebrated with an inauguration ceremony on 28 August, 2013. The ceremony was attended by representatives of the Swiss federal government, canton Grison, Davos county, and the World Meteorological Organisation (WMO). The Swiss WMO representative, Dr. Christian Plüss, Director of MeteoSwiss, attended on behalf of the Swiss confederation, the chief Administrator, Mr. Eugen Arpagaus, for the canton Grison, and Mr. Reto Dürst, member of the communal council, for the community Davos. The director of the WMO's World Climate Research Program, Dr. Ghassem R. Asrar, emphasised in his keynote speech the importance of the World Radiation Centre for observing and understanding the Global Climate System. It was very encouraging to hear the full support of all officials, who represent organisations that cover the costs of operating the World Radiation Centre.

The Davos Atmosphere and Cryosphere Assembly DACA-13 took place in Davos from 8 – 12 July 2013. The International Association of Meteorology and Atmospheric Sciences IAMAS and the International Association of Cryospheric Sciences IACS, both Associations of the International Union of Geodesy and Geophysics IUGG, had invited the science community to this unique assembly in the mountain resort of Davos, in the heart of the Swiss Alps. The PMOD/WRC was involved in the organisation of this event from its very beginning in July 2009, when Davos made its bid to host the next association's quadrennial meeting at the MOCA-09 meeting in Montreal, Canada. It was planned to jointly organise the meeting together with Prof. M. Lehning's group at the Institute for Snow and Avalanche Research, Davos. Numerous staff members were involved, not only administrative but also scientists and technical personnel, in ensuring that conference participants were looked after. I would like to express my special appreciation for their enthusiastic involvement and contribution to a very successful DACA-13 event. I would also like to extend my gratitude to the Swiss National Organisation Committee and in particular, to the project manager, Anja Schilling, who was essential for ensuring the success of the event.

In 2012, we recorded a decreasing demand for calibration services offered by the World Radiation sections. The demand recovered last year, and overall, the statistics indicate a stabilisation of the number of calibrations over the last four years. This development is very positive because it means that it allows us to cope with the Operational Services workload given the current levels of funding. A closer analysis of each Operational Service shows that the WRC expansion from a European Calibration Centre to a World Calibration Centre for UV (WCC-UV), mandated by the World Meteorological Organisation in 2013, has brought a larger workload for that section. We have thus observed a shift of attention from the calibration of integrated radiation instruments to those with selected wavelength ranges.

No Precision Filter Radiometers were sold, which in view of the fact that this instrument type had sold well in the past years, probably reflects the fact that potential customers are waiting for the newly developed precision spectroradiometer (PSR) to become available. For the institute's finances this implies that the income balance from instrument sales was lower. In addition, resources and funding were invested in the manufacturing of the first PSR instrument series. The result is that the statement of operations for 2013 closed with a financial loss. The difference was covered out of our reserves, with the understanding that it is a pre-financing of future instrument sales.

The PREMOS experiment on the French satellite PICARD performed well and fully covered the failing measurements of Total Solar Irradiance (TSI) by the American SORCE experiment. A new TSI experiment was launched at the end of 2013 by the USA, in their turn compensating the deactivation of PICARD by the Centre National d'Etudes Spatiales in March 2014. Thus, monitoring of the solar energy input to the Earth-Atmosphere system is secured from a long-term perspective, although from the PMOD/WRC's perspective it is extremely sad that a well-performing experiment was retired due to financial reasons.

CLARA will be the next space absolute radiometer to be built by the PMOD/WRC. The experiment will fly on bilateral terms on the Norwegian NORSAT-1 satellite. This is a very valuable contribution to worldwide efforts to ensure the continuity and stability of monitoring one of the key natural parameters that influences the terrestrial climate.

Besides calibration, characterising radiometers is an important step to fully understand an experiment. At the World Radiation Centre there is now the option to channel sunlight into one of the optical laboratories using a Heliostat. The device has now been successfully put into operation and CLARA will be the first space experiment to be characterised with this new facility.

Figure 1. Dr. Ghassem R. Asrar, director of the WMO's World Climate Research Programme (WCRP), gave a keynote speech during the inauguration of the renovated PMOD/WRC building. In his talk "Contributions of The World Radiation Centre to Earth System Science" he emphasised the importance of the PMOD/WRC in observing and understanding the global climate system.

Operational Services

Quality Management System

Manfred Gyo

Overview

One of the main milestones in 2013 was a re-evaluation of the Quality Management System (QMS). The QMS relates to the application of ISO standards, in our case ISO/IEC 17025 which specifies the general requirements for the competence to carry out tests and/or calibrations. It covers testing and calibration using standard and non-standard methods, as well as laboratory-developed methods. ISO/IEC 17025 is for use by laboratories in developing their management system for quality, administrative and technical operations.

The Quality Management annual report and the re-evaluation report were issued in early 2013. The annual meeting of EURAMET TC-Q was held in March 2013 in Sarajevo. The system and practical experience in using the Quality Management were presented in a talk at the meeting. The plenum of the annual meeting declared their confidence in the PMOD/WRC system.

At present, the QMS covers the WRC-SRS and the WRC-WCC-UV Sections. However, the WRC-IRS and WRS-WORCC sections worked on their documentation in 2013, enabling them to be integrated into the QMS in the near future.

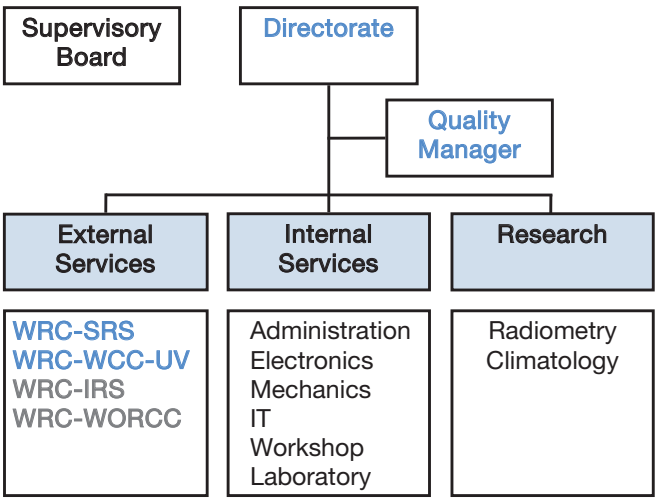

Figure 1. Organisational chart of the PMOD/WRC Quality Management System. The WRC-SRS and WRC-WCC-UV sections perform calibrations according to the EN ISO/IEC standard 17025.

Activities

Two calibration and measurement capabilities (CMC) are listed in the "Bureau International des poids et mesures" (BIPM) database: Responsivity, direct and global solar irradiation. The CMCs "Responsivity, global solar irradiance weighted (UV (280–400 nm), UVB (280–315 nm), UVA (315–400 nm), Erythema CIE)" were first submitted to EURAMET in 2012 and then to the inter-Regional Metrology Organisation (RMO), both are in the review process. It is expected that they will be approved in 2014.

ISO/IEC 17025 specifies the general requirements for the competence to carry out tests and/or calibrations, including sampling. It covers testing and calibration performed using standard methods, non-standard methods, and laboratory-developed methods. ISO/IEC 17025 is for use by laboratories in developing their management system for quality, administrative and technical operations.

Calibration Services

Manfred Gyo, Wolfgang Finsterle, Julian Gröbner, Christoph Wehrli

A re-organisation of the tasks performed by PMOD/WRC technicians was deemed necessary in 2013 due to an increase in the workload of the technology department. The development of hardware for space projects has become increasingly important, and is expected to continue in the future. The pool of technical positions was therefore divided into two, with two technicians providing dedicated support to the WRC section. Amongst other tasks, the WRC technicians will primarily support the calibration services in order to further uphold the present high standards.

Solar Radiometry Section (WRC-SRS)

In 2013, the WRC-SRS section calibrated two PMO6 instruments, 16 Pyrheliometers and 88 Pyranometers (see Figure 1).

Infrared Radiometry Section (WRC-IRS)

The WRC-IRS section again experienced a modest increase in the number of calibrations to 37 instruments. A total of 35 pyrgeometers were calibrated, as well as two Infrared Integrating Sphere Radiometer (IRIS) instruments.

Atmospheric Turbidity Section (WRC-WORCC)

The WRC-WORCC section calibrated 14 PFRs in 2013 against the WORCC Triad standard.

Ultraviolet World Calibration Centre (WRC-WCC-UV)

The WRC-WCC-UV section calibrated four spectroradiometers at their respective field sites using the QASUME travelling reference spectroradiometer.

Sixteen UVB, three UVA, one UV-Global and three dual channel (UVA/UVB) broadband radiometers, and five UV dosimeters were calibrated in 2013 at PMOD/WRC. The QASUME irradiance scale was transferred to three standard lamps at two European institutes.

In June 2013, 18 Brewer spectrophotometers were calibrated relative to the QASUME spectroradiometer during the 8th RBCC-E campaign (Figure 2) at INTA, El Arensillo, Spain.

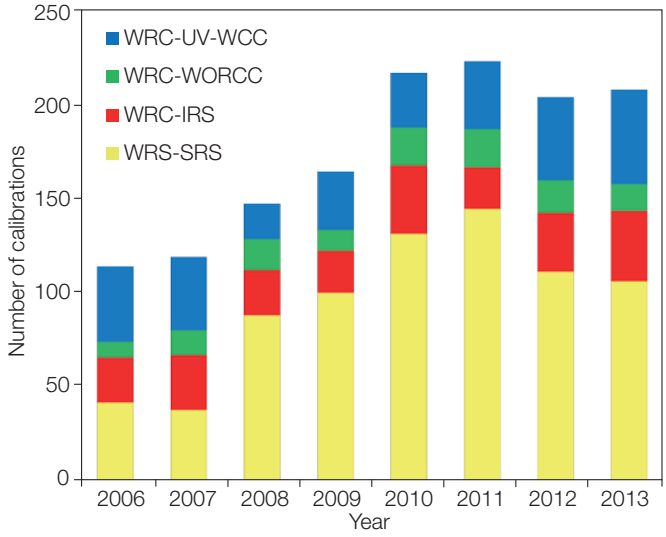

Figure 1. The annual number of instrument calibrations conducted in each WRC section at PMOD/WRC is shown for the 2006–2013 period.

Figure 2. Brewer spectroradiometers during a calibration campaign at INTA, Spain.

Solar Radiometry Section (WRC-SRS)

Wolfgang Finsterle

The Solar Radiometry Section of the WRC (SRS/WRC) is responsible for maintaining and disseminating the World Radiometric Reference (WRR). The WRR is the primary reference for shortwave solar irradiance measurements world-wide. It is established through a group of dedicated absolute cavity radiometers, the World Standard Group (WSG). In 2013, the SRS/WRC participated in the National Pyrehliometer Comparison (NPC-2013) at NREL in Golden, Colorado, USA. Other milestones in 2013 include the formal homologation of the new data acquisition system (DAQ10) for calibration services. The DAQ10 had its debut during the IPC-XI in 2010 and has been extended and successfully validated since then. Nathan Mingard joined the SRS/WRC in April 2013 as a new technical staff member.

Pyrheliometer comparison campaigns

Sustained confidence in the long-term stability of the WSG is a prerequisite for the SRC/WRC to perform its tasks. In September 2013, the National Radiation Center (NRC) in the USA organised the National Pyrheliometer Comparisons (NPC-2013). The SRS/WRC participated in this annual event with a group of three transfer standards (1 AHF and 2 PMO6-cc type cavity radiometers). The results of the comparison confirmed the stability of the WSG. Apart from validating the traceability of solar irradiance measurements world-wide, such inter-laboratory comparisons of standards also serve a key role in maintaining the WRR's status as a primary reference according to the ISO 17025 quality management system. Participation by the WRC is a strong incentive to National and Regional Radiation Centres to organise such intercomparisons in their respective countries and regions. Experience was shared between experts during seminar presentations and discussions. This building and sharing of knowledge during instrument comparison campaigns is a huge added value as opposed to just sending an instrument for calibration.

The new data acquisition system

The new data acquisition system (DAQ10) for the SRS/WRC's calibration facility had its debut during the IPC-XI in 2010, when it was used to read the signals of the six WSG instruments. After the IPC-XI, the DAQ10 software was extended to control the full set of 99 measurement and calibration channels. Fourteen digital multimeters (NI-PXI4065) are connected to two multiplexer cards to offer 84 voltage and 12 current channels for calibration items. The working references for direct and diffuse solar irradiance are connected to three additional and dedicated multimeters which are read out simultaneously with each multiplexer level. This is a clear improvement over the previous data acquisition system where the reference irradiance was read only once at the beginning of each calibration interval. Digitally controlled calibration items can be connected via 16 RS-232 ports. Work has started to implement MODBUS connectivity in order to communicate with the latest generation of pyranometers and pyrheliometers. The MODBUS capability is expected to become available for calibration purposes as of May 2014.
During the renovation of the PMOD/WRC building, the DAQ10 underwent extensive software testing and was ready to conduct calibrations under ISO17025 after the WSG had been moved back to its original site on the solar tracking platform.

Figure 1. Pyrheliometers measuring the solar irradiance during the US National Pyrheliometer Comparison (NPC-2013) in front of the foothills of the Rocky Mountains in Golden, Colorado.

Technical staff

As of April 2013, the SRS/WRC gained a dedicated technical staff position which was possible due to an internal re-organisation within PMOD/WRC. All technical staff previously belonged to the technical department and were only assigned to the SRS/WRC upon request. Since the work load in the calibration laboratory depends on weather conditions, the new and flexible staff structure greatly streamlines the calibration services. The new position was filled by Nathan Mingard, who started at PMOD/WRC in April 2013.

Heliostat light source

In December 2013, the SRS/WRC inaugurated the new Heliostat light source, which will be used to test and characterise space experiments and to facilitate instrument development (see Section on "Instrument Development").

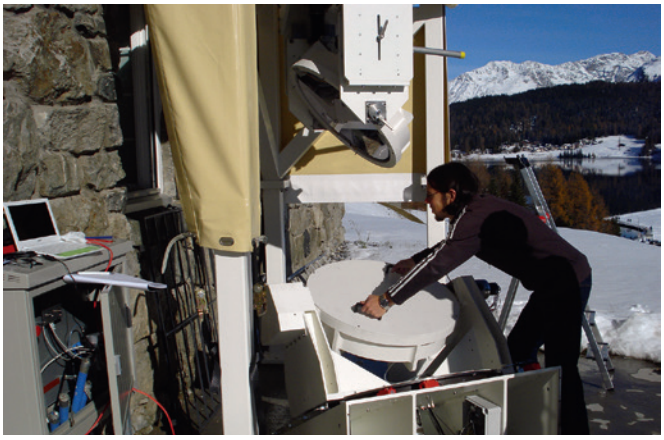

Figure 2. Markus Suter removing the cover from the Heliostat's primary mirror for "first light" on 16 November. Formal inauguration of the Heliostat was celebrated two weeks later.

Infrared Radiometry Section (WRC-IRS)

Julian Gröbner, Stephan Nyeki, and Stefan Wacker

The Infrared Radiometry Section of the WRC maintains and operates the World Infrared Standard Group of Pyrgeometers (WISG) which represents the world-wide reference for atmospheric longwave irradiance measurements.

The WISG time-series surpassed the mark of 10 years of continuous measurements in 2013. Since 1 January 2004, the four pyrgeometers comprising the WISG have been remarkably stable to within ±1 Wm^{-2} over this time period (Figure 1). A minor readjustment was performed on WISG No.4 in 2012 in order to compensate for the slight drift observed with respect to the remaining WISG.

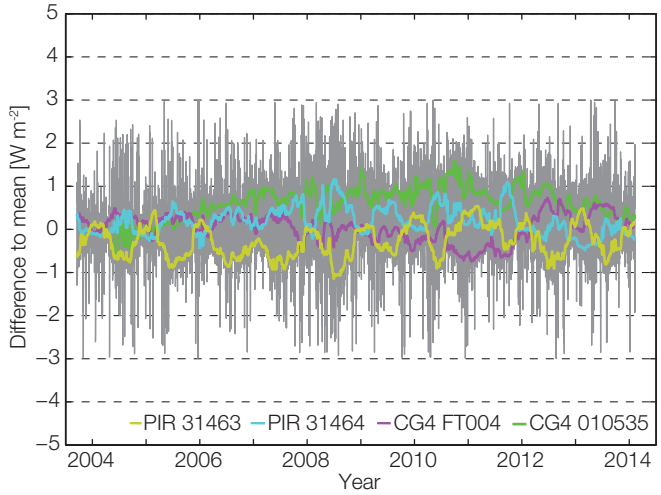

Figure 1. Internal night-time variability of the WISG pyrgeometers with respect to their average. The thick lines show the moving monthly averages, while the grey shaded area represents the nightly averages.

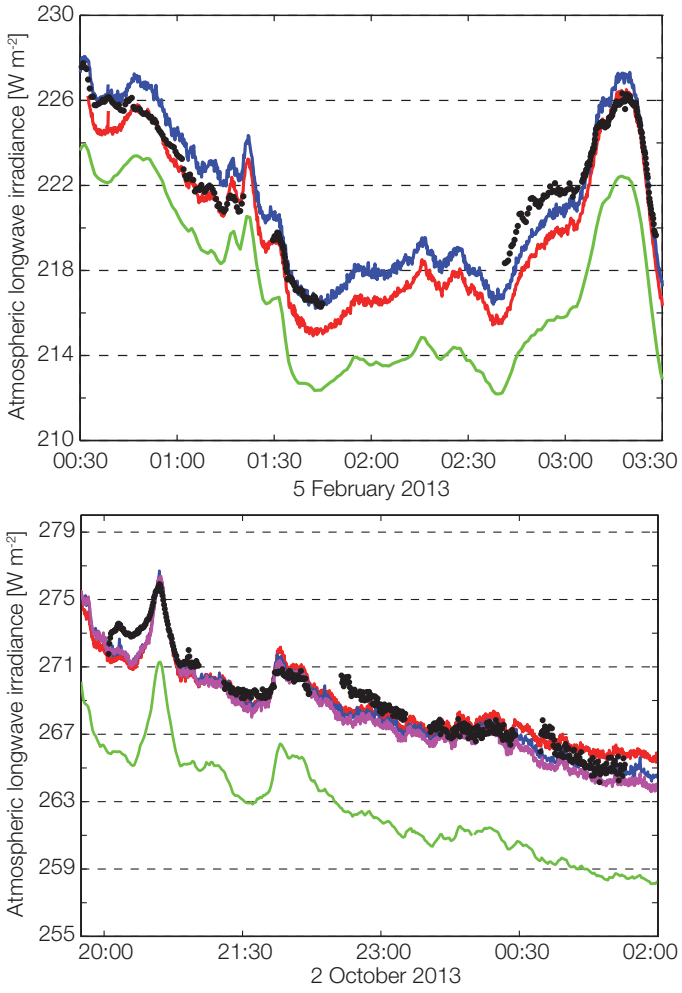

Figure 2. Downwelling longwave irradiance measurements between the ACP (black dots), IRIS (red, blue) and WISG (green) on 5 February (upper panel), and 2 October (lower panel). The magenta curve in the lower panel represents measurements from IRIS No.5.

IRIS No. 2 and 4 radiometers measured on 35 cloud-free nights to measure alongside the WISG. As in previous years, average WISG irradiance is 5 Wm^{-2} lower compared to the IRIS radiometers, with a slight dependence on atmospheric water vapour.

An independent verification of the WISG and IRIS measurements was obtained during two field campaigns organised at PMOD/WRC in February and October 2013 with the Absolute Cavity Pyrgeometer (ACP) developed by the National Renewable Energy Laboratory (NREL), Golden, USA. During two nights, simultaneous measurements between the ACP, IRIS and WISG showed excellent agreement of the two independent absolute references IRIS and ACP to within ±1 Wm^{-2}, while the WISG showed an offset of 3–5 Wm^{-2} relative to these (Figure 2). During the second campaign, the IRIS radiometers from the Deutsche Wetterdienst, Germany and from the Bureau of Meteorology, Australia, participated in the inter-comparison. The results from both campaigns are summarised in Table 1.

These findings suggest that the WISG, in its role as a working reference for atmospheric downwelling longwave irradiance, might require an offset of up to +5 Wm^{-2} in order to provide measurements consistent with the IRIS and ACP. This topic was discussed during the final meeting of the expert team on "in-situ technologies" of the Committee for Instruments and Methods of Observations (CIMO) in Geneva in September 2013. The expert team recommended a task force to be established to address this issue in accordance with WMO guidelines.

Instrument	Difference to IRIS average (Wm^{-2})	
	5 February	2–3 October
ACP	0.6	0.4
WISG	-3.8	-5.6
Atmospheric parameter		
Temperature	-5.2°C	+5.1°C
IWV	7.8 mm	14.7 mm

Table 1. Differences in downwelling longwave irradiance between the ACP and WISG with respect to IRIS on the nights of 5 February and 2–3 October 2013. The ambient temperature and integrated water vapour are also given.

Atmospheric Turbidity Section (WRC-WORCC)

Christoph Wehrli and Natalia Kouremeti

The Atmospheric Turbidity Section of WRC maintains a standard group of three Precision Filter Radiometers that serve as a reference for Aerosol Optical Depth (AOD) measurements within WMO. WORCC also operates the global GAW-PFR AOD network.

Operation of the GAW-PFR network and delivery of AOD to the World Data Centre of Aerosols (WDCA) continued as usual in the past year. Despite the growing number of stations with more than a 10-year AOD time-series, it was unfortunate to hear that Environment Canada closed down Bratt's Lake station at the end of 2012 due to internal re-organisation. The PFR was returned to WORCC after 11 years of continuous observations and will eventually be relocated to Japan as a link between GAW-PFR and SKYNET. The latter is a network to study aerosol-cloud-radiation interactions in the atmosphere where stations are mainly located in Asia. SKYNET is coordinated by Chiba University, Japan.

On the upside, measurements are still being conducted at Summit station (3250 asl) in central Greenland despite the extreme rugged environmental conditions experienced throughout the whole year. Figure 1 shows the PFR while measuring during the presence of ice crystals in the atmosphere. These are present close to the surface, and is then referred to as diamond dust, visible in the figure as speckles.

After the installation of a redundant PFR system at Izaña in 2012, the primary system was recalled to Davos for refurbishment of the data acquisition unit. Detailed inter-comparisons and consistency checks of the PFR reference Triad and the Izaña instrument have revealed drifts in two of the 368 nm channels of the Triad instruments. The Triad scale was thus adjusted by 0.66 % at 368 nm.

In 2013, seven instruments of the extended GAW-PFR network were calibrated against the reference Triad at Davos, and four instruments were calibrated by the Langley method at their respective GAW sites. Additional customer instruments were re-calibrated in the course of repair work. All calibrations were documented according to our Quality Management system.

Annual quality assured data from seven GAW-PFR stations were updated to 2012 and submitted to the WDCA. Daily AOD results from 24 stations are submitted in (quasi) near-real-time and are available at ebas.nilu.no within 24 hours.

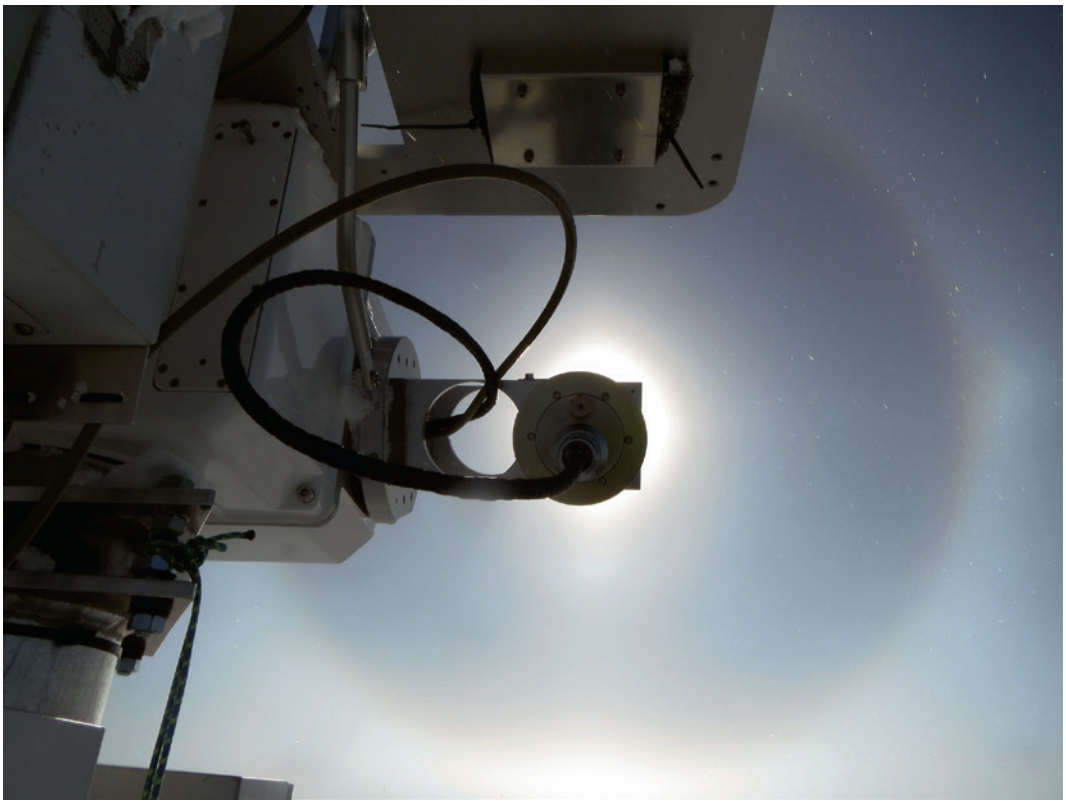

Figure 1. PFR at Summit station (Greenland, 72°N, 3250 m), looking at a 22° ice crystal halo on 4 April 2014. (Picture courtesy of Ward Handley).

World Calibration Centre for UV (WRC-WCC-UV)

Julian Gröbner, Gregor Hülsen, and Luca Egli

The Global Atmosphere Watch (GAW) Ultraviolet (UV) calibration centre aims to improve data quality in the Global GAW UV network and to harmonise the results from different stations and monitoring programs in order to ensure representative and consistent UV radiation data on a global scale.

Most of the activities concentrated on the EMRP project ENV03 "Traceability of spectral solar ultraviolet radiation" as it reached its half-term period and several key deliverables were due. Foremost was the validation of the QASUME spectral irradiance reference at the premises of the Physikalisch-Technische Bundesanstalt (PTB) against the primary standard for spectral irradiance. As shown in Figure 1, the black-body based calibration was found to be in excellent agreement with the irradiance reference realised by the portable lamp standards of QASUME, validating the irradiance scale realization of QASUME and decreasing the uncertainty to ±1.2 %. This is a significant improvement with respect to the previous validation performed in 2004. The subsequent calibration based on a tunable-laser system, aimed at realising the spectral irradiance scale using only a detector-based approach produced consistent results with the black-body calibration, demonstrating the potential of this new method. A follow-up calibration campaign is scheduled for March 2014 in order to demonstrate the reproducibility of the two calibration methodologies and to resolve the discrepancies observed in the 350–400 nm wavelength range. Additional information and ongoing activities can be found at the project web-site: http://projects.pmodwrc.ch/env03/.

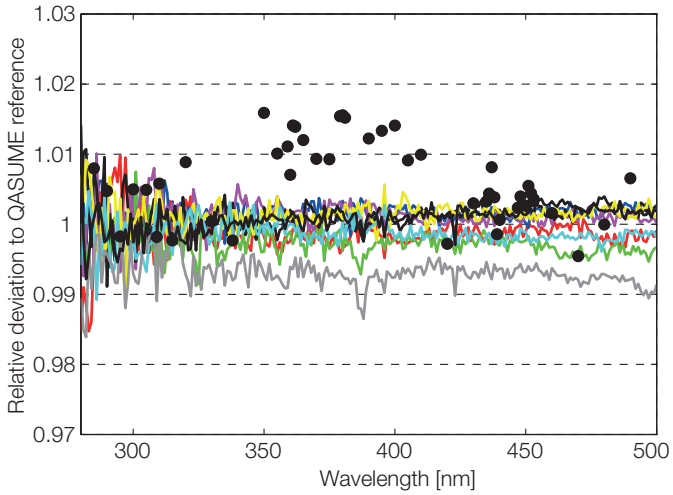

Figure 1. Relative differences between the QASUME scale realisation using secondary transfer standards (F300-F376), the black-body based realisations in 2004 and 2013 (grey and black line respectively), and the TULIP tunable-laser system (red dots). Legend: F300 (red line), F301 (dark blue), F304 (green), F324 (pink), F330 (black), F364 (yellow), F376 (light blue), BB2004 (grey), BB2013 (thick black), TULIP (black circle).

Figure 2. Participants of the QASUME site visit to St. Denis, La Reunion, France. The entrance optics of the two spectroradiometers can be seen in the background.

To round-up the successful news, the follow-up project EMRP ENV59-ATMOZ "Traceability for atmospheric total column ozone" was approved by the end of the year, and will begin in October 2014 to continue and expand the current activities on the metrology of solar UV irradiance measurements, focussing this time on the measurement of direct solar spectral UV irradiance with the aim of retrieving atmospheric total column ozone.

The transportable reference spectroradiometer QASUME was used during four quality assurance site visits. Most noteworthy was the site visit to the University of La Reunion, St. Denis, La Reunion (Indian Ocean), where QASUME was shipped by air freight for the first time. The resulting measurements were very successful, as is documented by happy faces on the last day of the campaign, see Figure 2.

In addition, QASUME measured at the National Meteorological Service of Spain in Madrid and participated in the 8th calibration campaign in the frame of the RBCC-E in El Arenosillo, Spain. The final site to be visited was the Regional Environmental Protection Agency in Aosta, Italy in September. Results of all the QASUME site audits can be found at the WCC-UV web-site: http://www.pmodwrc.ch/wcc_uv/wcc_uv.php?topic=qasume_audit.

Instrument Development

Improved Transportable Reference Spectroradiometer QASUME II

Gregor Hülsen and Julian Gröbner

A new transportable reference spectroradiometer has been built within the framework of the EMRP project ENV03. The principle design of the instrument is a copy of the current QASUME system. However, the key parts of the system were replaced by newly-developed state-of-the-art devices.

Since 2002, the QASUME spectroradiometer has acted as the European transportable UV reference instrument. It is operated by the World Calibration Centre for UV (WCC-UV) of the PMOD/WRC since 2006. Although this instrument records Solar UV irradiance with outstanding performance and stability, an improvement of this reference instrument was considered.

The core part of the current system is a Bentham DM150 double monochromator. However, its entrance optic deviates slightly from the nominal cosine response, which leads to diurnal variabilities of up to ±1.5 % during solar irradiance measurements. The photon detector, a photomultiplier tube (PMT), shows hysteresis effects after illumination which also adds to the measurement uncertainty.

The EMRP project ENV03 "Traceability of spectral solar ultraviolet radiation" enabled the construction of a new QASUME II unit. The principle design has been copied from the old system. The two main disadvantages of the system were overcome by the development of two new state-of-the-art components. First, the PMT was replaced by a Solid State Hybrid Detecting Device (SSDS). It consists of silicon diodes coupled to an electronic readout with high sensitivity. While these diodes have outstanding stability and linearity, they have low sensitivity in the UVB wavelength range. The SSDS was therefore equipped with a small commercial prototype USB photo counter by Hamamatsu. The hybrid system now has the same high sensitivity as the old QASUME PMT while performing as a stable reference detecting device.

The second improvement was the replacement of the input optic. The Teflon diffusor of the old optic was replaced by a new diffusing glass material. An important improvement is the negligible change in its transmission as a function of temperature and humidity, which is a severe problem with Teflon diffusors. In addition, the design of the optic is currently being optimised for an ideal cosine response.

The outlook for 2014 is that the new QASUME II system will be validated against the QASUME reference spectroradiometer. The input optic still needs to be improved for the goal of an ideal cosine response. The operating mode of the hybrid SSDS device will be developed in realistic outdoor intercomparisons.

Figure 1. QASUME (left) and QASUME II (right) during the construction and test phase in the PMOD/WRC optical laboratory.

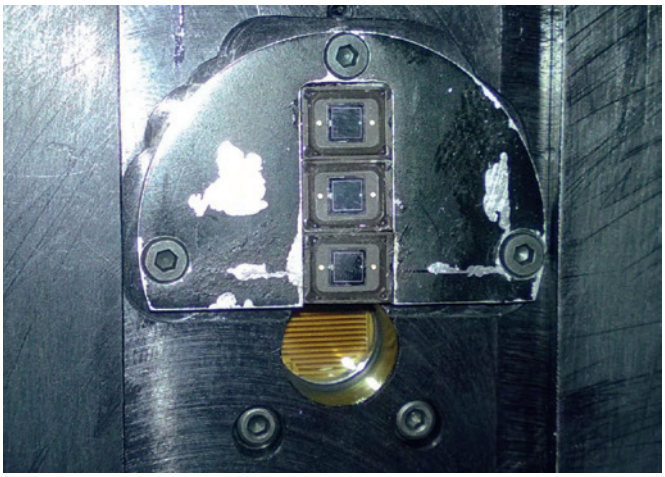

Figure 2. The Solid State Hybrid Detecting Device (SSDS). Visible are the three Si-diodes at the top and the commercial USB photo counter at the bottom.

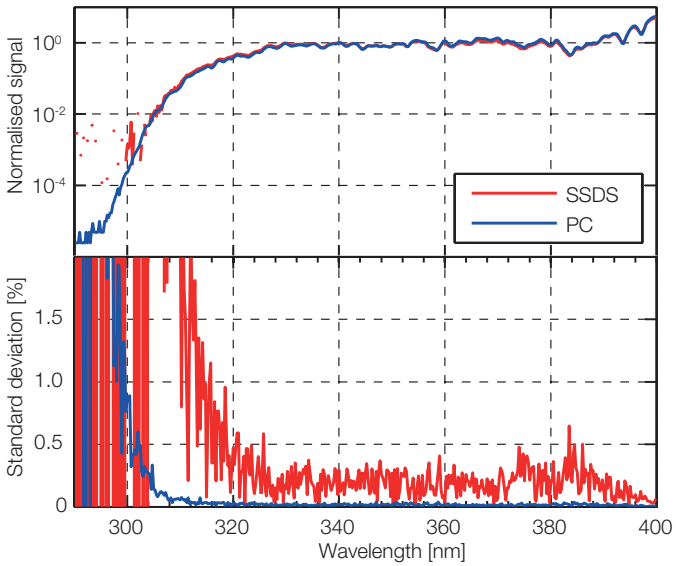

Figure 3. Solar irradiance measurement (top) and corresponding statistics (bottom) during the first QASUME II test at 14:00 UTC, on 7 November 2013.

The Monitor to Measure the Integral Transmittance of Windows (MITRA)

Benjamin Walter

Recent design improvements to the MITRA instrument significantly increased the accuracy of the integral transmittance measurements of the broad-band solar irradiance for windows. These transmittances are indispensable to correct the power reading of the Cryogenic Solar Absolute Radiometer (CSAR) for reflection and absorption losses at the entrance window. Measurements under laboratory conditions resulted in an uncertainty of 150 ppm, only slightly higher than the aim of 100 ppm. Environmental conditions such as wind and strong instrumental temperature changes have been found to significantly increase the uncertainty to 900 ppm for the intended outdoor measurements.

Operating a radiometer at cryogenic temperatures in a vacuum requires knowledge of the entrance window transmissivity. The MITRA instrument (Figures 1 and 2), built to measure the integral transmittance of the broad-band solar irradiance of the CSAR entrance window, aims to provide a high-accuracy correction factor to the CSAR power reading (Winkler, 2012). Because the solar spectral irradiance and thus the integral transmittance change during the course of a day, a week or a month, depending on the air mass and atmospheric conditions, the MITRA instrument determines the correction factor simultaneously to CSAR measurements.

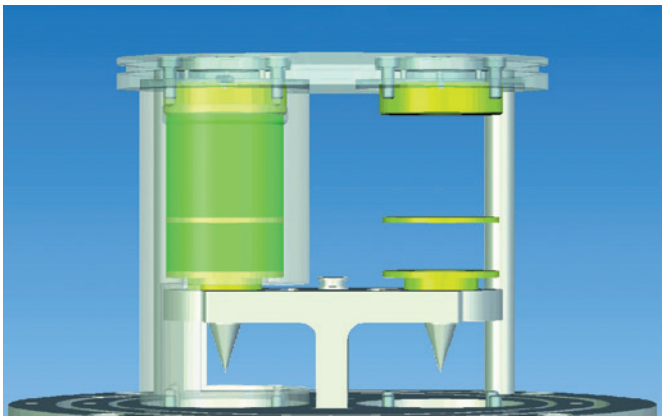

Figure 1. Schematic of the MITRA instrument with two absorbing cavities (upward facing cones) for measuring the temperature rise with respect to a common heat sink. One of the two cavities is periodically covered by a window from the same production batch as that used by the CSAR instrument. In the obstructed case, the temperature rise with respect to the heat sink is slightly reduced because of a reduced transmissivity and thus solar irradiance. Comparing the temperature rise of the obstructed with the unobstructed case defines the integral transmittance.

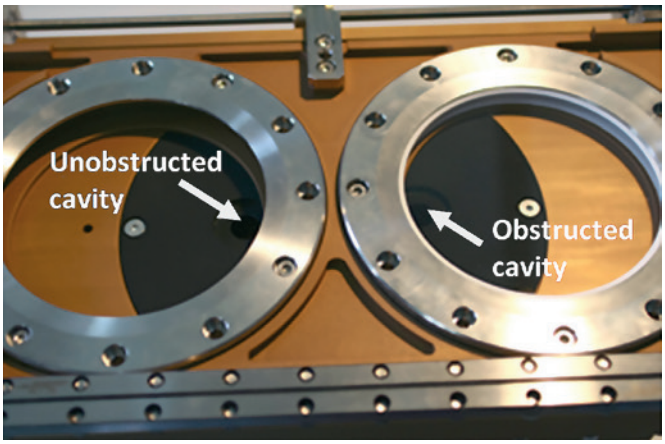

Figure 2. The sun-facing part of the MITRA instrument where a sledge periodically moves the window in front of one cavity. Here, the right-hand cavity (the hardly visible, small entrance hole close to the aluminum ring) is obstructed by a quartz window which is mounted in the circular window frame on the right-hand side of the sledge.

Recent design improvements to the MITRA instrument include: 1) the electrical separation and shielding of the motor driving the window sledge, and 2) the implementation of a high accuracy current measurement device and an additional voltmeter for measuring the voltage at the temperature sensing copper wires. The latter finally completes the MITRA setup so that all three voltages of the temperature sensing wires of both cavities and the sink can now be measured simultaneously, thereby reducing interferences from switching channels. These improvements have reduced the average measurement uncertainty of dark measurements from 395 ppm to 22 ppm (k = 1) for laboratory conditions. This result shows that the temperature-sensing and read-out electronics of the instruments perform well under laboratory conditions and meet the intended uncertainty goal of 100 ppm. As a consequence, further improvements need to focus on disturbances and electrical noise induced by illuminated outdoor conditions.

Figure 3 shows measurements of the integral transmittance t_{int} of a quartz window under laboratory conditions, where solar radiation is guided into the laboratory via two mirrors from the newly installed Heliostat. The results show that the improved MITRA instrument allows diurnal variations of the integral transmittance to be detected with high accuracy. After fitting and subtracting a 5^{th} order polynomial function, the uncertainty of the de-trended

variations is 150 ppm. The average level of t_{int} is higher than the range of average values, $0.9268 < t_{int} < 0.9271$, determined by simulations (Fehlmann, 2011), indicating that atmospheric conditions on the day of measurement were different to those used in the simulations. Furthermore, spectral variations of the TSI induced by the Heliostat resulting from a changing incidence angle of the radiation on the first mirror and a changing mirror temperature resulting in a varying infrared radiation emission towards the MITRA instrument, might cause additional deviations of t_{int} with respect to the simulations.

As the CSAR instrument measures TSI under outdoor conditions, MITRA should be operated similarly, including environmental influences such as wind and a changing ambient air temperature. Figure 3 shows an outdoor measurement of t_{int} on the WRR sun-tracking platform. The results show a lower average integral transmittance t_{int} compared to the laboratory measurement, which agrees well with the average value of $t_{int} = 0.9269$ predicted by simulations (Fehlmann, 2011). However, t_{int} values also show a significantly stronger scattering than the laboratory measurements as a result of environmental influences such as wind and changing air temperature. The uncertainty of the detrended t_{int} – variations is 900 ppm in this case. It was found that temperature drifts larger than $\pm 2°C.h^{-1}$ result in a significant decrease of the measurement accuracy. Future work on this project will focus on the elimination of wind influences and strong temperature drifts to reduce the measurement uncertainty from 900 ppm to the intended 100 ppm for outdoor conditions. In general, it needs to be mentioned that successful CSAR and MITRA measurements with the intended low uncertainty of 100 ppm can only be performed under perfect atmospheric and environmental conditions, which means no wind, a clear sky and small air temperature changes.

References: Fehlmann A.: 2011, Metrology of Solar Irradiance, PhD Thesis, University of Zürich.

Winkler R.: 2012, Cryogenic Solar Absolute Radiometer – a potential replacement for the World Radiometric Reference, PhD Thesis, University College London.

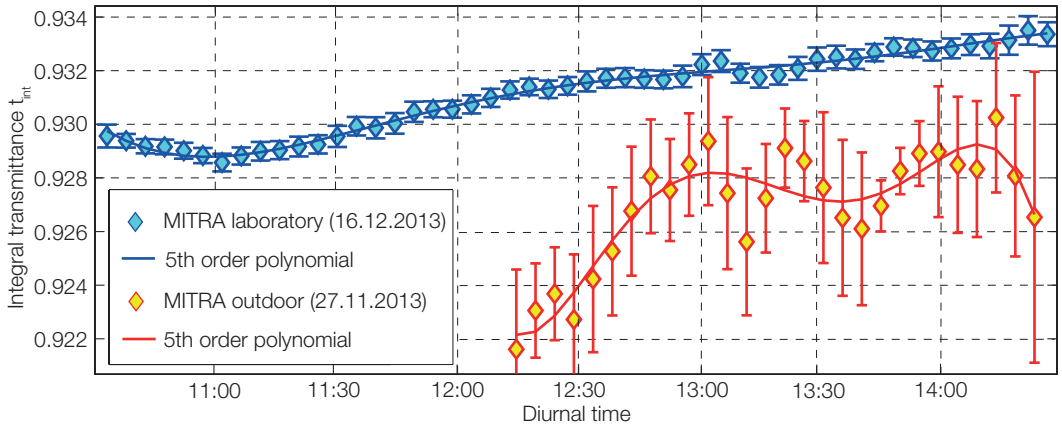

Figure 3. MITRA integral transmittance time-series measurements under laboratory and outdoor conditions.

Heliostat

Markus Suter

The new Heliostat system was installed and inaugurated in 2013. This project, which began in 2011, has entered its final phase, including manufacturing, installation and commissioning. The Heliostat had a successful "first light" test in November 2013, and was inaugurated soon after.

During renovation of the PMOD/WRC building (2011/2012), the old Heliostat system, which had been integrated into the building roof, was removed. It was then decided to build a new system that will not only replace the old system but offer more opportunities for a wider range of applications. With two flat mirrors the Heliostat feeds a high quality solar light beam into the optics laboratory where experiments will take place. It is also possible to feed the beam from the laboratory into the adjacent clean room, to test space experiments.

The Heliostat project began in 2011 with basic design studies and fundraising. The design was finalised in 2012, and the mirrors were manufactured (see Annual Reports 2011 and 2012). Manufacturing of the Heliostat structure began in December 2012 while the structure of the mirror support was then temporarily assembled in Sargans at G+P Engineering AG in spring 2013. During this period, first tests of the motion control were carried out. In addition, the rain cover was adapted to fit the structure. The controller software was developed and prepared in parallel.

After final inspection at G+P Engineering, the Heliostat was sent to the PMOD/WRC and installed on 20 June 2013. The Heliostat structure was lifted with a "Manitou" crane from the transport lorry, and precisely placed and fixed on its pre-prepared platform (Figures 1 and 2).

Figure 1. Heliostat structure on the "Manitou" crane in front of the PMOD/WRC building.

Figure 2. Installation of the Heliostat structure.

After the installation of the structure, the motion control system was integrated and cables were fixed. A low-grade mirror instead of the high-grade mirror was then temporarily installed to test the tracking system and software. After the tracking system had been proven reliable, the high-grade mirrors were unpacked and installed in October 2013. Figure 3 shows the integration of the mirrors into their holder.

The Heliostat saw "first light" on 16 November whereby the mirrors were uncovered for the first time in front of the sun (Figure

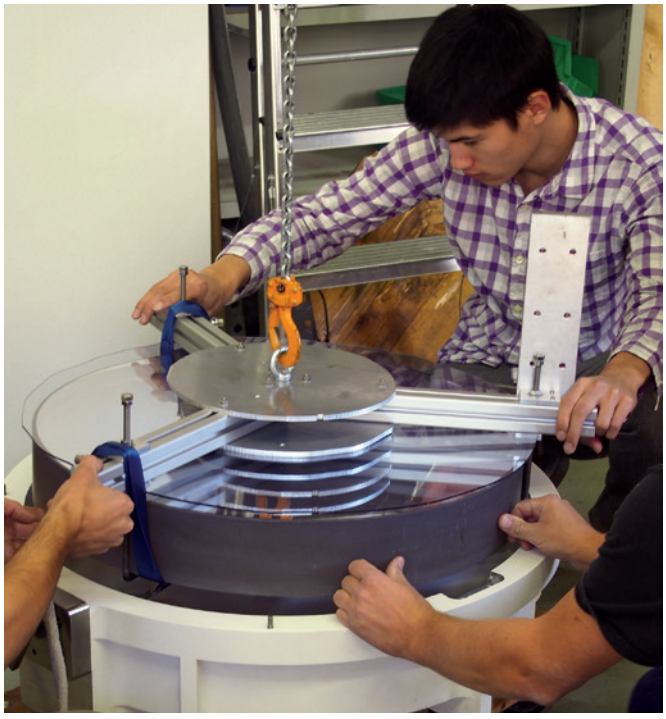

Figure 3. Nathan Mingard and two co-workers integrating one of the Heliostat mirrors.

Figure 4. "First light" test with Markus Suter uncovering the Heliostat mirror.

4). At 12:05 the beam was directed into the laboratory for the first time. Active tracking capability was then added to the system and several performance tests were conducted. An inauguration party took place on 2 December 2013. The Heliostat was demonstrated to the PMOD/WRC staff, and a small celebration took place (Figure 5). After the inauguration, the Heliostat was frequently used in December to test and improve the MITRA instrument.

It is planned to use the Heliostat in 2014 for the characterisation of the CLARA space radiometer as well as for the further development of the MITRA instrument.

Construction of the Heliostat was supported by the Swiss National Science Foundation Grant No 206021 139119 and Grant No 200021_132553.

Figure 5. Inauguration of the Heliostat with PMOD/WRC staff.

Instrument Sales

Manfred Gyo, Julian Gröbner, Etienne de Coulon, Fabian Dürig, Natalia Kouremeti, Dany Pfiffner, Ricco Soder, Marcel Spescha, Diego Wasser

Two PMO6-cc absolute radiometers were sold in 2013. The main focus was on the finalization of the new precision spectroradiometer (PSR).

While development of the PSR finished in 2013, improvements to the design were being continuously assessed and implemented throughout the year. A major improvement concerned the reduction of the instrument temperature sensitivity. The PSR bench is made of carbon fibre to minimise the thermal expansion coefficient as much as possible. The linear sensor is actively temperature-stabilised to maintain $\Delta T < 0.2$ K. The optics are also temperature-stabilised to cope with ambient temperature variations from -25 up to 40°C without a decrease in performance.

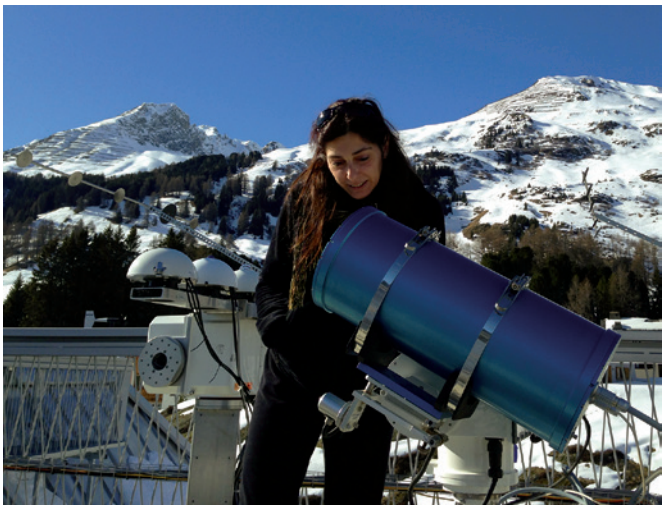

Figure 1. Precision Spectroradiometer (PSR) on the PMOD/WRC roof.

The instrument is sealed and filled with dry nitrogen to survive harsh environments. A customer request for an extra auxiliary channel was also implemented in the final design. It is now possible to connect external optics to the instrument. An internal data logger has been integrated, and the PSR can be operated via a USB connector or Ethernet connection in direct measurement mode or logger mode. A web-interface allows the PSR to be configured and monitored remotely or on-site (see Figure 2). In addition, to the instrument development a set of tools to support the manufacturing, integration and testing were developed. For instance, Figure 3 shows a view of the PSR sensor and optical components during assembly.

Figure 2. PSR web-interface for remote configuration and operation.

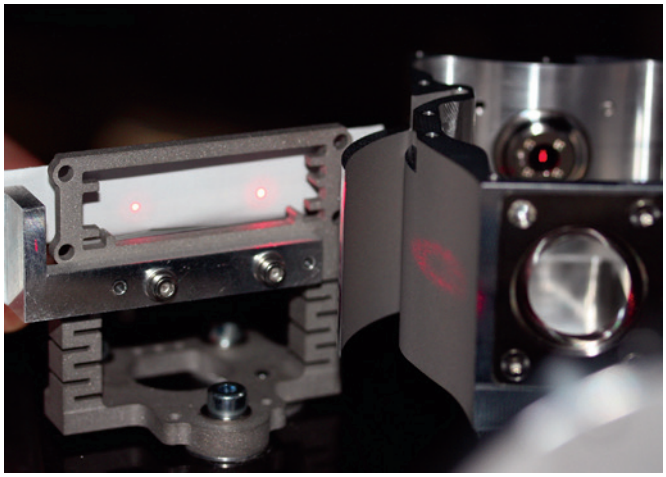

Figure 3. View of PSR sensor and optical components.

The first or so-called "zero" series was manufactured and assembled in autumn 2013. Final testing will be finished in spring 2014. Figure 4 shows results from a slit function test from the first production instrument which allows it to be characterised at a particular monochromatic wavelength. The new instrument will be available for customers in spring 2014.

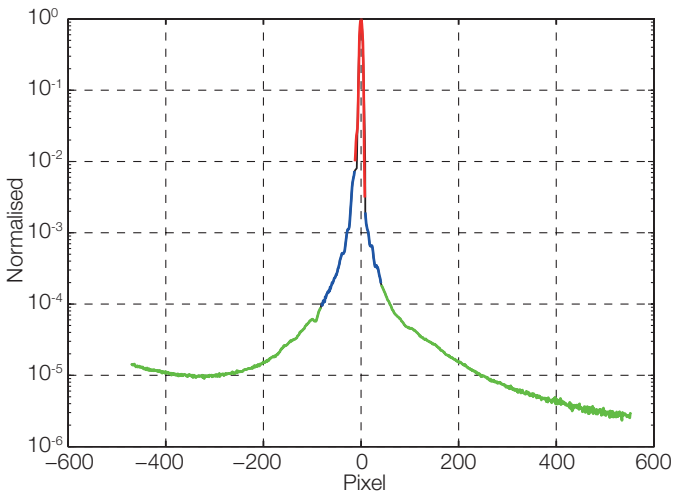

Figure 4. Slit function measurement of a PSR.

Space Experiments

Manfred Gyo, Werner Schmutz, Valeria Büchel, Etienne de Coulon, Fabian Dürig, Wolfgang Finsterle, Margit Haberreiter, Silvio Koller, Nathan Mingard, Dany Pfiffner, Ricco Soder, Marcel Specha, Diego Wasser

PREMOS

The PREMOS experiment, a payload aboard the French PICARD micro satellite.

PREMOS is still operating well. Figure 1 illustrates the evolution of the PREMOS on-board temperature. Compared with results from last year, a slight temperature increase is evident which is due to optical degradation of the front sun-shield and the radiator.

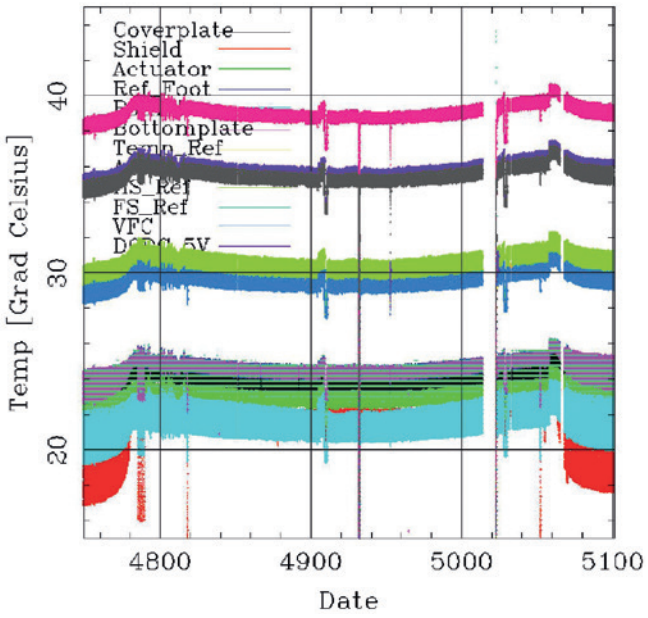

Figure 1. PREMOS package temperatures.

Despite a few minor events, described below, PREMOS is still measuring the total and spectral solar irradiance with great reliability and accuracy. Two minor technical issues occurred during 2013. The first incident in June concerned the backup radiometer shutter while the second incident in July concerned housekeeping measurements. Both problems were solved upon restarting PREMOS. Two further unconnected incidents occurred from 19–22 December but were automatically corrected by the periodic reloading of the onboard Application Specific Integrated Circuit (ASIC). Several special procedures were also conducted during 2013:

- 28 January: Dark current measurements with the filter radiometers.
- 10 February: Deep-space measurements with the absolute radiometers.
- 10 May: Observation of the solar eclipse with the filter radiometers
- 6 November: A new set-point of the heat-sink temperature was necessary.

All of the above special procedures were successfully completed. 2013 was the last full year of PREMOS measurement. PICARD and its payloads will be switched off at the end of March 2014.

EUI

The Extreme UV Imager (EUI) experiment, a payload aboard the ESA/NASA Solar Orbiter Mission.

The EUI instrument suite consists of a number of filter-graph telescopes designed for narrow-band Extreme Ultra Violet (EUV) imaging of the solar corona.

The instrument contains two high-resolution telescopes (HRI) and one Full-Sun Imager (FSI) in a single optical housing. The telescope channels operate in different pass-bands at UV wavelengths between 174 and 1216 Å.

The Manufacturing Readiness Review (MRR) for the structural model (STM) was held in April 2013. Dummy benches for alignment tests, the engineering model (EM) support structure and STM were delivered during the year.

Assembly of the EUI STM instrument was completed in December after which a thermal test was performed. Figure 2 shows the open EUI STM instrument during test preparation.

Solar UV radiation is known to lead to irreversible degradation of optical surfaces by photo-polymerization of molecular organic material outgassing from organic substances used for the construction of telescopes.

Figure 2. Extreme UV Imager (EUI) structural model in front of the consortium members.

Figure 3. Panel bake-out preparations at PMOD/WRC which are conducted in a clean-room environment.

It is therefore important to pay attention to cleanliness requirements. To meet these, every component of the instrument has to be baked-out under vacuum at its maximum operating temperature. A first bake-out procedure of STM structural elements was conducted in the clean-room facilities at the PMOD/WRC with a constructed heat case, placed in a large vacuum chamber (Figure 3).

SPICE

The SPICE experiment, a payload aboard the ESA/NASA Solar Orbiter Mission.

Low Voltage Power Supply (LVPS)

The LVPS is designed and manufactured by PMOD/WRC. The critical design review was approved in June 2013. The Assembly, Integration and Testing (AIT) of the Engineering Model (EM) began in July 2013.

The LVPS EM (Figure 4) was ready for shipping in October 2013, and was integrated into the SPICE Electronic Box at Southwestern Research Institute, US.

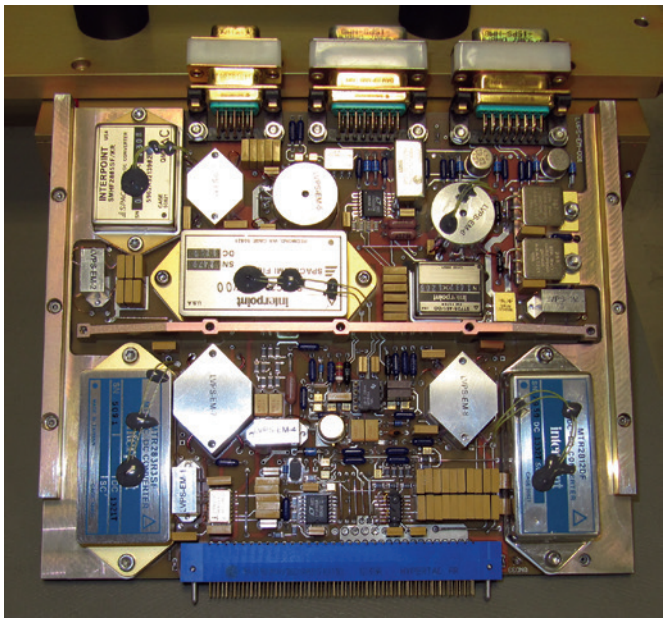

Figure 4. LVPS engineering model ready for shipping.

Slit Change Mechanism (SCM)

The SCM is designed to put one of four slits into position during measurements, and passed the critical design review in October 2013. The design was further optimised by our SCM industry partner, ALMATECH. The assembly and testing of the breadboard is currently ongoing. The qualification model, the flight model and the flight spare will be manufactured, assembled and tested in 2014. Part of the tests, namely the bake-out of the SCM components and models, will be performed at PMOD/WRC. Figure 5 shows the static slit holder model.

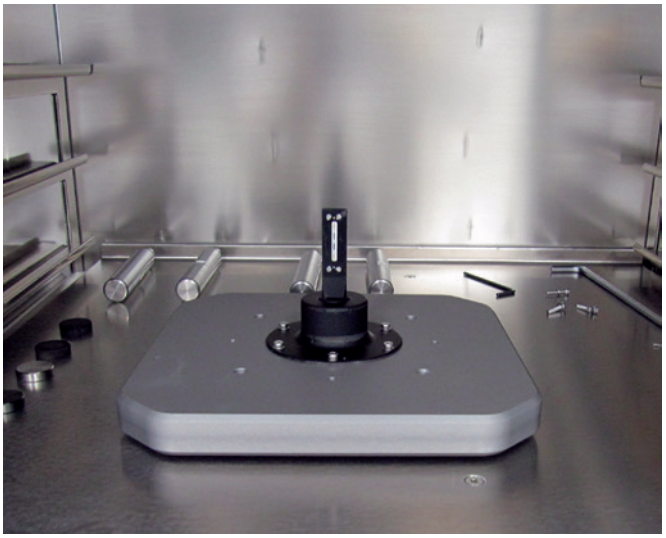

Figure 5. Static slit holder model during bake-out in a vacuum oven at PMOD/WRC.

SPICE Door Mechanism (SDM)

The SDM is designed to prevent instrument contamination while on the ground and in space. It also allows the instrument to be purged through a labyrinth seal during AIT and launch. The project passed the critical design review in October 2013. The design was completed by APCO Technologies, our industry partner for the SDM. The breadboard (Figure 6) which is similar to the flight model has been manufactured and is currently in the test phase.

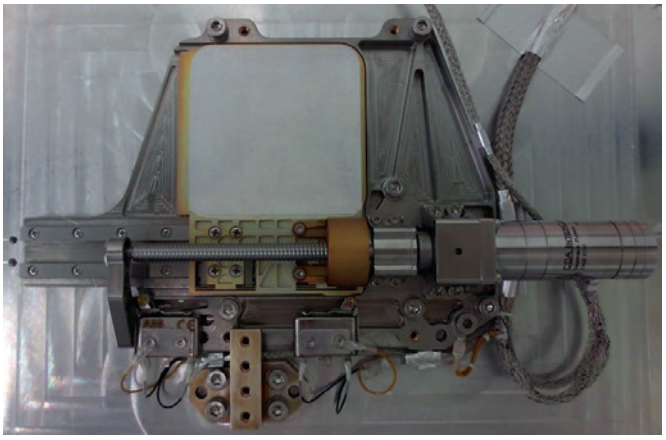

Figure 6. The SPICE Door Mechanism (SDM) breadboard.

CLARA

The Compact Lightweight Absolute Radiometer (CLARA) on the Norwegian nano-satellite NORSAT-1.

CLARA is an enhancement of the DARA radiometer, the new PMOD/WRC radiometer design. CLARA was selected as a payload instrument by the Norwegian Space Centre at the beginning of 2013. The satellite NORSAT-1 carries a next-generation AIS (automatic identification system) receiver system, a Langmuir probe (plasma detector), developed by the University in Oslo, and CLARA. The AIS is a GPS-based tracking system for large ships, which Norway has already integrated on previous satellites.

CLARA will continue the long-term series of total solar irradiation (TSI) measurements in space. Such measurements are of global importance to understand the Sun as well as the external forcing of Earth's climate system.

The CLARA design phase started in mid-2013. Besides design and development activities, industry tasks were defined, as CLARA will be supported by ESA PRODEX. Swiss companies will conduct software development, mechanical and thermal analyses and some manufacturing tasks.

A very ambitious schedule must be kept. The EM will have to be ready in spring 2014, and the flight units delivered by the end of 2014. Figure 7 shows a cross-section of the current instrumental design. The whole structure is divided into two parts: The right-hand compartment contains most of the electronics and the left-hand houses the radiometer sensors.

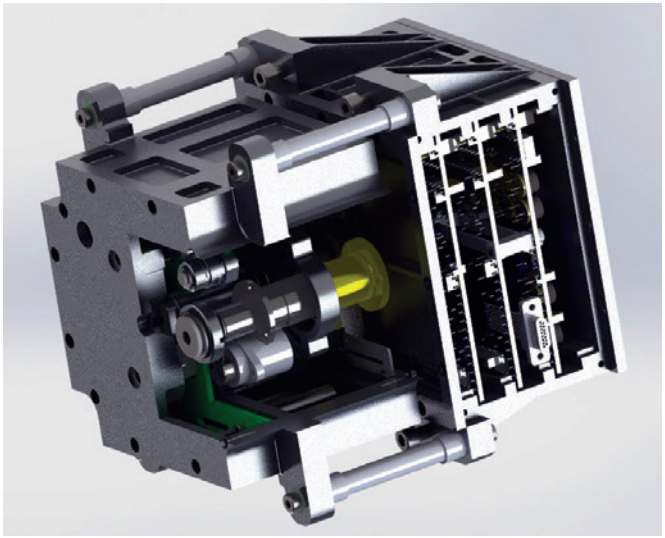

Figure 7. Compact Lightweight Absolute Radiometer (CLARA) cross-section.

Scientific Research Activities

Overview

Werner Schmutz

Projects at PMOD/WRC are related to solar radiation in which we address questions regarding the radiation energy budget in the terrestrial atmosphere as well as problems in solar physics to understand the mechanisms concerning the variability of solar irradiance. Hardware projects at our institute are part of investigations into Sun-Earth interactions by providing measurements of solar irradiance.

The choice of projects to be conducted at the institute is governed by the synergy between the know-how obtained from the Operational Services of the World Radiation Centre and other research activities. Basically, the same instruments are built for space-based experiments as are utilised for ground-based measurements.

The research activities can be grouped into three themes:

- Climate modeling
- Terrestrial radiation balance
- Solar physics

Research activities are financed through third party funding. Last year, five projects were supported by the Swiss National Science Foundation, two projects by the Swiss COST support, one project by MeteoSwiss, two projects by the seventh European Framework Programme FP7, and three projects by the European Metrology Research Programs. These funding sources are supporting three PhD Theses and eight post-doctoral positions. ESA's PRODEX programme funds the hardware development of space experiments. The institute's three PRODEX projects paid for the equivalent of six technical department positions.

The main project in climate research at PMOD/WRC is the project Future and Past Solar Influence on the Terrestrial Climate (FUPSOL), which is a collaborative multi-institute research with partners from the EAWAG, IAC ETHZ, Bern University, and Oeschger Centre for Climate Change Research. It was funded by a "Sinergia" 3-year grant from the Swiss National Science Foundation, which ended in December 2013. The successful collaboration resulted in three PhD Thesis, all based on published or submitted research articles in major international journals. In addition, many publications by the project's participants concern natural influences on the climate. Although several questions have been answered in the project, many other problems have surfaced – as is normal in any ambitious research project. Consequently, the collaboration has submitted a proposal for a follow-up project, FUPSOL – II, again led by the PMOD/WRC. A continuation was approved by the SNSF for another 3 years.

Most PMOD/WRC projects relate directly or indirectly to the goal of understanding natural climate change as well as forecasting the contributions from natural influences to future climate change. The results are reported in scientific research articles and the publications of the observatory have increasingly received attention in international scientific communities. As illustrated in Figure 1, this trend is testified by the increasing number of citations to articles including authors having a PMOD/WRC affiliation. In 2013, the annual number of citations surpassed a total of 1000; a number that duly reflects the success in the scientific community.

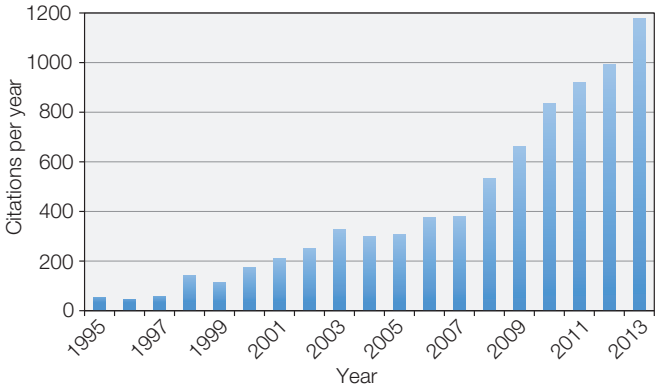

Figure 1. Number of annual citations to published papers including an author with a PMOD/WRC affiliation. In April 2014, there were in total 8278 citations to 422 articles included in Thomson Reuter's Web of Science. The articles are selected using the search criteria address = (World Rad C*) OR (PMOD* NOT PMOD Technol*) OR (Phys* Met* Obs*).*

Future and Past Solar Influence on the Terrestrial Climate (FUPSOL)

Werner Schmutz (PI), Eugene Rozanov (project manager) and Alexander Shapiro in collaboration with teams from EAWAG, IAC ETHZ, KUP and GIUB of University of Bern, and Oeschger Centre for Climate Change Research

FUPSOL is a Swiss collaboration project involving partners from the Institute for Atmosphere and Climate Sciences of the ETH Zürich (IAC ETH), the Swiss Federal Institute of Aquatic Science and Technology, Dübendorf (EAWAG), the Physics Institute (KUP) and Institute of Geography (GIUB) of the University of Bern and the Oeschger Centre for Climate Change Research. It aims to quantify the solar forcing and its influence on the Earth's atmosphere and climate in the past and future.

On the basis of the spectral analysis of solar activity in the past, we predict its steady decrease in the future reaching approximately the level of the Dalton minimum in the year 2100. From this time-series we derived the evolution of the energetic electron precipitation (EEP), solar proton events (SPE) and the spectral solar irradiance (SSI) for all years from 1600 to 2100 based on the Shapiro et al. (2011) approach. We have also prepared a novel, detailed stratospheric aerosol data-set which includes several volcanic eruptions in the future, defined from statistical properties of volcanic eruptions in the past.

The main efforts during the last year of the project were aimed at the simulation of the 21st century with the atmosphere-ocean-chemistry-climate model (AOCCM) SOCOL–MPIOM. Using this model we investigated the effects of a recently proposed decline in solar activity on the evolution of the Earth's climate and ozone layer. Three sets of two-member ensemble simulations, forced by an intermediate emission scenario (Intergovernmental Panel on Climate Change RCP4.5), were performed, one with constant solar activity, the other two with reduced solar activity and different strength of the solar irradiance forcing.

Our results revealed that a future grand solar minimum is able to compensate the global mean anthropogenic surface warming of 2 K between 1986–2005 and 2081–2100 by 0.2 to 0.3 K. In this case, the 2 K warming threshold will not be reached during the 21st century. However, it should be noted that in case of a high emission scenario (IPCC RCP 8.5 pathway) even the strongest possible decrease in solar activity would not lead to noticeable compensation of the greenhouse warming.

Furthermore, the decrease in solar activity followed by the limited availability of solar UV radiation leads to a significant depletion of the ozone layer in the future. Figure 1 illustrates global and annual mean total column ozone (DU) evolution from 1960 to 2100 simulated by AOCCM MPIOM for our three cases. If the present level of solar activity is kept constant in the future, the recovery in total ozone to the 1960/1980 level will be reached in 2060/2030 due to Montreal Protocol limitations on the production of ozone destroying substances.

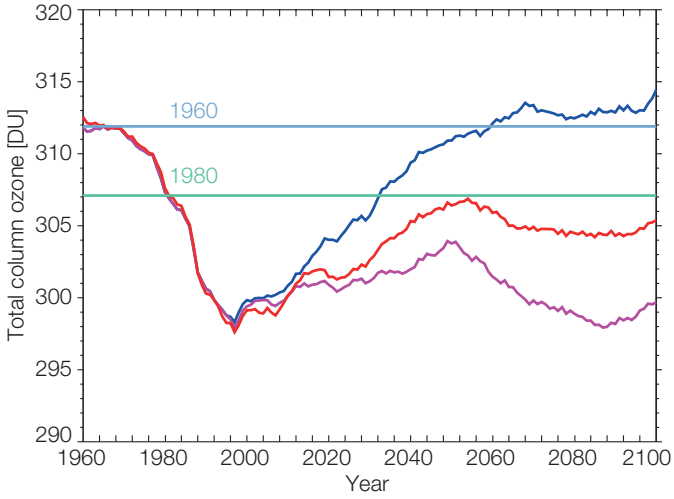

Figure 1. Global mean annual total column ozone (DU) evolution from 1960 to 2100 simulated by AOCCM MPIOM. The blue line represents the case with constant solar activity. Red/Pink lines represent the case with a strong decline in solar activity for weak/strong strength scenarios of SSI evolution as proposed by Shapiro et al., (2011). The results are smoothed with a 7-year running average.

In the two cases with a decline in solar activity, the global mean total ozone will never recover to pre-ozone hole conditions for both the strong and weak SSI change scenarios. Therefore, the effects of a decline in solar activity, should it occur, may interfere with international efforts for the protection of global climate and the ozone layer. The results of this study are presented by Anet et al. (2013) in greater detail.

References:

Anet J. G., et al.: 2013, Impact of a potential 21st century "grand solar minimum" on surface temperatures and stratospheric ozone, Geophys. Res. Lett., 40, 4420–442.

Shapiro A.I., Schmutz W., Rozanov E., Schoell M., Haberreiter M., Shapiro A. V., and Nyeki S.: 2011, A new approach to the long-term reconstruction of the solar irradiance leads to large historical solar forcing, Astronomy and Astrophysics, 529, A67.

Middle Atmospheric Ozone Changes

Anna Shapiro, Eugene Rozanov, Alexander Shapiro, Tatiana Egorova, Timofei Sukhodolov and Werner Schmutz in collaboration with Thomas Peter (IAC ETH, Zurich)

We compared 3-D modelled and measured middle atmospheric ozone changes between August 2004 and August 2008. The measurements detected a substantial increase in ozone changes at about 35–45 km altitude. This increase is not reproduced by the model. We believe that the origin of this feature could be due to the unforced sporadic variability of the atmosphere.

The recent Spectral Solar Irradiance (SSI) measurements by Spectral Irradiance Monitor (SIM) and SOLar STellar Irradiance Comparison Instrument (SOLSTICE) instruments onboard the SOlar Radiation and Climate Experiment (SORCE) suggest significantly larger ultraviolet (UV) changes than was previously estimated. A detailed discussion of different SSI data-sets has been given by Ermolli et al. (2013). The SSI changes influence the middle atmosphere. To find the SSI data-set which leads to the best agreement between modelled and measured atmospheric changes we applied the Chemistry-Climate Model (CCM) SOCOL and simulated ozone changes using SSI reconstructed by the Naval Research Laboratory (NRL) and measured by the SIM and SOLSTICE instruments. In addition we conducted a reference run (CONST SUN), during which the SSI was kept constant. For the measured changes we used the observations by SBUV/ NOAA, SABER/TIMED, MLS/AURA and SCIAMACHY/ ENVISAT. For the comparison of the modelled and measured differences in the similar dynamical states we considered the periods corresponding to the same QBO phases. Thus we calculated ozone changes between August 2004 and August 2008.

While the comparison showed a reasonable agreement between the measured and modelled results in the mesosphere, measurements indicated a remarkable feature at lower altitudes. At 35–45 km ozone changes measured by SABER/ TIMED, SBUV/ NOAA, MLS/AURA, and SCIAMACHY/ENVISAT are substantially larger than changes modelled with all considered SSI data-sets (Figure 1). Figure 2 shows that some event strongly affected the measured August ozone changes. The origin of this event has not been identified yet. The separate analysis of August 2004 and August 2008 measurements showed that the anomaly which affects ozone changes happened in August 2004. We suspect that the August anomaly is caused by processes, which are not taken into account by the free-running climate models.

To simulate this event we will run CCM SOCOL in the specified dynamics regime. In this mode, the meteorological data are nudged to the measured values for some specifically chosen altitudes. We think that modeling with SOCOL in the regime of specified dynamics will help us to reproduce the August 2004 event and improve the comparison of the modelled and measured ozone changes.

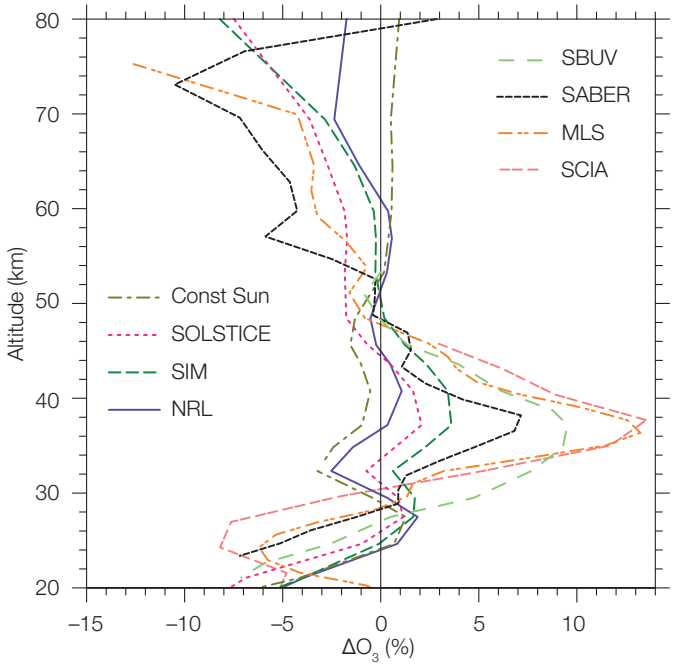

Figure 1. Ozone changes between August 2004 and August 2008.

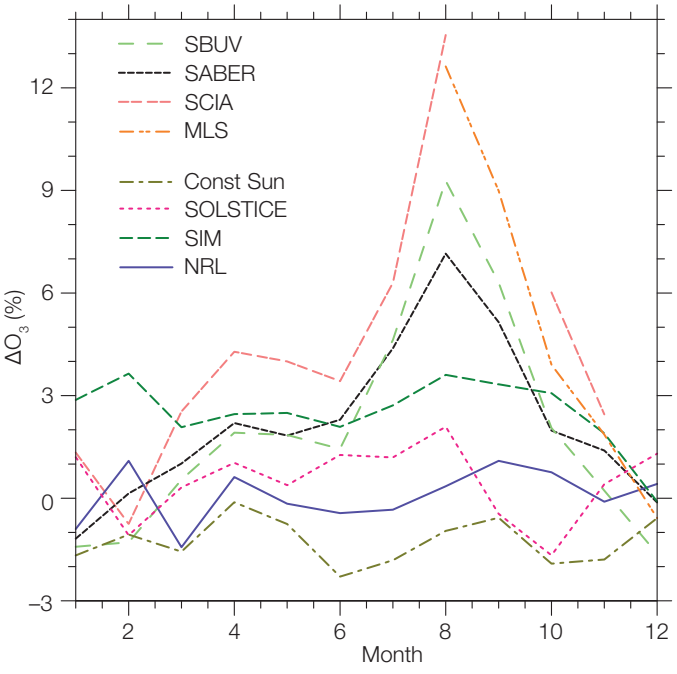

Figure 2. The dependency of ozone differences on month at an altitude of about 38 km.

References: Ermolli I., et al.: 2013, Recent variability of the solar spectral irradiance and its impact on climate modelling, Atmos. Chem. Phys., 13, 3945-3977, doi:10.5194/acp-13-3945-2013.

Evaluation of Tropospheric Climate Change during the Dalton Minimum with AOCCM SOCOL– MPIOM

Eugene Rozanov and Julien Anet in collaboration with the FUPSOL team (PMOD/WRC, EAWAG, IAC ETHZ, Bern University and Oeschger Centre for Climate Change Research)

The SNF supported FUPSOL project aims to evaluate the impact of solar variability on the climate and ozone layer. We analyze experimental results obtained with the Atmosphere-Ocean-chemistry-climate model (AOCCM) SOCOL–MPIOM to elucidate the climate response to spectral solar irradiance, volcanic eruptions and variability in energetic particle precipitation during the Dalton Minimum.

The SNF-Sinergia project "Future and Past Solar Influence on the Terrestrial Climate (FUPSOL) investigates the response of the Earth's climate to changes in solar spectral irradiance and ionisation by different energetic precipitating particles (EPP) from 1600 to 2100 using the AO-CCM SOCOL–MPIOM model.

The aim of this work is to elucidate the impact of changes in solar irradiance and energetic particles versus volcanic eruptions on tropospheric global climate during the Dalton Minimum (DM, 1780–1840 AD). Separate variations in the: (i) solar irradiance in the UV-C with wavelengths shorter than 250 nm, (ii) irradiance at wavelengths longer than 250 nm, (iii) in energetic particle spectrum, (iv) volcanic aerosol forcing were analysed separately, and (v) in combination, by means of small ensemble calculations. Global and hemispheric mean surface temperatures show a significant dependence on the solar irradiance for wavelengths longer than 250 nm. In addition, powerful volcanic eruptions in 1809, 1815, 1831 and 1835 significantly decreased the global mean temperature by up to 0.5 K for 2–3 years after each eruption. However, while the volcanic effect is clearly discernible in the Southern Hemisphere (SH) mean temperature, it is less significant in the Northern Hemisphere (NH), partly because: 1) the two largest volcanic eruptions occurred in the SH tropics, and during seasons when aerosols were mainly transported southward, and 2) partly because of the higher northern internal variability.

Figure 1 shows that in the simulation including all forcings, simulated temperature anomalies are in reasonable agreement with the tree-ring-based data for the NH. Interestingly, the model suggests that the changes in solar irradiance with wavelength shorter than 250 nm and energetic particles only have an insignificant impact on the climate during the Dalton Minimum. This downscales the importance of top-down processes relative to bottom-up processes. Reduction of the solar irradiance with wavelengths longer than 250 nm leads to a significant (up to 2 %) decrease of the ocean heat content (OHC) between depths of 0 and 300 m, whereas changes in shortwave solar irradiance or in energetic particles have virtually no effect. In addition, volcanic aerosol yields a very strong response, reducing the OHC of the upper ocean by up to 1.5 %. In the simulation with all forcings, the OHC of the uppermost levels recovers after 8-15 years after a volcanic eruption, while the solar signal and the different volcanic eruptions dominate the OHC changes in the deeper ocean and prevent its recovery during the DM.

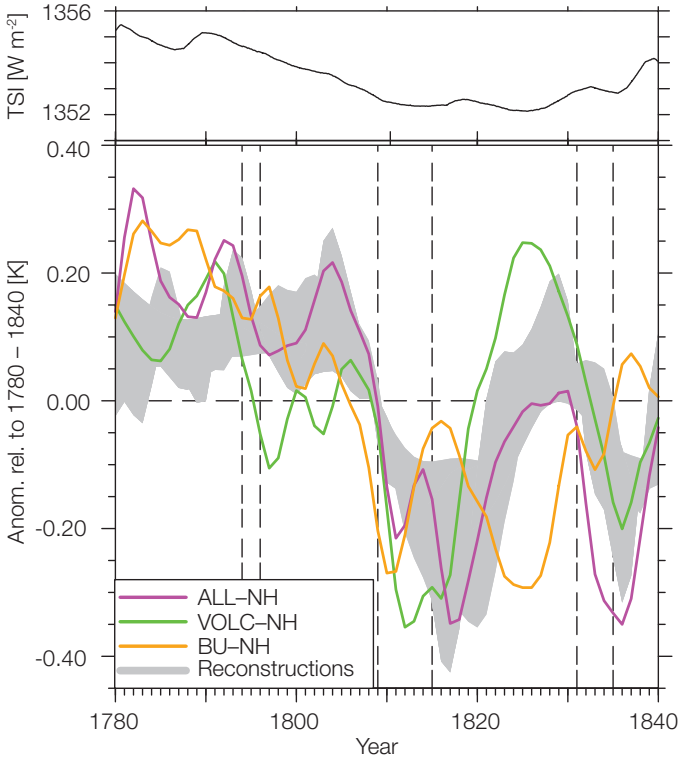

Figure 1. Top panel: Total solar irradiance from Shapiro et al. (2011). Lower panel: Model comparison with five NH temperature reconstructions from the IPCC AR4 (averaged). Magenta, green and orange lines are model curves, the grey envelope is the composite of a range of tree-ring-based reconstructions. Magenta thick: ensemble mean of NH temperatures (ALL-NH). Green: same, but for the VOLC experiment (VOLC-NH). Orange: same, but for the BU experiment (BU-NH). Vertical, dashed lines highlight the years, at which a volcanic eruption occurred.

Finally, the simulations suggest that the volcanic eruptions during the DM had a significant impact on the precipitation patterns caused by a widening of the Hadley cell and a shift of the intertropical convergence zone.

The results of this study are presented by Anet et al. (2013) in more detail.

References:

Anet, J., et al.: 2013, Impact of solar vs. volcanic activity variations on tropospheric temperatures and precipitation during the Dalton Minimum, Clim. Past Discuss., 9, 6179–6220.

Shapiro A.I., et al.: 2011, A new approach to the long-term reconstruction of the solar irradiance leads to large historical solar forcing, Astronomy and Astrophysics, 529, A67.

Development of the Sulphate Aerosol Module for CCM SOCOL

Eugene Rozanov in collaboration with J. Sheng and T. Peter, IAC ETH, Zurich

The SNF-supported IASSA project aims to study the behaviour of sulphate aerosol after proposed geo-engineering by injection of sulphur-containing gases. In the last phase of the project we completed the development of the coupled aerosol–CCM model (AER–SOCOL) and performed simulations of the atmospheric state after Mt. Pinatubo volcanic eruption. The simulation results were validated against observations and compared with other models.

The IASSA project aims to investigate the future climate and ozone evolution assuming different geo-engineering scenarios. For this project, we developed the coupled aerosol-chemistry-climate model SOCOL–AER which takes into account the main components of the climate system (atmosphere, clouds, land surface, ocean, sea ice, chemical species, and sulphate aerosol) and their interactions. For the treatment of sulphate aerosols, we introduced a size-dependent microphysical module and gas phase chemistry of the sulphur containing species. The model includes the emissions of SO_2 (anthropogenic, biomass burning, ships) and DMS, while the mixing ratio of OCS, CS_2 and H_2S are prescribed in the near-surface air in a manner similar to the AER 2–D model (Weisenstein et al., 1997). With the ACCM SOCOL–AER, we simulated the aerosol behavior for the background atmosphere and found good agreement with different observation data. The model was then applied to simulate the effects of the powerful eruption of Mt. Pinatubo in 1991, and to elucidate the role of different processes in the evolution of the sulphate aerosol layer.

The stratospheric aerosol burden from the reference case (REF) shown in Figure 1 is in reasonable agreement with the observed data. In the tropics, the aerosol burden reaches its maximum of 16 Tg H_2SO_4 / H_2O, which slightly exceeds satellite data but is still within its uncertainty range. The simulated tropical burden decay rate shows a deceleration after one year. The global aerosol burden peaks at 23 Tg and its decay rate is slightly faster than observed by HIRS, but agrees very well with the SAGE–II data.

The results of the sensitivity runs are also presented in Figure 1. In the absence of the QBO and radiation heating from aerosols (runs QBO/OFF, RAD/OFF and RQ/OFF) the aerosol burden is lower by 3–4 Tg with respect to the reference case which is mostly due to the aerosol deficit in the tropical stratosphere. It means that an additional initial sulphur mass injection into the stratosphere is required in order to match the observed maximum burden when the QBO and radiative heating are not properly included.

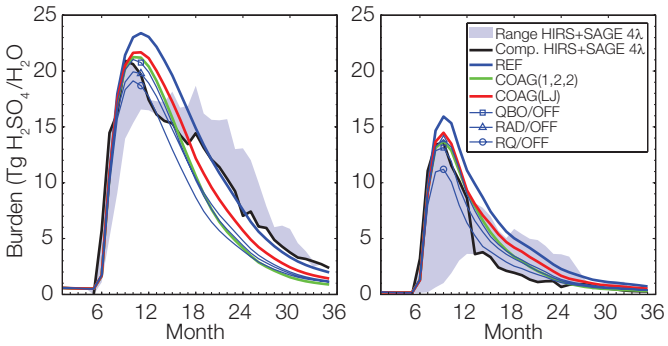

Figure 1. Evolution of the simulated global (left) and tropical (right) stratospheric sulphate aerosol burden (Tg H_2SO_4 / H_2O) compared to the composite of the available satellite data shown black line and shaded area.

The results of the simulations COAG(1,2,2) and COAG(LJ) show a more pronounced impact of the coagulation efficiency on the lifetime of volcanic aerosols. Particularly, in the tropical region COAG(1,2,2) (green curve, substantially faster coagulation rate) shows a noticeably accelerated decline in the sulphate aerosol burden in month 14 compared to COAG(LJ) (red curve, slightly faster coagulation rate) whose decay rate seems to be similar to the reference case. This is expected because the enhanced coagulation leads to a faster growth of particle size and thus more rapid sedimentation, while the reduced coagulation in the free molecular regimes tends to maintain the number density for the small particles and prevents their aggregation. The maximum global aerosol burden of COAG(1,2,2) and COAG(LJ) agrees well with the observations. However, the decay of their simulated aerosol burdens is slightly faster than in observations. This may be caused by a faster than observed meridional transport in the current CCM SOCOL v3.0 (Stenke et al., 2013) version which may lead to enhanced removal of aerosol in addition to sedimentation.

Overall, the newly developed model is able to successfully reproduce the main features of the sulphate aerosol distribution in the background and volcanic cases. The first experiments using geo-engineering scenarios are on-going.

References: Stenke A., Schraner M., Rozanov E., Egorova T., Luo B., Peter T.: 2013, The SOCOL version 3.0 chemistry-1 climate model: description, evaluation, and implications from an advanced transport algorithm, Geosci. Model Dev., 6, 1407–1427.

Weisenstein D.K., Yue G.K., Ko M.K., Sze N.D., Rodriguez J.M., Scott C.J.: 1997, A two-dimensional model of sulfur species and aerosols. J. Geophys. Res., 102, 13019.

Middle Atmosphere Heating Rate and Photolysis Response to the Uncertainties in Spectral Solar Irradiance Data

Timofei Sukhodolov, Eugene Rozanov, Alexander Shapiro

The uncertainties in the magnitude and spectral composition of the spectral solar irradiance (SSI) evolution during the declining phase of solar cycle 23 have substantial implications for the modelling of the middle atmosphere evolution, leading to pronounced differences in the heating-rates and also affecting photolysis rates. To estimate the role of SSI uncertainties we have compared the oxygen photolysis rates (JO_2) and heating rates calculated with the high-resolution radiation code libRadtran using SSI data-sets obtained from two models and SORCE observations.

The magnitude and spectral composition of changes in SSI can lead to a substantial alteration of heating-rates and also affect photolysis rates, resulting in significant ozone, temperature, and zonal wind responses in the stratosphere and mesosphere (Brasseur and Solomon, 2005). However, SSI observational and modelled data that are used by atmosphere models as input parameters for photolysis and heating-rate parameterizations are noticeably different from each other (Ermolli et al., 2013).

To evaluate the effect of the uncertainty of the available SSI data-

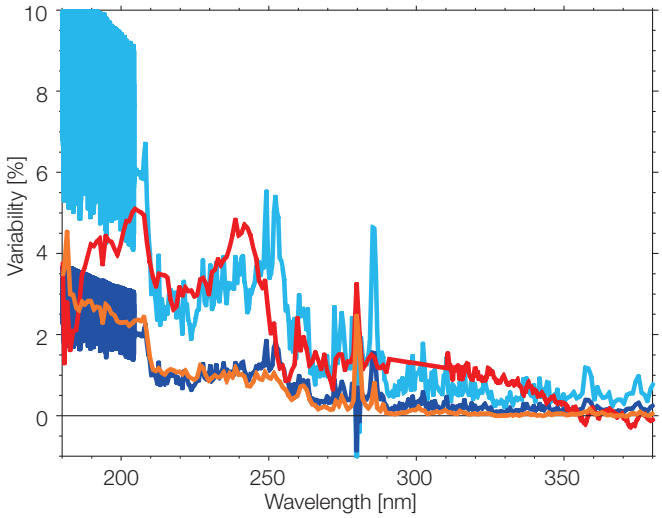

Figure 1. The relative difference (%) in SSI between June 2004 and February 2009 for NRL (orange), COSI (dark blue), SORCE (red) data-sets and the difference between solar maximum and minimum for the COSI full cycle (light blue).

sets, we performed calculations with SSI data for June 2004 and February 2009 (normalised to 1 AU) obtained from two models (NRL, COSI) and from SORCE observations. NRL and SORCE data-sets were chosen as representative of the lower and upper limits in the magnitude of UV SSI variability and COSI, as one of the closest reconstructions to SORCE (Ermolli et al., 2013). The chosen dates are limited by the availability of SORCE measurements, and reflect a difference of ~0.33 of the sunspot number difference between minimum and maximum (sunspot number = 40.5). In addition, we used the full cycle from COSI (sunspot

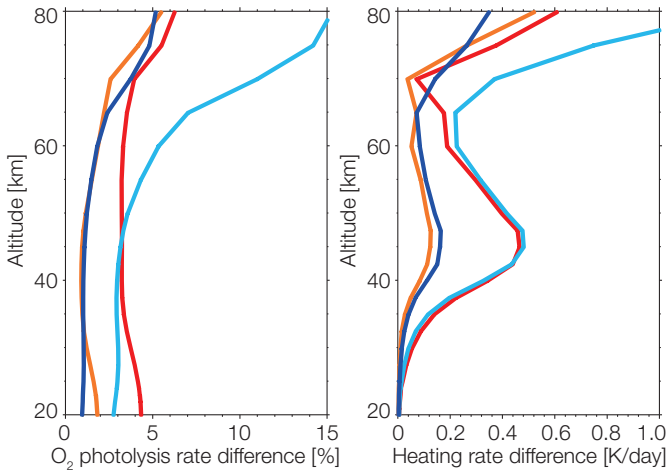

Figure 2. The relative difference (%) in JO_2 (left) and the difference (K/day) in the heating rates (right) between June 2004 and February 2009 for the SSI data-sets: NRL (orange), COSI (dark blue), SORCE (red) and the COSI full cycle (light blue).

number = 120) to give a rough overview of the potential of SORCE data for the full cycle. All calculations were performed for the tropical standard atmosphere model and a zenith angle equal of 10° using the high spectral resolution libRadtran code (Mayer and Kylling, 2005).

Figure 1 illustrates the relative SSI difference between the given dates for the 180–380 nm spectral range. The calculated differences in JO_2 and changes in heating-rate between different data-sets (Figure 2) are mostly defined by SSI variability in this spectral range and the Lyman-alpha line. Since the agreement between both model reconstructions is good, their results are also quite close to each other compared to SORCE, however, in the higher stratosphere NRL heating rates are ~25 % less compared to those for COSI. The response of the heating rates and JO_2 to SSI variability using SORCE data is approximately three times higher than for NRL and COSI in the entire stratosphere and at some altitudes is even higher than the solar signal calculated using the COSI full cycle. The observed differences imply noticeable consequences for modelling the atmosphere, and can influence not only the stratosphere-mesosphere region but also the surface response following the "top-down" mechanism.

References:

Brasseur G. P., Solomon S.: 2005, Aeronomy of the Middle Atmosphere, 658 pp., Springer, New York.

Ermolli I. et al.: 2013, Recent variability of the solar spectral irradiance and its impact on climate modelling, Atmos. Chem. Phys., 13, 3945–3977, doi:10.5194/acp-13-3945-2013.

Mayer B. and Kylling A.: 2005, Technical note: The libradtran software package for radiative transfer calculations – description and examples of use, Atmos. Chem. Phys., 5, 1855–1877, doi:10.5194/acp-5-1855-2005.

Solar Variability and Climate Change during the First Half of the 20th Century (SOVAC)

Tatiana Egorova, Eugene Rozanov, and Werner Schmutz in collaboration with the FUPSOL project team

In the SOVAC project we study the causes of observed climate warming during the first half of the 20th century. To address this question we have simulated the climate from 1880 to 1950 using different versions of the atmosphere-ocean-chemistry-climate model (AOCCM) SOCOL–MPIOM and compare the results with the observations and other models results.

The results of IPCC CMIP–5 experiments (Jones et al., 2013) confirmed that the multi-model mean is only able to reproduce just over 50 % of the observed global warming during the first half of the 20th century. This problem remains important and should be investigated given the noticeable recent progress in modelling and understanding of past solar irradiance variations.

We address this problem with a series of multi-year ensemble runs of the AOCCM SOCOL–MPIOM (Muthers et al., 2014) driven by all known anthropogenic and natural forcings taken in different combinations to elucidate the effects of anthropogenic factors as well as natural phenomena such as solar spectral irradiance, energetic particle precipitation and volcanic aerosol loading. We compare the simulated seasonal and geographical patterns of climate change against available observation data to establish the robustness of the model results. During the year, we collected and analysed several observational data-sets.

Figure 1 illustrates the geographical distribution of the surface air temperature trend during 1900–1940 obtained from the NCDC (National Climatic Data Centre) data-set. In agreement with the analysis of Brönnimann (2009) the warming is more pronounced over Northern Europe and the US.

We also compare our results with those of some other models, which participated in the CMIP–5 activity. These models have different sensitivity to greenhouse gases and volcanic aerosol, and exploited the solar irradiance changes with smaller magnitude in comparison to our model. Figure 2 illustrates the surface air warming (K) trend during 1900–1940 obtained from the NCDC data-set, and simulated with the AOCCM SOCOL–MPIOM and other models which participated in the CMIP–5 activity.

The presented results reveal that the increase of the surface air temperature from 1900 to 1940 simulated with AOCCM SOCOL–MPIOM is in good agreement with observations. Our model simulates a slightly more pronounced warming than in most other models. The interpretation of these results is in progress. We are considering several hypotheses including: 1) the application of larger irradiance changes than in CMIP–5, and 2) a significant increase in tropospheric ozone (see Muthers et al., 2014) simulated by our model as a result of anthropogenic activities. A re-evaluation of the obtained trends is also necessary because for some models (such as CESM1) the warming trend is caused by the overestimated cooling after volcanic eruptions at the beginning of the century.

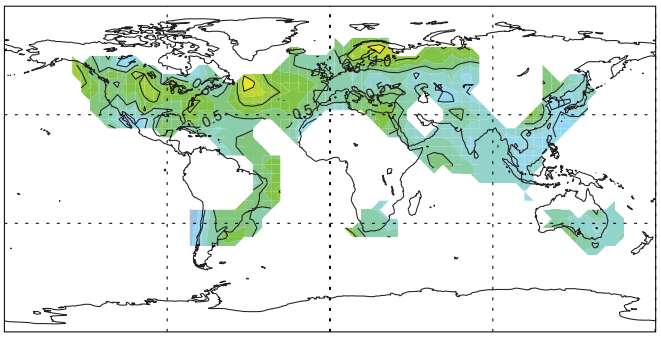

Figure 1. Surface air temperature warming (K) trend during 1900–1940 obtained with observations (NCDC data-set).

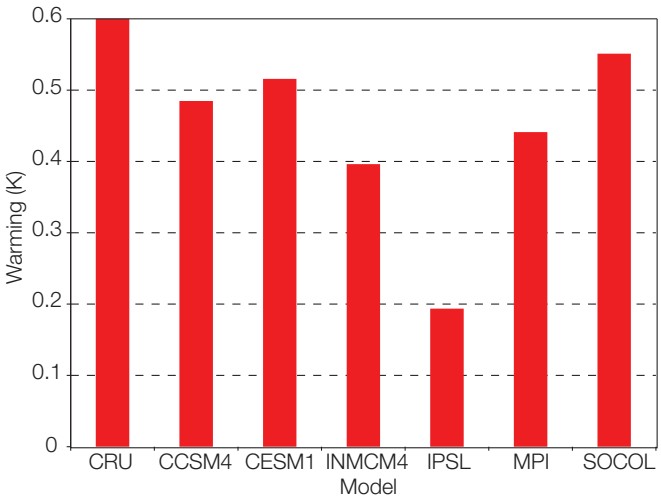

Figure 2. Surface air temperature increase (K) during 1900–1940 obtained with observations (NCDC data-set) and simulated with the AOCCM SOCOL–MPIOM and several other models, which participated in the CMIP–5 activity.

References:

Brönnimann S.: 2009, Early twentieth-century warming, Nature Geosci.,2, 735–736, doi :10.1038/ngeo670.

Jones G. et al.: 2013, Attribution of observed historical near-surface temperature variations to anthropogenic and natural causes using CMIP5 simulations, J. Geophys. Res., 118, 4001–4024.

Muthers S., et al.: 2014, The coupled atmosphere-chemistry-ocean model SOCOL–MPIOM, submitted to GMD.

Simulations of the Climate, Chemistry and Ozone in Support of the Chemistry-Climate Modelling Initiative CCMI

Eugene Rozanov, Timofei Sukhodolov in collaboration with IAC ETHZ

With the chemistry-climate model (CCM) SOCOL v3.0 we are participating in the SPARC Chemistry-Climate Modelling Initiative (CCMI). This project aims at the focused analysis of contemporary CCMs by their validation against observational data. It is planned to carry out a number of climate, chemistry and ozone simulations for the 1960–2100 period. The results of the experiments will be made available for analysis by international teams of experts. During 2013, we prepared the model version according to CCMI recommendations and began spin-up runs.

The SPARC CCMI activity (Eyring et al., 2013) was organised to provide necessary data for the future WMO Ozone depletion assessments. One of the CCMI requests was to simulate climate, chemistry and ozone trends in the recent past (1960–2012) and in the future (1960–2100) using prescribed natural and anthropogenic forcings such as: sea surface temperatures, sea ice concentrations, greenhouse gases, ozone destroying substances, emissions of carbon monoxide and reactive nitrogen oxides, solar spectral irradiance, geomagnetic Ap index, ionisation rates by solar protons, stratospheric sulphate aerosol loading, and the tropical quasi-biennial oscillation.

During 2013, we modified the basic version of CCM SOCOL v3.0 described by Stenke et al. (2013) to take into account the CCMI requirements by installing new modules for the treatment of tropospheric chemistry, solar heating rates, production of nitrogen and hydrogen radicals by particle ionisation or lightning, and by introducing completely new post processing procedures. After intensive testing the model was initialised to run spin-up simulations from 1950 to 1960.

To illustrate the model behavior during the 10-year long spin-up run we plotted the global mean HCl mixing ratio in the middle mesosphere around 1 hPa (60 km altitude). This quantity was chosen because it illustrates the convergence of the model to the quasi-equilibrium state which in the case of chlorine is far from the initial state. The decrease of the HCl mixing ratio in Figure 1 reflects the model adaptation to much lower anthropogenic chlorine loading during 1950–1960 compared to the model initialization fields.

Figure 2 illustrates the geographical distribution of the zonal mean total column ozone in March 1959. The improved version of CCM SOCOL reproduces the main features of the total ozone distribution very well. The first maximum is located near the Aleutian high where downward motion brings down ozone from the tropical stratosphere. Strong winter-time westerlies transport ozone and form the secondary maximum over Northern Canada. Full analyses of the obtained results will be conducted by the scientific community next year.

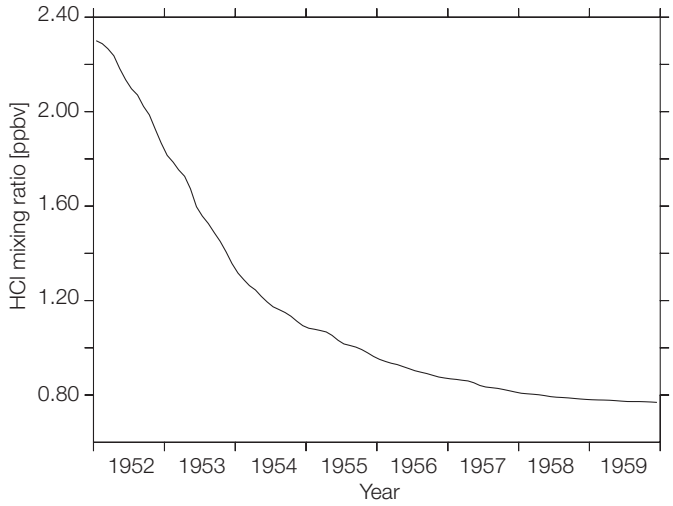

Figure. 1. Time evolution of the global mean HCl mixing ratio at 0.1 hPa.

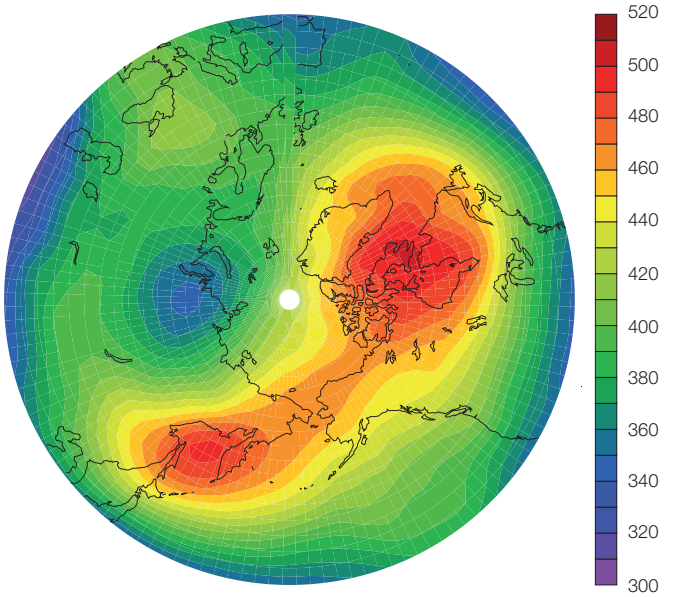

Figure 2. Geographical distribution of the total column ozone (DU) for March 1959.

References: Eyring V., et al.: 2013, Overview of IGAC/SPARC Chemistry-Climate Model Initiative (CCMI) Community Simulations in Support of Upcoming Ozone and Climate Assessments, SPARC newsletter, 40, 48-66.

Stenke A., et al.: 2013, The SOCOL version 3.0 chemistry-climate model: description, evaluation, and implications from an advanced transport algorithm, Geosci. Model Dev., 6, 1407–1427.

Radiation Measurements during the 2013 Charmex Campaign at Lampedusa, Italy

Julian Gröbner, Natalia Kouremeti, Stefan Wacker, Florian Henschel in collaboration with ENEA, Laboratory for Earth Observations and Analyses, Italy.

A comprehensive set of surface-based radiation measurements was performed at the ENEA station for Climate Observations "Roberto Sarao", Lampedusa, Italy, from June to September 2013, during the Chemistry-Aerosol Mediterranean Experiment (CHARMEX) Special Observation Period in order to quantify the direct aerosol radiative forcing for the short and longwave radiation components.

Radiation measurements conducted on Lampedusa are traceable to the reference standards of the World Radiation Centre at the PMOD/WRC, Davos, Switzerland. The aerosol optical depth (AOD) was measured simultaneously with an AERONET CIMEL sunphotometer and a MultiFilter Rotating Shadowband Radiometer (MFRSR). A precision spectroradiometer (PSR) measured the direct spectral solar irradiance from 320 nm to 1040 nm to retrieve the spectral AOD and integrated water vapor (IWV), while two Satlantic Hyperspectral Ocean Colour Radiometers (HyperOCR) measured global and diffuse spectral irradiance from 350 to 800 nm.

The quality of the measurements was assessed by comparing measurements between different radiometers belonging to PMOD/WRC and ENEA. A preliminary analysis showed that the ENEA and PMOD/WRC radiometers agreed to within ±2 Wm^{-2} for the longwave, and ±15 Wm^{-2} in the shortwave radiation. In the core measurement period between June and July, the radiometers were cleaned at least twice daily in order to remove sea-spray from the instrument domes, while daily cleaning was conducted during the rest of the period.

Several Saharan dust events were observed during the measurement period, of which three events were analysed with respect to a clear day with very low aerosol burden (17 June). Figure 1 shows the AOD diurnal variation on each of these three days. The direct longwave radiative effect of a Saharan dust outbreak is shown in Figure 2, where the net longwave irradiance increases by 50 Wm^{-2} during the day as the optical depth of the Saharan dust event increases. The effect of aerosols on longwave irradiance was quantified by using a pyrgeometer which was only sensitive in the 8–14 μm wavelength range. As can be seen in Figure 3, the longwave irradiance correlates with the observed AOD, yielding a radiative forcing effect of 90 Wm^{-2} per unit AOD.

Conclusions: Saharan dust intrusions significantly enhance the downwelling and net longwave radiation, while the shortwave radiation is attenuated. The 24–averaged net radiation budget (shortwave and longwave) increases during Saharan dust events with respect to clean reference conditions. The Saharan dust events produce a significant increase in the net longwave irradiance with respect to clean reference conditions. The 24-hour averaged net radiation budget increased from 11 to 17 Wm^{-2} in the presence of Saharan dust aerosols. The net energy deposition over 24 hours increased from 13 to 19 %.

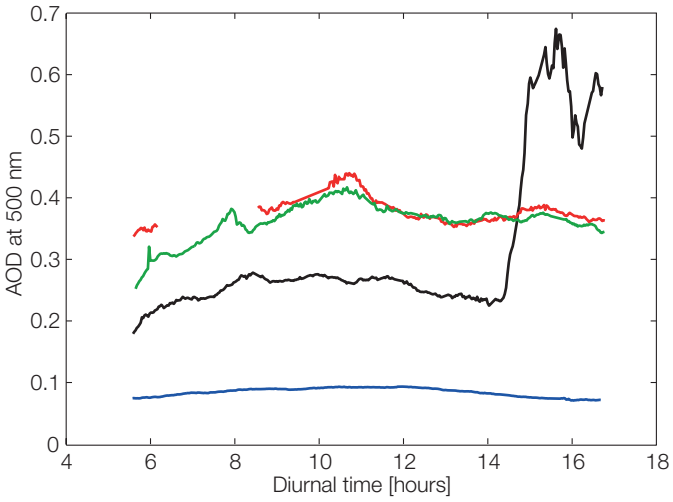

Figure 1. Aerosol optical depth at 500 nm on 9 June (black), 17 June (blue), 22 June (red) and 2 July (green).

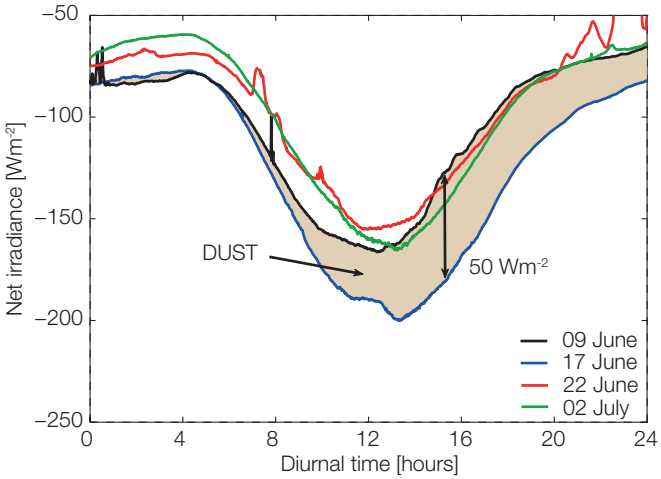

Figure 2. The net longwave irradiance is enhanced by up to 50 Wm^{-2} on 9 June in the presence of dust aerosols with respect to the clear reference day.

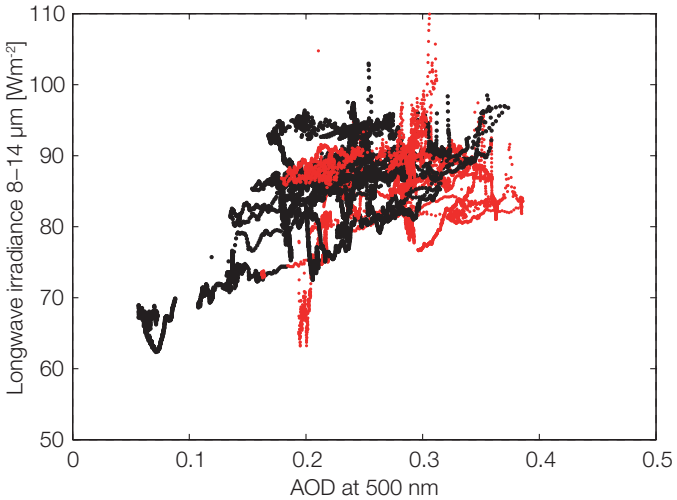

Figure 3. The longwave irradiance in the atmospheric window (8–14 μm), with respect to AOD. The black and red dots are for an Ångström exponent alpha larger and smaller than 1, respectively.

UV Exposure, Vitamin D and Their Relationship in a Group of Highschool Students in Davos

Julian Gröbner, Matthias Gröbner (Schweizerische Alpine Mittelschule Davos), and Gregor Hülsen

The relationship between UV exposure and vitamin D status was investigated in a group of seven high-school students from Davos, Switzerland. The personal UV exposure was recorded with electronic dosimeters between March and August 2013, while blood samples were taken at monthly intervals to determine their 25(OH)D3 concentration.

Study design: It is well known that the body's primary source of vitamin D results from cutaneous exposure to sunlight. Seven male students of similar age from the Schweizerische Alpine Mittelschule Davos (1590 m asl), recorded their personal UV exposure using electronic dosimeters and had blood samples taken at monthly intervals to determine their 25(OH)D3 concentration.

UV dosimetry: Personal UV exposure was measured by using state-of-the-art electronic UV dosimeters (Sherman, 2010). Throughout the study the dosimeters sampled UV irradiance from 7 am to 10 pm in 5 second intervals. With these settings, the daily number of gathered UV data points per participant exceeded 10,000, i.e. the whole study consists of over 10 million UV data points. Previous studies have shown that the wrist is a representative site for UV body monitoring (Knuschke et al. 2007). On these grounds participants wore their dosimeters like wristwatches on their wrist whenever they were outside.

Vitamin D: 7 blood samples were taken at monthly intervals starting in March. The blood samples taken at the Hochgebirgsklinik of Davos were assayed at the Labormedizinisches Institut Dr Risch (LI) using ultra-high-performance liquid chromatography (UHPLC) and vitamin D status was reported in terms of the serum concentration of 25(OH)D3 (CV 10 %).

Results: During schooldays the students gathered just a small fraction of the available ambient UV radiation. As solar UV radiation is absent inside buildings, they were mainly exposed to radiation on their way to and from school (see Figure 1). On average, the school UV exposure represented only 1.7 % of the ambient UV dose with a variability during the study period of ±2.4 % across all pupils. As expected, this fraction slightly increased in summer and with higher ambient temperatures. On the other hand, more than 85 % of the UV exposure was acquired outside normal school days. Personal UV exposure increased significantly during the holidays. Depending on the student's activity, the total UV dose over the study period varied from 93 to 370 SED (Standard Erythemal Dose).

Throughout the study, the average vitamin D insufficiency from the beginning of March (11.6 ng ml^{-1} 25(OH)D3) increased to a sufficient vitamin D supply of 42.4 ng ml^{-1} 25(OH)D3 in mid-August. The largest increase in vitamin D occurred during the spring and summer holidays, where the status increased on average by 68 %. For half of the students vitamin D levels declined again by an average of 34 % between spring and summer due to reduced UV exposure during school (see Figure 2).

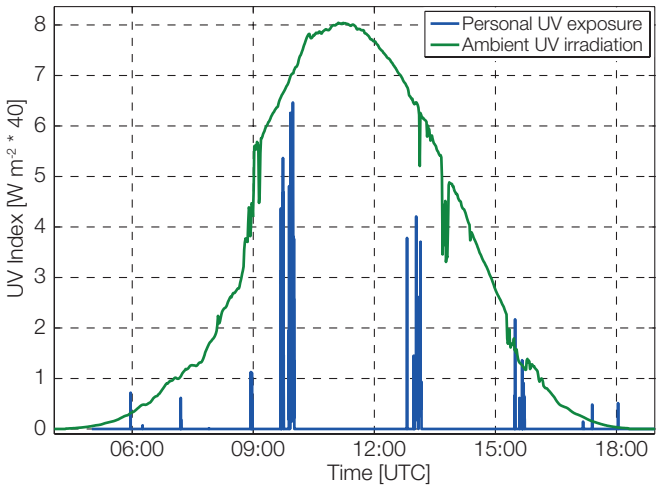

Figure 1. An example of a typical UV exposure profile during a school day (blue line) on 23 April 2013. The daily personal UV exposure is 50 J m^{-2}, which represents 1.25% of the ambient UV dose (green line).

Conclusions: The UV exposure and vitamin D status of a group of seven high-school students in Davos were monitored from March to August 2013. During the study period, the vitamin D status increased significantly, from initially insufficient concentrations to a sufficient level of more than 40 ng ml^{-1}. The average observed 25(OH)D3 concentration increase was 0.36 ± 0.24 ng ml^{-1} per 100 J m^{-2} of vitamin D weighted UV exposure.

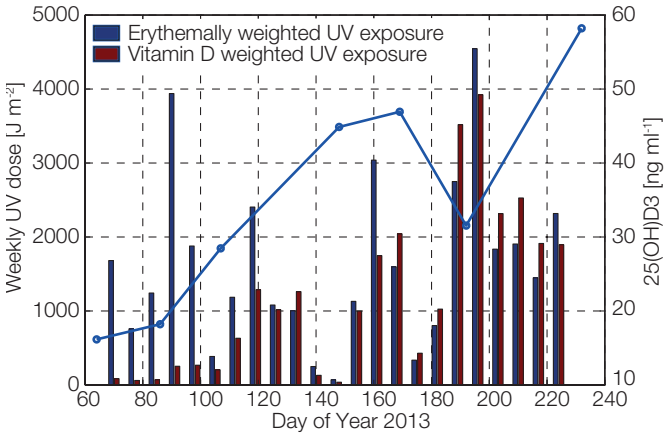

Figure 2. Summary of one student's weekly averaged UV exposure (blue bar, erythemally weighted, and red bar, vitamin D weighted) for the study period. The blue line represents the 25(OH)D3 concentration. Note that the vitamin D weighted UV exposure was corrected for skin area and sunscreen factor.

References: Sherman D: 2010, Personal UV dosimeter badges: Mark II. NIWA UV Workshop, Queenstown.

Knuschke P., Unverricht I., Ott G., Janssen M. : 2007, Personenbezogene Messungen der UV-Exposition von Arbeitnehmern im Freien, Bundesamt für Arbeitsschutz und Arbeitsmedizin.

The GAW-PFR Aerosol Optical Depth Network: 2008–2014 Time-Series at Cape Point Observatory, South Africa

Stephan Nyeki, Christoph Wehrli, Natalia Kouremeti, Julian Gröbner in collaboration with the South African Weather Service, Stellenbosch, South Africa

Measurements of aerosol optical depth (AOD) in the GAW-PFR network are conducted at a number of representive background sites located around the globe. This study reports the 2008–2014 AOD time-series at Cape Point, South Africa, for the first time.

As one of the World Meteorological Organisation's (WMO) Global Atmosphere Watch (GAW) background stations, Cape Point (CPT; 34°21' S, 18°29' E, 230 m asl; South Africa) has a unique mid-latitude location to monitor the remote marine environment in the southern hemisphere. In order to augment the monitoring program, in-situ and remote aerosol measurements began in 2007–2008, including the aerosol optical depth (AOD). Long-term ground-based AOD measurements are rare in southern Africa which is not surprising considering the size of this region. Only two time-series longer than 5 years exist to date: at Mongu (15°15' S, 23°09' E, 1107 m; Zambia) and at Skukuza (24°59' S, 31°35' E, 150 m; South Africa). Both sites are part of the AERONET sun-photometer network, and began operation in June 1995 and July 1998, respectively.

Measurements were conducted with a Precision Filter Radiometer (PFR). GAW-PFR algorithms (e.g. Nyeki et al., 2012) were used for the determination of AOD. The combined uncertainty related to instruments and retrieval algorithms was estimated to result in an AOD uncertainty <0.010 at λ = 500 nm. A graph of the 2008–2014 CPT AOD time-series (λ = 500 nm) shown in Figure 1 is rather notable for its apparent lack of any seasonal features. Continental sites usually have a clear annual cycle with a maximum in summer and minimum in winter, as recently reported for several GAW-PFR sites in central Europe (Nyeki et al., 2012). This contrasts the AOD cycle at the GAW-PFR Mace Head station in Ireland which is strongly influenced by the prevailing westerlies, advecting air-masses from the North Atlantic. Similar conditions occur at CPT where winter months (June–August) are characterised by either deep frontal systems from the South Atlantic or by occasional local inversions. In contrast, summer (December–February) months are characterised by strong SE to SW winds which bring clean marine air-masses from the South Atlantic and the Southern Ocean.

Along with back-trajectory analysis, another powerful tool to characterise the origin of air-masses is the use of radon-222 (half-life 3.824 days). It is produced by the radioactive decay of radium-226, and primarily emanates over continental regions where the flux is more than 2 to 3 magnitudes greater than over oceanic regions. It may thus be considered as an unambiguous indicator of air-masses which have had recent contact with large continental regions. According to thresholds defined by Brunke et al. (2004), air-masses can be classified into marine (radon-222 concentration <350 mBq m^{-3}), mixed (350–1200) or continental (>1200) types. Figure 2 illustrates a preliminary analysis of AOD versus radon-222 concentration. Radon-222 appears to cluster at concentrations <700 mBq m^{-3} indicating that air-masses during sun-photometer measurements are mainly of marine or mixed

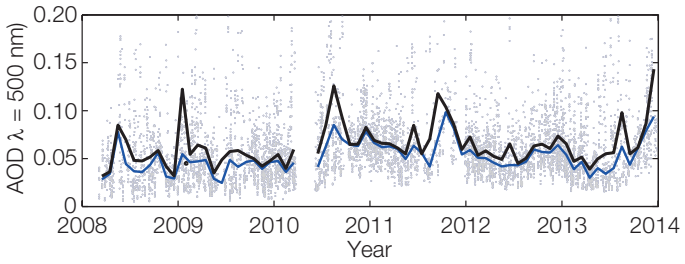

Figure 1. Aerosol optical depth 2008–2014 time-series at the GAW-PFR Cape Point station, near Cape Town, South Africa. Lines illustrate the 1-month average (black) and median (blue) values, while grey circles are 1-hr values.

origin with AOD < 0.1. There appears to be some evidence that air-masses of continental origin are not necessarily associated with elevated AOD (circled area on left in Figure 1). On the other hand, marine air-masses are frequently characterised by AOD up to about 0.15 (circled area on right). Elevated values most probably indicate the presence of high sea-salt aerosol concentrations in the marine boundary layer, generated by sea-spray and bubble-bursting mechanisms. A more in-depth analysis along with other parameters is currently ongoing.

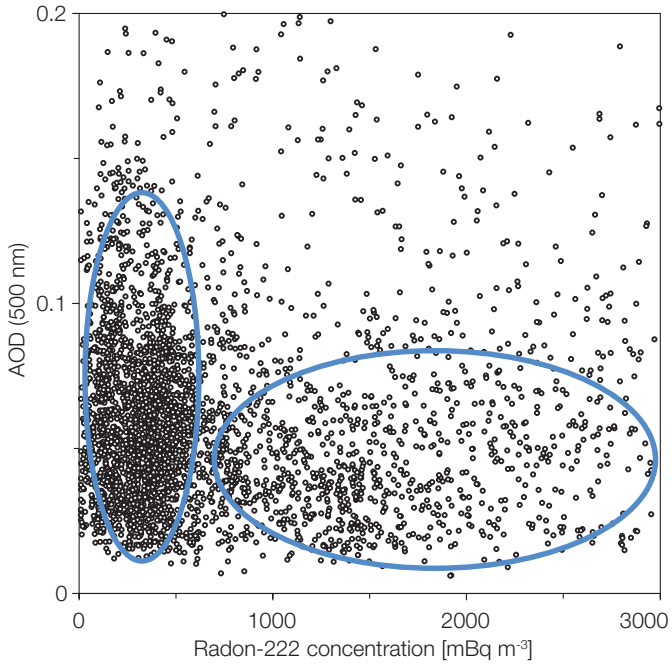

Figure 2. Aerosol optical depth versus radon-222 concentration. See text for a description of the circled areas.

References: Brunke E-G. et al.: 2004, Baseline air mass selection at Cape Point, South Africa: Application of ^{222}Rn and other filter criteria to CO_2. Atmos. Environ. 38, 5693-5702.

Nyeki S. et al.: 2012, Ground-based aerosol optical depth trends at three high-altitude sites in Switzerland and southern Germany from 1995 to 2010, J. Geophys. Res., 117, D18202, doi:10.1029/2012JD017493.

UV Aerosol Optical Depth Retrieved by UVPFR and CIMEL Sunphotometers and a Brewer Spectrophotometer

Natalia Kouremeti, Julian Gröbner, Christoph Wehrli in collaboration with AEMET

AOD measurements using a UVPFR, Brewer spectrophotometer and CIMEL–AERONET sunphotometer were compared and shown to be within ±0.02 at wavelengths between 310 and 332 nm. The results of this comparison shows that the UVPFR provides reliable AOD measurements at three channels between 311 and 332 nm, opening the possibility of using this instrument as a travel standard for in-situ calibrations of AOD for Brewer spectrophotometers which is a stated goal of the COST Action ES1207 EUBREWNET.

The common data-set of AOD measurements from three independently calibrated instruments was retrieved during a 3-month campaign in 2008 at the Observatory of Izaña, Tenerife, Canary Islands. The Brewer spectrophotometer used is, a MKIII Brewer (#185), and is the traveling standard of the Regional Brewer Calibration Centre for RA-VI Region (Europe) (RBCC-E). The AOD is determined from standard ozone procedures using solar irradiance measurements at 303.2, 306.3, 310.0, 313.5, and 320.0 nm, and by applying an appropriate calibration and retrieval procedure. The UVPFR #002, is one of a series of four sunphotometers developed at PMOD/WRC, and has four channels at 305, 311, 317 and 332 nm whose spectral response has been measured for one of the instruments of the series (Figure 1). The collocated CIMEL sunphotometer which is part of AERONET has been used as a reference, using AOD at 340 nm and the Angstrom exponent in the 340–440 nm range (Level 2) to extrapolate AOD values to the UVPFR and Brewer #185 wavelengths.

In the UVPFR, two interference filters with a bandpass of less than 2 nm each are placed on top of each other to achieve a stray light rejection of better than 10^{-6}. Nevertheless, as shown in Figure 1 some radiation leakage at longer wavelengths was observed in the relative spectral response of all four channels as measured in the laboratory. Even though this leakage is more than four orders of magnitude less than the maximum, it has significant effects on the measurements, since the solar irradiance decreases by several orders of magnitude between 300 and 320 nm. We determined the contribution of this out-of-range stray light to the AOD retrievals at the four wavelengths using radiative transfer calculations (LibRadTran) for different atmospheric conditions covering ozone values from 250 to 450 DU, AOD from 0 to 1.4 (at 440 nm) and Angstrom alpha exponents from 0.2 to 2.2. The stray light contribution ranges from 0.2 to 1 % at 332 nm, 0.4 to 4 % at 317 nm, 1 to 8 % at 311 nm and 2 to 50 % at 305 nm, for SZA between 10 and 65°. Based on the uncertainties introduced by using radiative transfer calculations instead of measured information, we decided to apply this correction only to the lower two channels, ie. 305 and 311 nm.

In total, 5715 points were compared resulting in a correlation coefficient better than 0.99 at 317 and 332 nm, and 0.98 and 0.97 at 311 and 305 nm, respectively (Figure 2). The AOD difference as a function of airmass reveals a fairly strong dependency for the 305 nm channel leading to the conclusion that the applied stay

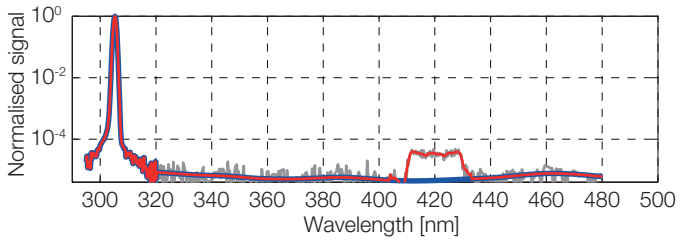

Figure 1. Relative spectral responsivity of UVPFR#004 at 305 nm. The grey line represents the measurement, the red the smoothed function used in the analysis and the blue the "ideal" transmittance without leakage. The transmittance function of the other three channels is similar to that shown here.

light correction is overestimated. The same, to a lesser extent, also applies to the 311 nm channel. Between 60 and 86 % of measurements from both instruments are within the WMO criterion of ± (0.005 + 0.010/airmass) for wavelengths between 311 and 332 nm, while the lowest channel at 305 nm shows significant discrepancies which precludes its use for reliable AOD and ozone determination. A similar comparison of Brewer #185 with respect to the extrapolated CIMEL values gave a correlation coefficient of 0.95 at 320 and 317 nm, and 0.94 and 0.91 for 310 and 306 nm, respectively, with a bias offset of less than 0.01 in AOD. This comparison revealed an agreement of ±0.02 in AOD between the 3 instruments and opens the possibility of using the UVPFR as a travel standard for in-situ AOD calibration transfer of Brewer spectrophotometers.

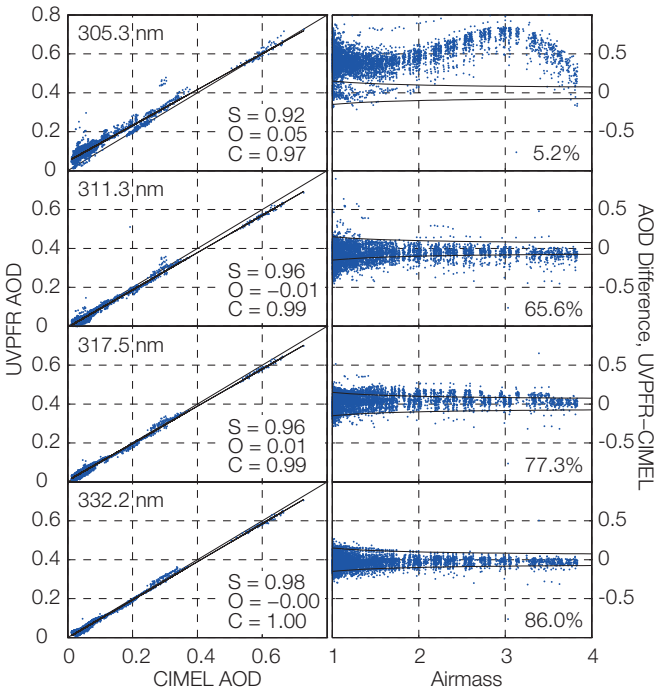

Figure 2. Comparison of AOD between UVPFR and CIMEL (first row) and AOD difference as a function of airmass (second row). The red lines represent the WMO traceability criterion. S = slope, O = offset, C = correlation coefficient.

Lunar AOD in the Arctic

Christoph Wehrli, Natalia Kouremeti, and Diego Wasser

We have modified a PFR instrument for AOD observations using the Moon for use during the Polar night in the Arctic. A joint project of one US and five European institutions under the lead of NILU was proposed to the Svalbard Science Forum (SSF). After successful tests at Davos, the Moon-PFR was deployed for initial measurements at Ny Ålesund in February 2014.

A PFR instrument has been in operation at Ny Ålesund (78.9°N), Spitzbergen since 2005 as a station of the GAW-PFR network. Situated above the Polar circle, the measurement season only lasts from mid-March to mid-September. Lunar photometry can substitute solar photometry during the polar night in order to partly fill in the 6-month gap in AOD climatology, and to further understanding the onset of the Arctic haze season.

Scientists from six institutions: NILU (Norway), ISAC/CNR (Italy), AWI (Germany), PMOD/WRC (Switzerland), NOAA/ CIRES (US), and IGF/PAS (Poland) are collaborating in coordinated aerosol observations by active and passive remote sensing on Spitzbergen and are aiming to establish Svalbard as a key satellite validation site.

A joint project, under the lead of NILU, was thus proposed to the SSF in 2013. The research proposal covering 24 months was accepted in January 2014.

The contribution of PMOD/WRC to the project is mostly instrumental by providing a PFR instrument suitable for lunar measurements.

A lunar ephemeris algorithm was developed to remotely control one of our solar trackers during the night.

Figure 1. Full Moon over Ny Ålesund in February 2014. (Picture courtesy of Mauro Mazzola, ISAC/CNR).

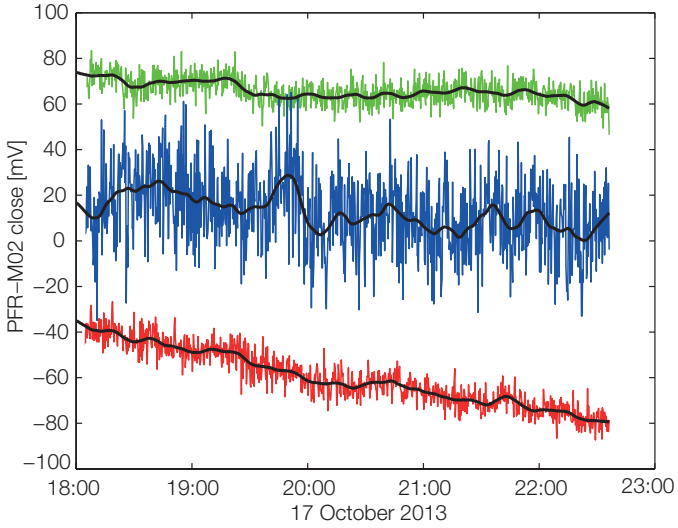

Figure 2. Test measurements with Moon PFR illustrating noise and dark signal drift.

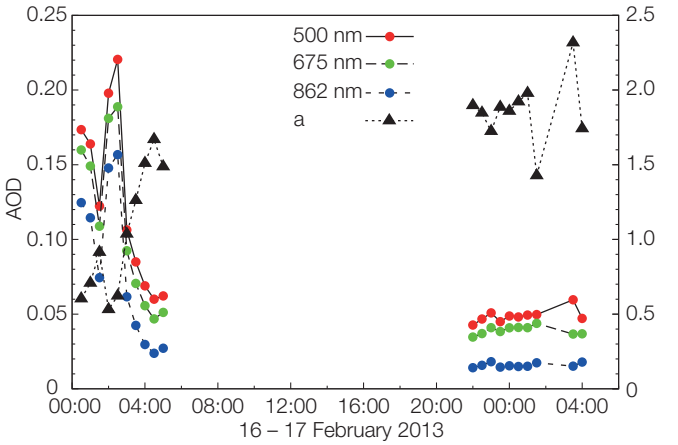

Figure 3. First AOD measurements using the Lunar PFR at Ny Ålesund.

While the solar irradiance changes slowly over the course of a year, lunar irradiance may change during a given observation night. Project partners at ISAC have successfully implemented a semi-empirical model (Kiefer and Stone, 2005) to calculate the instantaneous lunar irradiance.

After a series of tests at Davos, the Moon-PFR was deployed at Ny Ålesund in February 2014 where it took a number of measurements. Weather conditions were rather cloudy (see Figure 1), but a proof-of-concept was nevertheless established. The instrument was returned to Davos for further improvement of the S/N ratio.

References: Kiefer H. H., Stone T. C.: 2005, The spectral irradiance of the Moon, Astron. Journal, 129, 2887–2901.

Effective Solar UV Albedo to Monitor Snow Covered Area during Snow Melt

Luca Egli, Julian Gröbner and Gregor Hülsen in collaboration with WSL- Institute for Snow and Avalanche Research SLF, Institute of Geography University of Bern and Oeschger Centre for Climate Change Research Bern

We present a new radiation based remote sensing technique to monitor the seasonal course of snow covered area around the Davos region by measuring global solar UV radiation at PMOD/WRC. The method does not require a line-of-sight to the observed snow-covered regions, which makes it well suited to monitor integral snow-cover properties on complex mountainous terrain.

In snow climatology, past and future snow availability is investigated by estimating the total volume of snow in snow dominated mountainous areas (Marty, 2008). Monitoring of the temporal evolution of the snow-covered area (SCA) during the melt season and the use of snow-melt models allows the total volume of snow at the winter snow maximum for an entire area to be reconstructed.

From solar UV science it is known that global solar UV radiation in the 315–400 nm spectral range is affected by the surrounding terrain, in particular by the reflectance on snow due to multiple backscattering. The radius of the influence of the surrounding terrain is estimated to be in the 5–40 km range, which roughly corresponds to the dimensions of a snow micro-climatological region in the Swiss Alps. Figure 1 illustrates the backscattering of UV radiation of snow and snow-free areas reaching the Brewer double monochromator.

Figure 1. Illustration of solar UV snow and atmospheric backscattering on snow-covered areas reaching the dome of the Brewer double monochromator located on the PMOD/WRC observatory roof.

The reflectance of the surrounding terrain can be quantified in terms of effective albedo, which is an input parameter for the radiative transfer model LibRadtran (Mayer and Kylling, 2005). By comparing the model results with global solar UV measurements provided by the Brewer double monochromator in the 320–360 nm wavelength range an estimate of the effective solar UV albedo is derived. Figure 2 (red points) shows the temporal evolution of the effective albedo during the snow-melt season in 2009. In addition, the temporal development of the fractional SCA (Figure 2, blue stars) during this season at the Wannengrat catchment near Davos is displayed (Egli et al. 2012). A catchment area of about 1 km^2 was observed using a terrestrial laser scanner. Evidently, this curve does not agree with the observed albedo at PMOD/WRC. Since the radius of albedo observations covers a much larger snow-free area than the observed area at

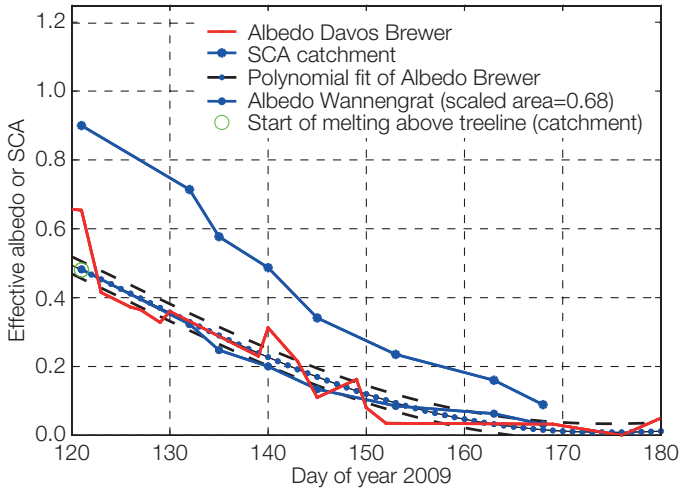

Figure 2. Albedo observations at PMOD/WRC (red points) show good agreement with scaled snow-covered area (blue points) from the Wannengrat catchment near Davos.

Wannengrat, the Wannengrat-SCA was scaled by an additional snow-free dimensionless area of A = 0.68 at the beginning of melt season (Figure 2, green circle.)

After this scaling, the SCA-Wannengrat values (Figure 2, blue points) agree well with the polynomial fit of the observed effective albedo (Figure 2, black points). Similar good agreement was found for the 2008 melt season. Applying a simple snow-model in Monte-Carlo based simulations and the use of albedo observations at PMOD/WRC, the total snow volume in the Wannengrat catchment area at the winter maximum before the start of melt was reconstructed. The results for the 2008 and 2009 seasons revealed that the total snow volume can be reconstructed backwards with an uncertainty of <10 %, which is validated by using spatial high-resolution snow-depth measurements obtained with terrestrial laser scanner measurements at Wannengrat (Egli et al., 2012).

We conclude that global solar UV measurements constitute an alternative approach to monitoring integral snow-cover characteristics such as fractional snow covered area which can be applied to reconstruct the total volume of snow for snow climatological investigations. Moreover, effective solar UV albedo may be applied to monitor available snow water resources in Alpine watersheds.

References:

Egli L., Jonas T., Grünewald T., Schirmer M., Burlando P.: 2012, Hydrological Processes, 26, 1574–1585, doi: 10.1002/hyp.8244.

Mayer B., Kylling A.: 2005, Atmos. Chem. Phys., 5, 1855-1877.

Marty C.: 2008. Geophys. Res. Lett., 35, 280L12501, doi:10.1029/208GL033998.

SOLID – First European Comprehensive Solar Irradiance Data Exploitation – Technical and Scientific Management

Margit Haberreiter and Werner Schmutz in collaboration with the SOLID consortium

The SOLID Project started in December 2012. All "Tasks and Deliverables" were accomplished in the first year. Here, we summarise key activities of the Technical and Scientific Management for which PMOD/WRC as Coordinator is responsible.

SOLID Kick-off Meeting: The SOLID Kick-off Meeting was held on 12 – 14 February, 2013 at PMOD/WRC in Davos, Switzerland. The meeting was attended by representatives from all project partners.

SOLID Annual Meeting: The First Annual Meeting of the SOLID consortium was held on 15 – 18, October, 2013 at LPC2E in Orléans, France. All project partners were represented by one or more representatives. Furthermore, two members of the Advisory Board, Prof. Farzad Kamalabadi, and Dr. Matt DeLand, also attended the meeting and were actively involved.

Review of Periodic Report: The successful SOLID review meeting was held on 5 December, 2013 in Brussels (Figure 1), and the first SOLID Reporting Period was reviewed and approved.

Figure 1. Attendees of the First Annual Meeting of SOLID: (from left to right, Gerard Thuillier, Farzad Kamalabadi, Klairie Tourpali, Stergios Misios, Yvonne Unruh, Véronique Delouille, Mark Weber, Jean-François Hochedez, Marty Snow, Alain Hochecorne, Giulio Del Zanna, Christian Erhardt, Matt Deland, Laure Levefre, Gaël Cessateur, Maira Dasi-Espuig, Rami Qahwaji, Benjamin Mampeay, Christophe Marqué, Wissam Chehade, Matthieu Kretzschmar, Margit Haberreiter, Thierry Dudok de Wit (not in the picture).

SOLID Webpage and Database: The SOLID webpage and database were developed in the first year, and is accessible through the following links: 1) Webpage: http://projects.pmodwrc.ch/solid, 2) Database:http://projects.pmodwrc.ch/solid-visualization/makeover/. Four different categories of data-sets are currently being implemented. The solar spectral irradiance (SSI) data-sets that can be displayed as a function of time (for a specific spectral range) or as a function of wavelength (for a given point in time). Moreover, reference spectra can also be visualised. Finally, the proxy data-set can also be plotted. All the data-set in the database can be overplotted and also downloaded, if required. An example of an irradiance time-series is shown in the middle panel of Figure 2. Furthermore, the web-based tool also allows us to display segmentation maps that are closest to a point in time selected in the time-series.

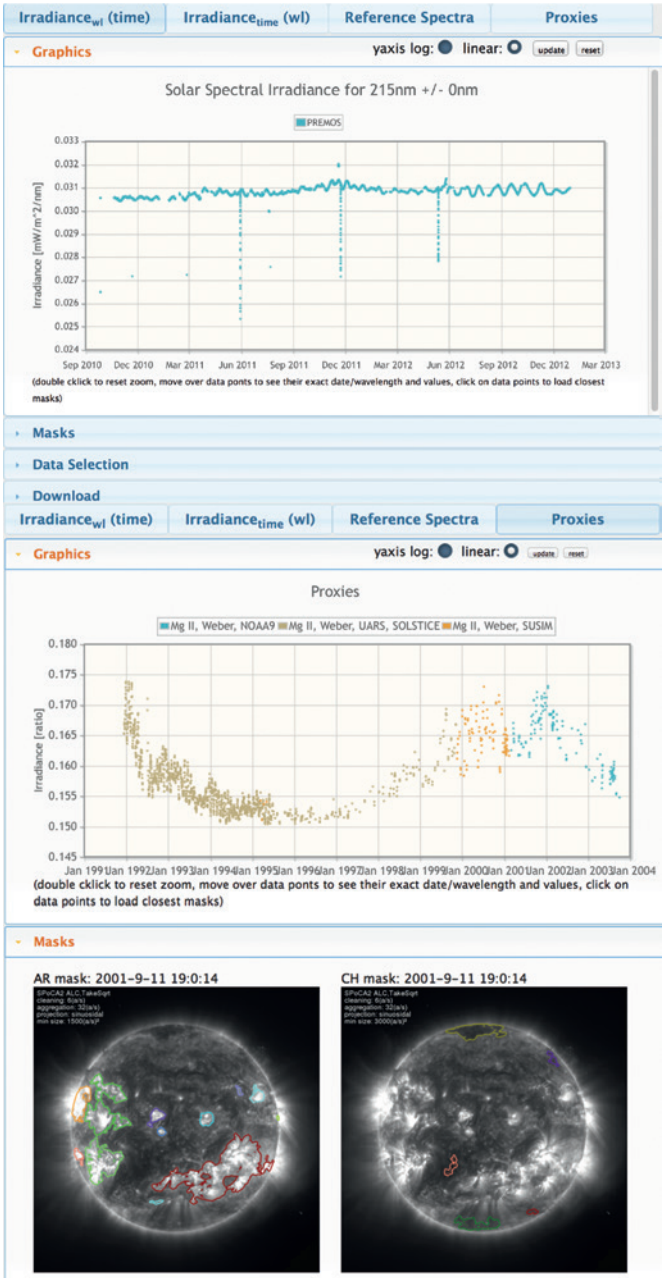

Figure 2. Web-based visualisation tool on the SOLID homepage showing the PREMOS irradiance time-series (upper panel) and several Mg II proxy time-series (middle panel). The SOLID Database also allows segmentation maps to be visualised (lower panel) for a particular point in time chosen interactively from the selected time-series.

Upcoming Activities: A SOLID Error Analysis Workshop will be held at the beginning of April at Imperial College, London. This will be an important meeting in order to discuss and establish consistent error estimates when analysing the solar irradiance time-series.

Acknowledgement: Funding from EC FP7 2012 under grant agreement No. 313188 (SOLID) has been gratefully received.

Modelling of the Spectral Solar Irradiance with COCOSIS

Gaël Cessateur, Alexander Shapiro, Werner Schmutz in collaboration with MPI, Lindau, Germany

We present a new kind of irradiance model, the Combination of COSI Spectra (COCOSIS), and directly compare it with measurements from the PICARD/PREMOS radiometer. We employ the COSI radiative transfer code convolved with solar disk area with different magnetic features as deduced from SDO/HMI data.

Calculation of the synthetic profile of the solar spectral irradiance will be focussed on. We follow here a well-developed approach based on the principle that the solar spectrum is a linear superposition of reference spectra that originate in different regions of the solar disk, i.e. the quiet Sun and different active features.

We employ here a 5-component model which separately treats the contribution from the quiet Sun, sunspots (umbra and penumbra), and active network and plage regions. The solar disk was divided into 100 concentric rings over different heliocentric angles.

Network regions and faculae, as well as sunspots were identified in daily HMI data (Yeo et al., 2013). A generic spectra associated with each magnetic structure is then obtained with the COSI model (Shapiro et al., 2010). COCOSIS then reproduces the spectral solar irradiance variability for every wavelength from the UV to the infrared part of the solar spectrum.

In the following comparative analysis of PREMOS and COCOSIS, we present irradiacne curves at 215 nm and 607 nm over the three years of the PICARD mission. Figure 1 displays the irradiance at 215 nm as seen by PREMOS and modelled with COCOSIS. The relative difference in absolute values does not exceed 1 % over three years, which is quite remarkable compared to the intrinsic variability of the solar signal at this wavelength (more than 10 % over three years).

The absolute contributions to the solar irradiance also reveal that the faculae and the network regions are responsible for 2 % and 7.5 %, respectively, while penumbrae and umbrae regions do not participate respectively more than 0.06 % and 80 ppm to the solar variability. These results then justify that filling factors from umbra and penumbra are not required to reconstruct the UV part of the solar spectrum.

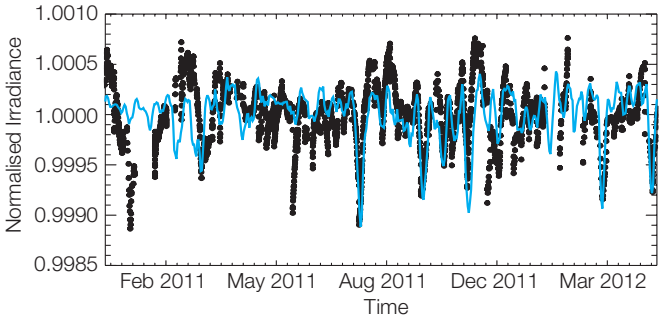

Figure 1. Irradiance at 607 nm from PREMOS observations (black dots) and the COCOSIS model (red line) over 18 months.

A similar reconstruction was conducted for irradiance at 607 nm as shown in Figure 2. The intrinsic variability of the solar irradiance is less than 0.1 % over 18 months at this wavelength. The variability, modulated by solar rotation, is clearly visible for both curves, especially the appearance of a large sunspot in July 2011. By closely examining the different contributions to the overall variability, we have found that the faculae do play an important role even for rotational modulation. For example, the presence of large faculae close to December 2011 explains the sudden increase of intensity.

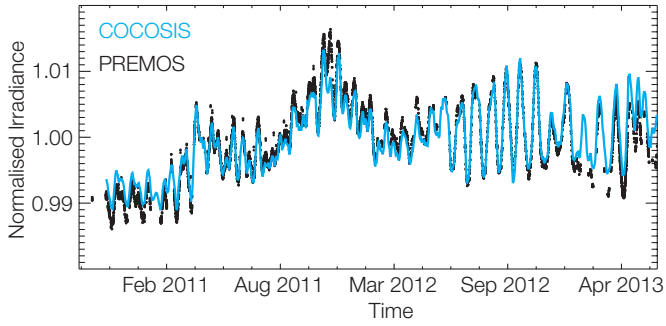

Figure 2. Daily spectral solar irradiance comparison at 215 nm from PREMOS and the COCOSIS model from September 2010 to July 2013.

References: Shapiro A.I., Schmutz W., Schoell M., Haberreiter M., Rozanov E.: 2010, NLTE solar irradiance modeling with the COSI code. Astron. Astrophys., 517, A48.

Yeo K.L., Solanki, S.K., Krivova, N.A.: 2013, Astron. Astrophys., 550, A95.

Understanding the Implication of Small-Scale Heating Events in the Solar Upper Atmosphere

Nuno Guerreiro, Margit Haberreiter and Werner Schmutz in collaboration with the University of Oslo

The coronal heating problem is still a key science question in solar physics. Here, we use 3D MHD simulations to understand the role of small-scale heating events in coronal heating, and report the latest results from our analysis.

Levine (1974) suggested that the coronal heating problem could be explained by a multitude of small reconnection events. Parker (1988) built on Levine's ideas and coined the term "nanoflare". Nanoflares are considered to have an average energy of 10^{24} erg which lie at the limit of detectability. In order for them to significantly contribute to the heating of the corona they must have an energy distribution given by a power law, $dN/dt \sim E^{-\alpha}$, where α has to be greater than 2.

Simulations using the "Bifrost" code (Gudiksen, 2011) are used to study the small-scale events and their properties. An example is shown in Figure 1. We have identified the events at every time-step and conclude that the number of events is roughly constant over time, as shown in Figure 2.

In order to account for the energy associated with each event at any instant, we define the spatial extent of the event to be the volume containing energy values that are above a certain percentage of the individual event's maximum energy at a certain instant. For the volume of each event only cells in the surrounding are taken into account. By "surrounding" we mean all the cells that have path-connectivity to the single event's maximum and the energy value is above the threshold. Figure 3 shows the total amount of energy of all identified events at each instant. This figure shows that the energy from the events lies within 2–6 x 10^6 erg cm^{-2} s^{-1}.

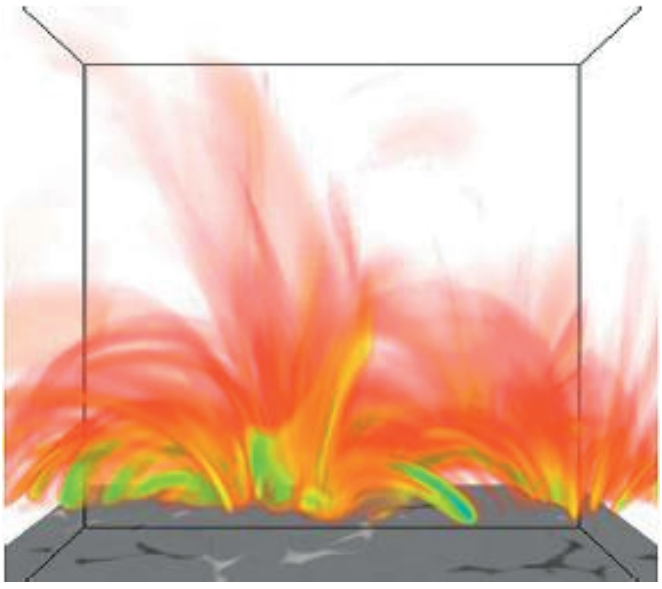

Figure 1. Current density squared per particle: red/yellow weakest, green/blue strongest. Low current density regions are given low opacity and are therefore transparent. The B_z component of the magnetic field in the photosphere at z = 0 Mm, where τ_{500}=1, is shown in grey.

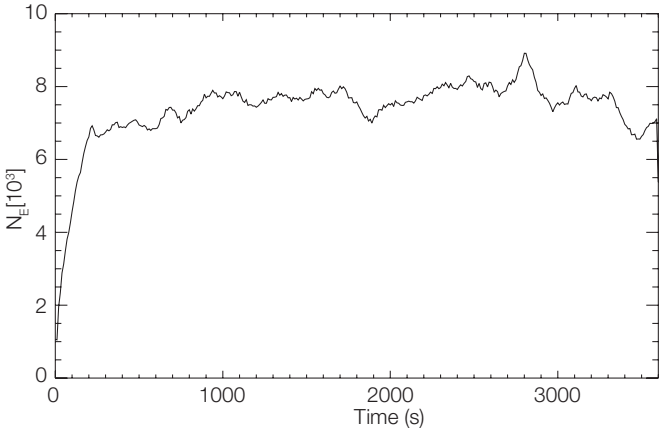

Figure 2. Number of small-scale events (N_E) versus time. The number of events in the simulation is almost constant over one hour.

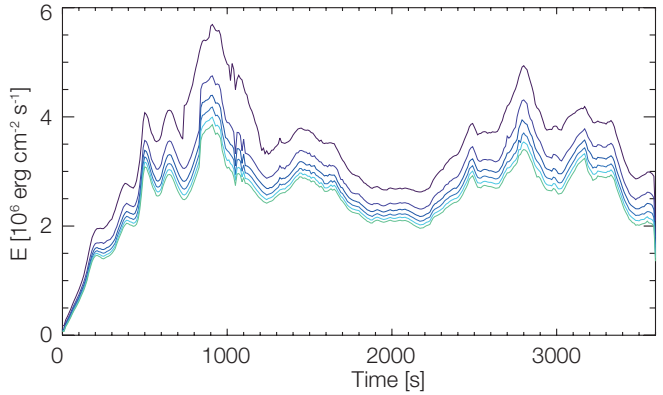

Figure 3. Total energy from the small heating events at each instant. The different colored lines represent the different thresholds used to identify the extent of the events. The threshold ranges from 5 % (purple) to 25 % (green) in 5 % steps.

Finally, we have computed the vertical extent of the events in the simulation box. This parameter is difficult to estimate from observations but is very important for an accurate calculation of the thermal energy of the events. Our results give an average value of about 1 Mm which is between 25 % (Parnell and Jupp, 2000) and 50 % (Krucker and Benz, 1998) larger than the values previously used to estimate the thermal energies from observationally detected events.

Acknowledgement: NG thanks SNSF for financial support and VH for the provided data. MH acknowledges support from the FP7 SOLID project.

References:

Gudiksen B. V., Carlsson M., Hansteen V. H., Hayek W., Leenaart J., Martinez-Sykora J.: 2011, Astron. Astrophys., 531, A154.

Krucker S, Benz A.O.: 1998, ApJ. Lett., 501, L213.

Levine R. H.: 1974, ApJ., 190, 457–466.

Parker E. N.: 1988, ApJ., 330, 474.

Parnell C.E., Jupp P.E: 2000, ApJ., 529, 554–569.

Sensitivity of Atmospheric Emissions Modelling to Solar/Stellar UV Flux

Gaël Cessateur, in collaboration with IPAG, Université Joseph Fourier, Grenoble, France.

The solar UV flux is one of the main energetic inputs for planetary upper atmospheres. It drives various processes such as ionisation/excitation, which give rise to atmospheric emissions. Through several examples, we explore the impact of uncertainties in solar/stellar UV flux regarding the modelled emissions.

We focus here on three different examples which summarise the specific problems caused by the non-perfect characterisation of the solar UV flux (Barthelemy and Cessateur, 2014).

Ganymede

Due to a thin atmosphere, the link between the solar UV flux and atmospheric emissions could not be more direct. Figure 1 displays the electron production rate for three different solar irradiance spectra: one directly measured with TIMED/SEE, one obtained with a Bandpasses model (Cessateur et al., 2012), and the last one obtained with the HEUVAC model using the F10.7 solar proxy (Richards et al., 2006).

While the disagreement reached only 3 % with the Bandpasses model, the HEUVAC model underestimates the electron production by about 13 %. The evaluation of the total electronic content within Ganymede's atmosphere is more disconcerting: the Bandpasses model overestimates by about 1.8 % while HEUVAC underestimates by about 11 %. It therefore appears that a model based only on the F10.7 proxy, clearly cannot be used for ionospheric calculations. We have also shown that several specific solar lines are mostly responsible for atmospheric emissions such as the red line at 630 nm. More than 25 % of the red line emission comes from the H-Lyman α, which directly outlines the need for a better understanding of the formation process of such a solar line.

Uranus

Recent Hubble Space Telescope (HST) observations of Uranus in the FUV allowed an auroral event to be detected on the 29 November 2011. Most of the light observed (90 %) by HST is composed of solar reflected light, while the remaining part concerns airglow and H_2 emissions induced by electron precipitation.

Thus, any uncertainty in the solar flux estimate can strongly affect estimates of the other components. We have estimated that a flux error of about 1 % can give rise to an error of about 10 % in the airglow estimate as well as of the precipitation contributions which lead to planetary upper atmosphere and auroral processes (Barthelemy and Cessateur, 2014). Moreover, the intrinsic variability on time-scales of a few days also has to be considered. Since the spectra are only measurements from an Earth-based orbit, this could lead to major errors if the angle between the observed planet and Earth is too large.

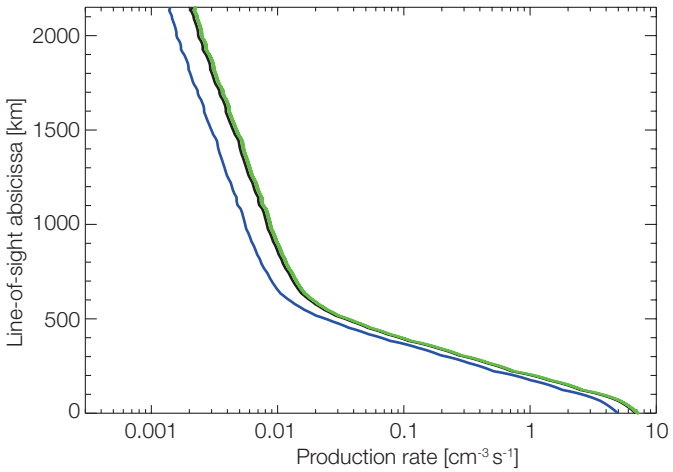

Figure 1. Electron production rate for three different solar irradiance spectra: The reference spectrum (in black), the Bandpasses model (in green), and the HEUVAC model (in blue).

Optically thick cases

Some solar lines, such as H-Lyman α or O I triplet at 130 nm, are optically thick in most planetary atmospheres, and are powerful tools for characterising the upper atmosphere dynamics and composition. The centre of the line is mostly scattered by the atmosphere: A small change in the line shape can then lead to an error of the modelled atmospheric parameters. In the case of H-Lyman, modelled by a double Gaussian shape, an enhancement in the width by about 15 % can lead to a 5 % overestimate of the atmospheric emission (Menager et al., 2010). The line profile of intense solar lines is also critical when considering the fluorescence especially for molecular species (i.e. H_2 in the case of Jupiter).

Finally, the question of whether the upper atmosphere of exoplanets can be characterised is currently a new field of research. More than 1000 exoplanets have so far been discovered, which underlines the need for a future UV space telescope in order to fully characterise the local environment.

References:

Barthelemy M., Cessateur G.: 2014, JSWSC, submitted.

Barthelemy M., Lamy L., Menager H., Schulik M., Bernard D., Abgrall H., Roueff E., Cessateur G., Prange R., Lilensten J.: 2014, JSWSC, submitted.

Cessateur G., Lilensten J., Barthelemy M., Dudok de Wit T., Simon Wedlund C., Gronoff G. Menager H., Kretzschmar M.: 2012, Icarus, 218, 308-319.

Menager H., Barthelemy M., Lilenten J.: 2010, Astron. Astrophys., 529, A56.

Richards P.G., Woods T.N., Peterson W.K.: 2006, Adv. Space Res., 37, 315–322.

Irradiance Reconstruction in the EUV based on SOHO/EIT 6-Component Image Segmentation

Margit Haberreiter in collaboration with the Royal Observatory Belgium

The solar EUV spectrum has important effects on the Earth's upper atmosphere. For detailed investigation of these effects it is necessary that a consistent data series of the EUV spectral irradiance is available. We present a six-component reconstruction of the solar EUV irradiance based on the segmentation of SOHO/EIT images, along with synthetic spectra calculated for the different coronal features.

As a starting point for reconstruction of the solar EUV irradiance we use the approach by Fontenla et al. (2009), further developed by Haberreiter (2011, 2012). Synthetic solar intensity spectra are calculated with the Solar Modelling (SOLMOD) code (Haberreiter, 2011) for five components of the intensity distribution of the solar corona: quiet corona (QS1), coronal quiet network (QS2), coronal active network (AR1), active regions (AR2), and bright active regions (AR3). The Coronal Hole (CH) intensity is calculated with a fixed contrast of c = 0.5 with respect to the quiet corona (QS1).

In collaboration with the Royal Observatory of Belgium, images taken with the Extreme Ultraviolet Imaging Telescope (EIT) onboard the SOHO satellite were segmented into six classes using the SPoCA2 tool (Verbeeck et al., 2013). The analysis spanning 16 years of data (1996 to 2012) is based on theoretical contrast values determined from the synthetic spectra calculated with SOLMOD. Figure 1 shows the contrast values for the employed components normalised to the quiet network (Class 3).

The area coverage of the six components is determined using the SPcCA2 tool on each day. Figure 2 shows an example of the image segmentation. Weighting the intensity spectra with the area covered by each of the feature yields the temporal variation of the EUV spectrum. The reconstructed spectrum is then validated against the spectral irradiance as observed with SOHO/SEM, shown in Figure 3. A considerable improvement in the reconstruction of the EUV spectral irradiance has been achieved with the six-component model.

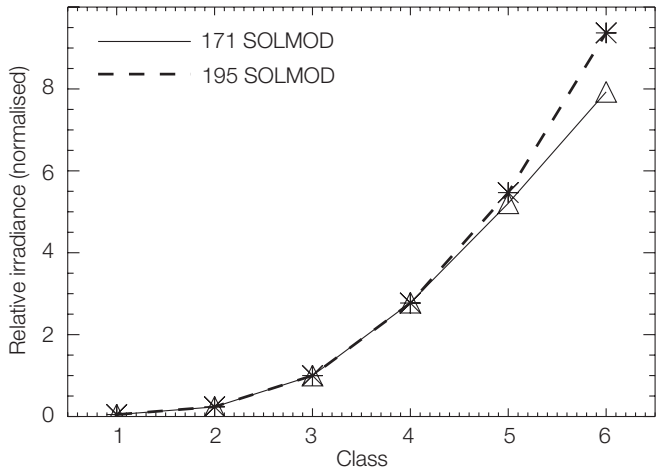

Figure 1. The theoretical EIT 171 and 195 Å contrast as calculated with the SOLMOD code. The contrasts are given for all six components and normalised to the quiet network (QS2, or Class 3).

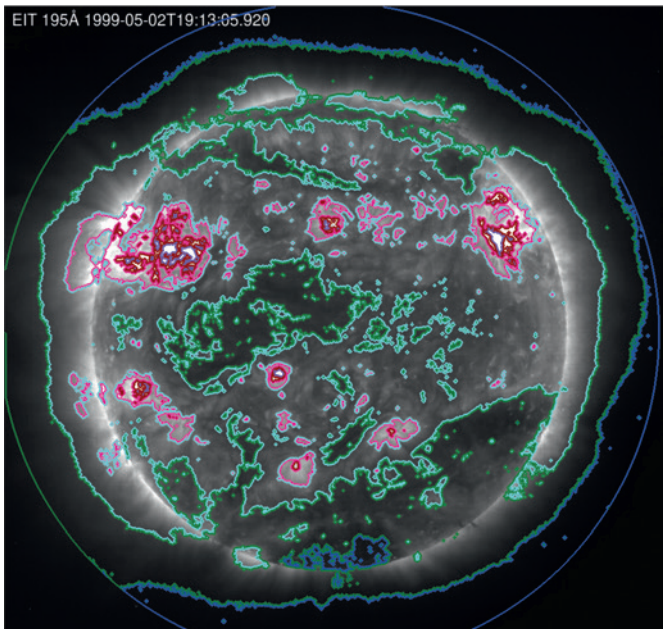

Figure 2. Example of an overlay of the segmentation map onto an EIT image (λ = 195 Å) from 2 May 1999. The coloured contours represent: blue: CH, dark green: QS1, light green: QS2, dark violet: AR1, red: AR2, violet: AR3.

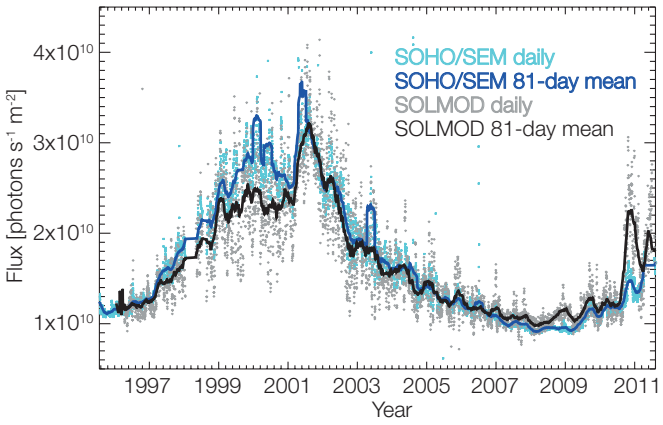

Figure 3. Comparison of the daily SOLMOD reconstruction (grey dots) with the SOHO/SEM irradiance data (light blue dots). The solid black and blue lines represent the respective 81-day running means. For further details see Haberreiter et al. (2014).

Acknowledgement: Funding from EC FP7 2012 under grant agreement No. 313188 (SOLID) has been gratefully received.

References:

Fontenla J., Curdt W., Haberreiter M., Harder J.: 2009, ApJ., 707, 482.

Haberreiter M.: 2011, Sol. Phys., 274, 473-479.

Haberreiter M.: 2012, Proceedings IAU Symposium 286, 97-100.

Haberreiter, M., Delouille, V., Mampeay, B., Verbeeck, C., Wieman, S.: 2014, J. Space Weather Space Clim., under review.

Verbeeck C., Delouille C., Mambaey B., De Visscher R.: 2013, Astron. Astrophys., 561, A29.

Accelerating COSI Lambda-Iterations with the Line Local Operator

Rinat Tagirov, Alexander Shapiro, Gaël Cessateur, and Werner Schmutz

We have been working on the implementation of a fast and reliable non-LTE radiative transfer numerical scheme within COde for Solar Irradiance (COSI), developed at the PMOD/WRC for solar spectrum modelling.

In short, a non-LTE line radiative transfer problem in a stellar atmosphere can be described by two equations. The first is the radiative transfer equation:

$$J = \Lambda[S], \quad (1)$$

where J is the mean intensity in a given line or continuum frequency, Λ is the so-called lambda-operator and S is the source function. The source function depends on populations of levels involved in the transition which in turn depend on the intensity by means of the second, statistical equilibrium equation:

$$\Sigma P_{ij}(J) n_i = n_j \Sigma P_{ji}(J), \quad (2)$$

where n_i is the population of the i-th level and P_{ij} is the total transition rate from level i to level j. The problem cannot be solved analytically in the general case. The numerical way to solve it is by means of iterating between the intensity and source function. Such iterations are called Λ-iterations and at step n can be described as follows:

$$J_{n+1} = \Lambda[S_n] \quad (3)$$

$$\Sigma P_{ij}(J_{n+1}) n_i = n_j \Sigma P_{ji}(J_{n+1}). \quad (4)$$

The iterations start with S_0 – a plausible initial approximation for the source function. From (4) we obtain S_{n+1} and then apply (3) again. Unfortunately Λ-iterations have a property of stabilising long before the correct solution is reached in atmospheric regions where optical depth for a given line is large (Hubeny, 2003) and therefore such a straightforward approach cannot be used. To circumvent this behavior one has to implement the Accelerated Lambda-Iterations (ALI) – a technique in which the problematic locations are dealt with by means of Λ-operator splitting (Cannon, 1973):

$$J_{n+1} = \Lambda^*[S_n] + (\Lambda - \Lambda^*)[S_n] \approx \Lambda^*[S_{n+1}] + (\Lambda - \Lambda^*)[S_n]$$

$$= \Lambda[S_n] + \Lambda^*[S_{n+1} - S_n] = J_n + \Lambda^*[S_{n+1} - S_n], \quad (5)$$

where Λ^* is the approximate Λ-operator and can take any form as long as it is easily invertible and serves as a good physical approximation to the initial Λ-operator. Equations (4) and (5) constitute the essence of the ALI scheme.

The goal of this project is to employ the local Λ^*-operator (Olson et al., 1986) in the ALI scheme within the code's co-moving system of reference framework. As has been done in the observer's frame, we adopt $\Lambda^* = \mathrm{diag}(\Lambda)$. This has not yet been described in the literature for a practical realisation. Accomplishment of our objective will expand the computational capabilities of COSI. Namely, such new capabilities, among others, will include proper calculation of the emergent intensity in the Lyman-α line and in the radio continuum (0.1 mm – 30 cm), both of which are crucial for a number of parallel and future projects.

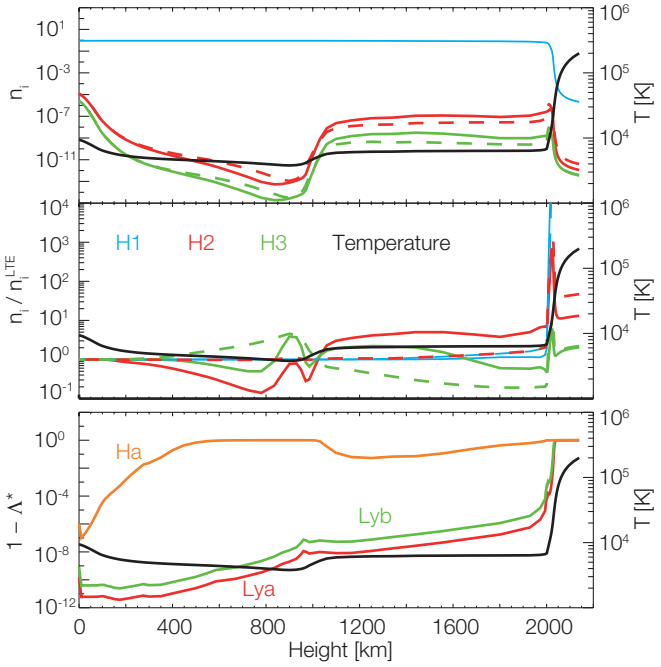

Figure 1. Upper Panel: Populations of the first, second and third levels of neutral hydrogen calculated with (solid) and without (dashed) local operator ALI implementation. Middle Panel: Zwaan departure coefficients for the second and third levels of neutral hydrogen obtained under the same conditions. Lower panel: The local Λ^*-operator values for some of the main lines governing the populations of corresponding levels.

The upper and middle panels of Figure 1 provide evidence of a significant impact on COSI output by implementing the local Λ^*-operator. The result is in reasonable agreement with calculations by Rutten and Uitenbroek (2012).

References:

Cannon C.: 1973, Frequency-quadrature perturbations in radiative-transfer theory, Astrophysical Journal, 185, 621–630.

Hubeny I.: 2003, Accelerated lambda iteration: an overview, Stellar Atmosphere Modeling, ASP Conf. Ser., 288, 17–30.

Olson et al.: 1986, A rapidly convergent iterative solution of the non-LTE line radiation transfer problem, Quant. Spectr. Rad. Tran., 35, 431–442.

Rutten R. and Uitenbroek H.: 2012, Chromospheric backradiation in ultraviolet continua and Hα, Astron. Astrophys, 540, A86.

Search for the Most Variable Part of the Solar Spectrum

Alexander Shapiro, Werner Schmutz, Eugene Rozanov, Gaël Cessateur, Rinat Tagirov, Wilnelia Adams in collaboration with Max-Planck Institut für Sonnensystemforschung, Goettingen, Germany; Blackett Lab. Imperial College London, UK

We present a model which attributes the variability of the stellar radiative energy flux to the imbalance between the contributions from dark starspots and bright faculae. Our approach allows us to model the stellar photometric variability as a function of an activity index and reproduce the transition from faculae-dominated to spot-dominated regimes of variability.

The solar irradiance varies on different time scales. The two most striking features in records are the 11-year solar activity and 27-day solar rotational cycles. We show that while the spectral profiles of the solar irradiance variability on the rotational and activity time-scales are completely different they have a common maximum. The position of the maximum coincides with the CN violet system, one of the most prominent features in the solar spectrum.

Most of the available data-sets yield fairly similar amplitudes and spectral profiles of the spectral solar irradiance (SSI) variability on the solar rotational time-scale. On longer time-scales the accumulated uncertainty in the instrumental degradation becomes larger and renders the interpretation of the SSI measurements rather difficult. To overcome this problem a number of models of solar irradiance variability have been created. Modern physics-based models attribute the variability of the solar spectrum to the imbalance between the contributions from dark (e.g. sunspots or pores) and bright (e.g. faculae or network) magnetically-active features in the solar atmosphere. The rotation of the Sun causes the irradiance modulation with a 27-day period, while changes in the overall magnetic activity (and consequently in the surface area coverage of active features) lead to the 11-year activity cycle and long-term changes in solar irradiance.

To calculate the spectral profiles of the SSI variability we convolved solar disk area coverages by active region, calculated by Ball et al. (2012) from the SOHO/MDI full-disc continuum images and magnetograms, with spectra of these features calculated by Shapiro et al. (2010). The spectral profile of the SSI change between 2004 and 2008, which is a good representative of the SSI variability on the activity time-scale, is plotted in Figure 1. The highest peak in the profile is the CN violet system, the peak at 430 nm is the CH G-band. To estimate the contribution from molecular lines we also calculated the spectra by artificially putting the molecular opacity to zero. Such an elimination of the molecular lines significantly reduces the SSI variability in the visible part of the spectrum and reduces TSI variability by approximately 25 %. Hence a quarter of the TSI variability on the activity time scale is coming from the molecular lines. Figure 2 presents the spectral profiles of the SSI variability on the rotational time-scale. While the CN violet system is still the highest peak of the profile, the overall contribution of the molecular lines is substantially smaller.

Interestingly the elimination of the atomic lines would completely reshape the spectral profile of the SSI variability and lead to the 11-year TSI variability being anti-correlated with solar activity.

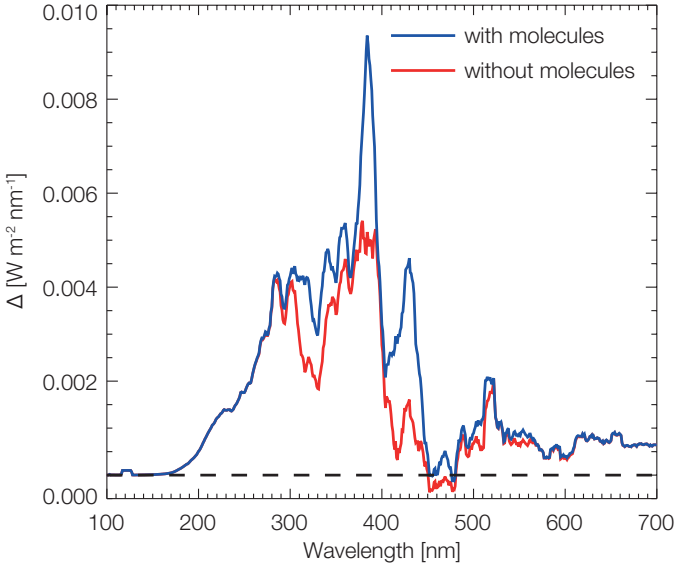

Figure 1. Absolute change between annual SSI values in 2004 and 2008 calculated taking molecular lines into account (blue curve) and ignoring them (red curve) vs. wavelength.

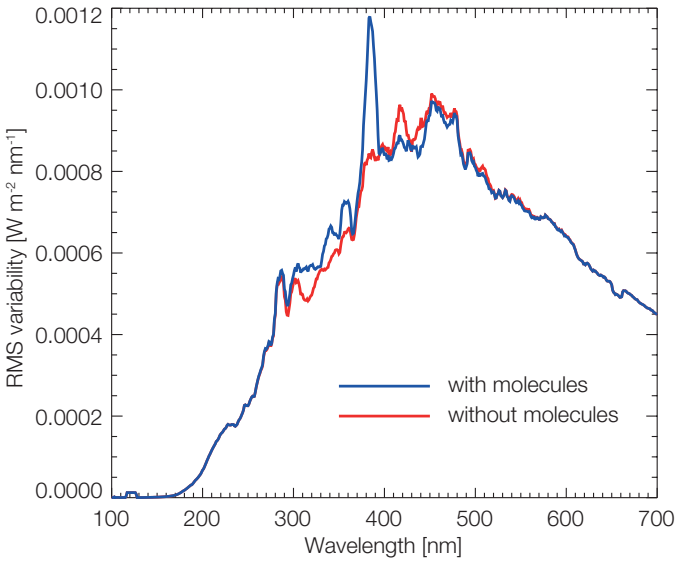

Figure 2. The RMS values of the SSI variability on the rotational time-scale calculated for the 1999–2010 period taking molecular lines into account (blue curve) and ignoring them (red curve) vs. wavelength.

Thus solar irradiance variability is almost exclusively defined by the behavior of the spectral lines and has very little connection with the continuous spectrum.

References: Ball W.T., Unruh Y. C., Krivova N.A., Solanki S., Wenzler T., Mortlock D.J., Jaffe A.H.: 2012, Astron. Astrophys., 541, A27.

Ermolli I., et al.: 2013, Atmos. Chem. Phys., 13, 3945–3977, 2013, doi:10.5194/acp-13-3945-2013.

Shapiro A. I., Schmutz W., Schoell M., Haberreiter M., Rozanov E.: 2010, Astron. Astrophys., 517, A48.

Publications

Refereed Publications

Anet J., Muthers S., Rozanov E., Raible C., Peter T., Stenke A., Shapiro A.I., Beer J., Steinhilber F., Brönnimann S., Arfeuille F., Brugnara Y., Schmutz W.: 2013, Forcing of stratospheric chemistry and dynamics during the Dalton Minimum, Atmos. Chem. Phys., 13, 10951–10967, doi:10.5194/acp-13-10951-2013.

Anet J., Rozanov E., Muthers S., Peter T., Bronnimann S., Arfeuille F., Beer J., Shapiro A.I., Raible C., Steinhilber F., Schmutz W.: 2013, Impact of a potential 21st century "grand solar minimum" on surface temperatures and stratospheric ozone, Geophys. Res. Lett., 40, 4420–4425, doi:10.1002/grl.50806.

Arfeuille F., Luo B., Heckendorn P., Weisenstein D., Sheng J.-X., Rozanov E., Schraner M., Brönnimann S., Thomason L., Peter T.: 2013, Modeling the stratospheric warming following Mt. Pinatubo eruption: uncertainties in aerosol extinctions, Atmos. Chem. Phys., 13, 11221–11234, 2013, doi:10.5194/acpd-13-4601-2013.

BenMoussa A., Gissot S., Schühle U., Del Zanna G., Auchère F., Mekaoui S., Jones A.R., Walton D., Eyles C.J., Thuillier G., Seaton D., Dammasch I.E., Cessateur G., Meftah M., Andretta V., Berghmans D., Bewsher D., Bolsée D., Bradley L., Brown D.S., Chamberlin P.C., Dewitte S., Didkovsky L.V., Dominique M., Eparvier F.G., Foujols T., Gillotay D., Giordanengo B., Halain J.-P., Hock R.A., Irbah A., Jeppesen C., Judge D.L., Kretzschmar M., McMullin D.R., Nicula B., Schmutz W., Ucker G., Wieman S., Woodraska D., Woods T.N.: 2013, On-Orbit Degradation of Solar Instruments, Sol. Phys. 288, 389–434, doi: 10.1007/s11207-013-0290-z.

Brönnimann S., Bhend J., Franke J., Flückiger S., Fischer A., Bleisch R., Bodeker G., Hassler B., Rozanov E., Schraner M.: 2013, A global historical ozone data set and prominent features of stratospheric variability prior to 1979, Atmos. Chem. Phys., 13, 9623–9639, doi: 10.5194/acp-13-9623-201.

Brugnara Y., Brönnimann S., Luterbacher J., Rozanov E.:2013, Influence of the sunspot cycle on the Northern Hemisphere wintertime circulation from long upper-air data sets, Atmos. Chem. Phys., 13, 6275–6288, doi:10.5194/acp-13-6275-2013.

Calisto M., Usoskin I., Rozanov E.: 2013, Influence of a Carrington-like event on the atmospheric chemistry, temperature and dynamics: revised, Environ. Res. Lett., 8, 045010 (10pp), doi:10.1088/1748-9326/8/4/045010.

Dominique M., Hochedez J.-F., Schmutz W., Dammasch I.E., Shapiro A.I., Kretzschmar M., Zhukov A.N., Gillotay D., Stockman Y., BenMoussa A.: 2013, The LYRA Instrument onboard PROBA2: Description and in-flight performance, Sol. Phys. 286, 21–42, doi: 10.1007/s11207-013-0252-5.

Dudok de Wit T., Moussaoui S., Guennou C. et al.: 2013, Coronal Temperature Maps from Solar EUV Images: A Blind Source Separation Approach, Sol. Phys., 283, 31–47, doi: 10.1007/s11207-012-0142-2.

Egorova T., Rozanov E., Gröbner J., Hauser M., Schmutz W.: 2013, Montreal Protocol benefits simulated with CCM SOCOL, Atmos. Chem. Phys., 13, 3811–3823, doi:10.5194/acp-13-3811-2013.

Ermolli I., Matthes K., Dudok de Wit T., Krivova N., Tourpali K., Weber M., Unruh Y., Gray L., Langematz U., Pilewskie P., Rozanov E., Schmutz W., Shapiro A.I., Solanki S., Thuillier G., Woods T.: 2013, Recent variability of the solar spectral irradiance and its impact on climate modelling, Atmos. Chem. Phys., 13, 3945–3977, doi: 10.5194/acp-13-3945-2013.

Fröhlich C.: 2013, Total Solar Irradiance: What have we learned from the last three cycles and the recent minimum?, Space Sci. Rev., 176, 237–252, doi: 10.1007/s11214-011-9780-1.

Lachat D., Wehrli C.: 2013, Dimming and brightening trends in direct solar irradiance from 1909 to 2010 over Davos, Switzerland: Proportions of aerosol and gaseous transmission, J. Geophys. Res., 118, 3285–3291, doi: 10.1002/jgrd.50344.

Petzold A., Ogren J. A., Fiebig M., Laj P., Li S.-M., Baltensperger U., Holzer-Popp T., Kinne S., Pappalardo G., Sugimoto N., Wehrli C., Wiedensohler A., Zhang X.-Y.: 2013, Recommendations for reporting "black carbon" measurements, Atmos. Chem. Phys., 13, 8365–8379, doi:10.5194/acp-13-8365-2013.

Schmutz W., Fehlmann A., Finsterle W., Kopp G., Thuillier G.: 2013, Total solar irradiance measurements with PREMOS/PICARD. In: R.F. Cahalan, J. Fischer (eds.) Radiation Processes in the Atmosphere and Ocean (IRS2012), Proceedings of the International Radiation Symposium (IRC/IAMAS), AIP Conf. Proc. 1531, p. 624–627, AIP Publishing LLC, Melville, New York, doi: 10.1063/1.4804847.

Refereed Publications

Shapiro A. V., Rozanov E., Shapiro A.I., Egorova T., Harder J., Weber M., Smith A., Schmutz W., Peter T.: 2013, The role of the solar irradiance variability in the evolution of the middle atmosphere during 2004–2009, J. Geophys. Res. 118, 3781–3793, doi:10.1002/jgrd.50208.

Shapiro A.V., Shapiro A. I., Dominique M., Dammasch I., Wehrli C., Rozanov E., Schmutz W.: 2013, Detection of solar rotational variability in the Large Yield RAdiometer (LYRA) 190 – 222 nm spectral band, Sol. Phys., 286, 289–301, doi:10.1007/s11207-012-0029-2.

Shapiro A.I., Schmutz W., Cessateur G. and Rozanov E.: 2013, The place of the Sun among the Sun-like stars, Astron. Astrophys., 552, A114, doi: 10.1051/0004-6361/201220512.

Shapiro A.I., Schmutz W., Dominique M., Shapiro A.V.: 2013, Eclipses observed by Large Yield RAdiometer (LYRA) – a sensitive tool to test models for the solar irradiance, Sol. Phys., 286, 271–287, doi: 10.1007/s11207-012-0063-0.

Simoniello R., Jain K., Tripathy S. C., Turck-Chièze S., Baldner C., Finsterle W., Hill F., Roth M.: 2013, The Quasi-biennial periodicity as a window on the solar magnetic dynamo configuration, ApJ., 765, 100S.

Stenke A., Hoyle C., Luo B., Rozanov E., Gröbner J., Maag L., Brönnimann S., Peter T.: 2013, Climate and chemistry effects of a regional scale nuclear conflict, Atmos. Chem. Phys., 13, 9713–9729, doi: 10.5194/acp-13-9713-2013.

Stenke A., Schraner M., Rozanov E., Egorova T., Luo B., Peter T.: 2013, The SOCOL version 3.0 chemistry-1 climate model: description, evaluation, and implications from an advanced transport algorithm, Geosci. Model Dev., 6, 1407–1427, doi:10.5194/gmd-6-1407-2013.

Tsagouri I., Belehaki A., Bergeot N. Cid C., Delouille V., Egorova T., Jakowski N., Kutiev I., Mikhailov A., Núñez M., Pietrella M., Potapov A., Qahwaji R., Tulunay Y., Velinov P., Viljanen A.: 2013, Progress in space weather modeling in an operational environment, J. Space Weather Space Clim., 3, A17, doi:10.1051/swsc/2013037.

Wehrli C., Schmutz W., Shapiro A. I.: 2013, Correlation of spectral solar irradiance with solar activity as measured by VIRGO, Astron. Astrophys., 556, L3, doi:10.1051/0004-6361/201220864.

Zubov V., Rozanov E., Egorova T., Karol I., Schmutz W.: 2013, Role of external factors in the evolution of the ozone layer and stratospheric circulation in 21st century, Atmos. Chem. Phys., 13, 4697–4706, doi:10.5194/acp-13-4697-2013.

Zuccarello F., Balmaceda L., Cessateur G. et al.: 2013, Solar activity and its evolution across the corona: recent advances, J. Space Weather Space Clim., 3, A18, doi:10.1051/swsc/2013039.

Other Publications

Anet J., Muthers S., Rozanov E., Raible C., Stenke A., Shapiro A.I., Brönnimann S., Arfeuille F., Brugnara Y., Beer J., Steinhilber F., Schmutz W., Peter T.: 2013, Impact of solar vs. volcanic activity variations on tropospheric temperatures and precipitation during the Dalton Minimum, Clim. Past Discuss., 9, 6179–6220, doi:10.5194/cpd-9-6179-2013, 2013.

Arfeuille F., Weisenstein D., Mack H., Rozanov E., Peter T., Brönnimann S.: 2013, Volcanic forcing for climate modeling: a new microphysics-based dataset covering years 1600–present, Clim. Past Discuss., 9, 967–1012, doi:10.5194/cpd-9-967-2013, 2013.

Blumthaler M., Gröbner J., Egli L., Nevas S.: 2013, A guide to measuring solar UV spectra using array spectroradiometers, AIP Conf. Proc., 1531, 805, doi:10.1063/1.4804892.

Cessateur G., Shapiro A., Schmutz W., Krivova N. Solanki S.K., Yeo K.L., Thuillier G.: 2013, What can we learn about the Sun with PREMOS/PICARD?, EGU General Assembly Conf. Abstracts 15, 11720.

Cessateur G., Shapiro A., Schmutz W., Rozanov E.: 2013, The Sun among the Sun-like stars, EGU General Assembly Conf. Abstracts 15, 8980.

Diemoz H., Egli L., Gröbner J., Siani A. M., Diotri F.: 2013, Solar ultraviolet irradiance measurements in Aosta (Italy): An analysis of short- and middle-term spectral variability, AIP Conf. Proc. 1531, 856, doi:10.1063/1.4804905.

Dudok de Wit T., Fröhlich C.: 2013, How to build a new composite of the total solar irradiance out of disparate observations?, EGU General Assembly Conf. Abstracts 15, 8675.

Egli L., Gröbner J., Smid M., Porrovecchio G., Burnitt T., Nield K. M., Gibson S., Dubard J., Nevas S. and Tormen M.: 2013, New technologies to reduce stray light for measuring solar UV with array spectroradiometers, AIP Conf. Proc. 1531, 825, doi:10.1063/1.4804897.

Finsterle W., Shapiro A., Schmutz W., Krivova N.: 2013, The latitudinal dependence of the solar radiance, EGU General Assembly Conf. Abstracts 15, 11672.

Finsterle W.: 2013, "An upcoming TSI mission and a new pre-flight calibration facility (invited)", AGU2013 GC54A-07.

Fludra A., Griffin D., Caldwell M., Eccleston P., Cornaby J., Drummond D., Grainger W., Greenway P., Grundy T., Howe C., McQuirk C., Middleton K., Poyntz-Wright O., Richards A., Rogers K., Sawyer C., Shaughnessy B., Sidher S., Tosh I., Beardsley S., Burton G., Marshall A., Waltham N., Woodward S., Appourchaux T., Philippon A., Auchere F., Buchlin E., Gabriel A., Vial J.C., Schühle U., Curdt W., Innes D., Meining S., Peter H., Solanki S., Teriaca L., Gyo M., Büchel V., Haberreiter M., Pfiffner D., Schmutz W., Carlsson M., Haugan S. V., Davila J., Jordan P., Thompson W., Hassler D., Walls B., Deforest C., Hanley J., Johnson J., Phelan P., Blecha L., Cottard H., Paciotti G., Autissier N., Allemand Y., Relecom K., Munro G., Butler A., Klein R., Gottwald A.: 2013, SPICE EUV spectrometer for the Solar Orbiter mission, SPIE Conf. Ser. 8862, 88620F-1, doi:10.1117/12.2027581.

Gröbner J., Wacker S.: 2013, Longwave irradiance measurements using IRIS radiometers at the PMOD/WRC-IRS, AIP Conf. Proc. 1531, 488, doi:10.1063/1.4804813

Haberreiter M.: 2013. In: Beyond the Sky, European Commission, Directorate General Enterprise and Industry, Unit Policy and Space Research (G1), p. 83.

Haberreiter M., Dasi M., Delouille V., Del Zanna G., Dudok de Wit T., Ermolli, I., Kretzschmar M., Krivova N., Mason H., Qahwaji R., Schmutz W., Solanki S., Thuillier G., Tourpali K., Unruh Y., and Verbeeck C., Weber M., Woods T.: 2013, A Collaborative FP7 Effort towards the First European Comprehensive SOLar Irradiance Data Exploitation (SOLID), EGU General Assembly Conf. Abstracts 15, 13079.

Junk J., Feister U., Rozanov E., Krzyścin J.: 2013, Reconstruction of daily erythemal UV radiation values for the last century –The benefit of modelled ozone, AIP Conf. Proc. 1531, 872 (2013); doi: 10.1063/1.4804909.

Lakkala K., Arola A., Heikkila A., Karhu J. M., Kaurola J., Koskela T., Kyro E., Karha P., LindforsA. V., Meinander O., Gröbner J., Hülsen G.: 2013, Two decades of spectral UV measurements at Sodankyla, AIP Conf. Proc. 1531, 883, doi:10.1063/1.4804912.

Muthers S., Anet J.G., Raible C.C., Brönnimann S., Arfeuille F., Peter T., Rozanov E., Shapiro A., Beer J., Steinhilber F., Brugnara Y., Schmutz W.: 2013, Stratospheric ozone levels and their role for the dynamic response to volcanic eruptions, EGU General Assembly Conf. Abstracts 15, 6906.

Nezval Y., Chubarova N., Gröbner J., Ohmura A.: 2013, Variations of longwave downwelling irradiance (LDI) due to different atmospheric factors in Moscow, AIP Conf. Proc. 1531, 580, doi:10.1063/1.4804836.

Nyeki S., Gröbner J., Wehrli C.: 2013, Ground-based aerosol optical depth inter-comparison campaigns at European EUSAAR super-sites, AIP Conf. Proc. 1531, 584, doi:10.1063/1.4804837

Porrovecchio G., Smid M., Gröbner J., Rajteri M., Portesi C., Nield K.M., Egli L.: 2013, New detection systems for UV solar reference scanning spectroradiometers, AIP Conf. Proc. 1531, 837, doi:10.1063/1.4804900

Schoell M., Haberreiter M., Schmutz W., Shapiro A.: 2013, Modeling the detailed Lyman-α line profile, EGU General Assembly Conf. Abstracts 15, 12813.

Shapiro A., Knaack R., Krivova N., Schmutz W., Solanki S., Unruh Y.: 2013, Modeling the variability of Sun-like stars, EGU General Assembly Conf. Abstracts 15, 9981.

Shapiro A., Rozanov E., Shapiro A., Egorova T., Harder J., Weber M., Smith A., Schmutz W., Peter T.: 2013, The stratospheric response to a discrepancy of the SSI data, EGU General Assembly Conf. Abstracts 15, 10373.

Swift N., Hülsen G., Nield K., Gröbner J., Hamlin J.: 2013, Calibration of erythemally weighted broadband instruments: A comparison between PMOD/WRC and MSL, AIP Conf. Proc. 1531, 817, doi:10.1063/1.4804895.

Thuillier G., Melo S., Lean J., Krivova N., Bolduc C., Fomichev V., Charbonneau P., Shapiro A., Schmutz W., Bolsee D.: 2013, Analysis of Different Solar Spectral Irradiance Reconstructions From The 17th century to 2010, EGU General Assembly Conf. Abstracts 15, 5411.

Wacker S., Gröbner J., Vuilleumier L.: 2013. Trends in surface radiation and cloud radiative effect over Switzerland in the past 15 years, AIP Conf. Proc., 1531, 672–675, doi:10.1063/1.4804859.

Administration

Personnel Department

Sandra Kissling

The New Year began in a relaxed way after a hectic time in 2012. Although many challenges stood in front of us, we began the year with the final preparations for the Davos Atmosphere and Cryosphere assembly 2013 (DACA-13). The PMOD/WRC staff had many tasks to fulfill and things to organise and thanks to all the helping hands and to the project manager Anja Schilling. The conference was held from the 8 – 12 July and turned out to be a great success. The next important event was on 28 August when the newly renovated building was officially inaugurated. International and swiss officials from the WMO attended the inauguration and gave keynote speeches. The efforts and dedication of staff, building workers, officials and all involved were praised.

Several new staff members arrived in 2013. At the beginning of the year, Seraina Egartner joined the Administration while Stephanie Ebert left in November 2012 but continued working part-time during 2013 to support the administration, in particular by editing and laying out the annual report. Christian Stiffler joined the administration in August and is responsible for the accounts. Seraina Egartner left the institute in November after 11 months to pursue her career in the retail branch. We thank her for her contribution and effort in supporting our institute. Alison Gustavsson was hired to fill the vacancy and began in November. We are glad to have her at PMOD/WRC.

Timofei Sukhodolov started as a PhD student in January. In the first half of the year, André Fehlmann and Daniel Lachat left the institute. Both of them did a great job and supported the institute with a lot of commitment.

Nathan Mingard was hired as the new lab assistant in April and we are proud to have such a determined and young person in our team. Together with Christian Thomann who changed departments, they are now both responsible for the direct technical support of the science department. Two new post-docs joined our solar physic group in July, Benjamin Walter and Nuno Guerreiro. Both are very welcome and we wish them a successful time.

Anja Schillings contract ended after DACA-13 and we would like to take this opportunity to thank her for her contribution and outstanding organisation of this conference in which more than 900 scientists participated.

Florian Henschel joined us in November as a trainee in the science department. A very warm welcome to him and we hope he will be able to gain as much experience as possible. At the end of 2013, Stefan Wacker left the PMOD/WRC. He completed his PhD at the institute and then stayed on as a Post-Doc in the IR-Section. We appreciate his devotion and commitment and wish him all the best for the future.

In addition, many thanks to the numerous civilian conscripts who did an excellent job in helping wherever help was needed. It has always been a great pleasure to have them at the institute.

Scientific Personnel

Prof. Werner Schmutz	Director, physicist
Dr. Gaël Cessateur	Postdoc, Solar Physics Group, physicist
Dr. Luca Egli	Scientist WCC-UV section, physicist
Dr. Tatiana Egorova	Scientist Climate Group, meteorologist
Dr. André Fehlmann	Postdoc, solar physics group, physicist (until 16.04.2013)
Dr. Wolfgang Finsterle	Head WRC-section solar radiometry, physicist
Dr. Julian Gröbner	Head WRC-sections IR, WORCC and WCC-UV, physicist
Dr. Nuno Guereirro	Scientist, solar physics group, physicist (since 08.06.2013)
Dr. Margit Haberreiter	Scientist, solar physics group, physicist
Dr. Gregor Hülsen	Scientist WCC-UV section, physicist
Dr. Natalia Kouremeti	Scientist WORCC section, physicist
Dr. Daniel Lachat	Postdoc WORCC section, physicist (until 04.07.2013)
Dr. Stephan Nyeki	Scientist WORCC and IR sections, physicist
Dr. Eugene Rozanov	Head Climate Group, physicist
Dr. Alexander Shapiro	Postdoc Solar Physics Group, physicist
Dr. Anna Shapiro	Postdoc Climate Group, physicist
Dr. Stefan Wacker	Postdoc IR section, physicist (until 31.12.2013)
Dr. Benjamin Walter	Postdoc solar physics group, physicist (since 01.07.2013)
Dr. Christoph Wehrli	Scientist WORCC section, physicist
Markus Suter	PhD student, UNIZH
Timofei Sukhodolov	PhD student, ETHZ (since 01.01.2013)
Rinat Tagirov	PhD student, ETHZ
Florian Henschel	Trainee (since 01.11.2013)

Technical Personnel

Manfred Gyo	Head technical department, electronic engineer, Quality System manager
Valeria Büchel	Mechanical engineer and part time project manager space experiments
Etienne de Coulon	Software development engineer
Fabian Dürig	Mechanical engineer
Silvio Koller	Project- and system engineer Space and Science Instruments (since 01.12.2013)
Daniel Pfiffner	Project manager space experiments, deputy head technical department and Quality System, electronic engineer
Marco Senft	Software developer
Ricco Soder	Research engineer
Marcel Spescha	Technician
Christian Thomann	Technician (until 31.03.2013)
Diego Wasser	Electronic technician
Thierry Hartmann	Electronics apprentice, 3rd and 4th year
Andri Morandi	Electronics apprentice, 2nd and 3rd year

Technical Personnel within the Science department

Christian Thomann	Technician (since 01.04.2013)
Nathan Mingard	Laboratory assistant (since 01.04.2013)

Administration

Sandra Kissling	Head administration/Human Resources
Seraina Egartner	Administration, book-keeping (from 01.01.2013 to 31.11.2013)
Stephanie Ebert	Administration, book-keeping (until 26.11.2013)
Alison Gustavsson	Administration, book-keeping (since 18.11.2013)
Edith Schaller	Book-keeping (from 13.06.2013 to 26.07.2013)
Christian Stiffler	Book-keeping (since 01.08.2013)
Irene Keller	Administration, import/export
Eliane Tobler	Administration apprentice, 2nd and 3rd year

DACA-13 (Project-Staff)

Anja Schilling	Project manager DACA-13 conference (until 31.08.2013)

Caretaker

Maria Sofia Ferreira Pinto	General caretaker, cleaning
Sonja Veras Araujo	General caretaker, cleaning (from 26.04.2013 to 26.05.2013)

Civilian Service Conscripts

Laurin Diener	08.10.2012 – 04.01.2013
Amos Schaub	03.01.2013 – 27.02.2013
Simon Corrodi	25.02.2013 – 23.07.2013
Patrik Langer	01.07.2013 – 31.08.2013
Nicolas Duchoud	23.09.2013 – 30.11.2013
Christoph Zysset	29.07.2013 – 27.12.2013

Meeting Organisation

DACA – 13	Davos Congress Center, 8 – 2 July 2013 Davos Atmosphere and Cryosphere Assembly. Assemblies of the IUGG associations IAMAS and IACS (Organisation with SLF and the ad-hoc Swiss National Organisation Committee)
UV Workshop	Davos PMOD/WRC, 27 – 28 August 2013 UV Workshop 2013
Inauguration	Davos PMOD/WRC, 28 August 2013 Inauguration of the renovated PMOD/WRC Building

Public Seminars

07.02.2013	Dr. Ibrahim Reda, NREL, USA, "Absolute infrared cavity radiometer"
04.03.2013	Dr. Benjamin Walter, SLF, "From solar cells to wind erosion"
04.03.2013	Dr. Mathias Gergely, SLF, Davos, "Ocean color measurement uncertainty", and "Snow characterization by optical properties" Dr. José Abreu, EAWAG, "Past and future solar activity and Bayesian data analysis
13.06.2013	Dr. Antonio Ferriz-Mas, CSIC, Spain, "Potential physical mechanisms of how planets can influence the long-term solar activity"
12.09.2013	Michael Kozubek, Inst. Atmospheric Physics, Prague, Czech Republic, "Changes in the middle latitude stratosphere"
04.11.2013	Krzysztof Barczynski, MPI for Solar System Research, Germany, "A study of velocities in solar polar plumes"
14.11.2013	Wilnelia Adams, University Innsbruck, "Sun-climate relations: The effect of UV irradiance on stratosphere O_3 over the 11-yr solar cycle"
05.12.2013	Sheng Jianxiong, IACETH, Zürich, "Modelling stratospheric aerosols: New results from the CCM SOCOL/AER"
23.12.2013	Sowmya. K., "F-state interference in the Paschen-Back regime" Dr. Michele Bianda, IRSOL, "Exploring chromospheric magnetic fields with the Forward Scattering Hanle effect"

Lecture Courses, Participation in Commissions

Werner Schmutz	Lecture course in Astronomy, HS 2013, ETH-ZH Examination expert in Astronomy, BSc ETH-ZH President of the International Radiation Commission (IRS, IAMAS) Comité consultatif de photométrie et radiométrie (CCPR, OICM) Science Programme Committee, ESA Expert group on space weather of the UN Committee on the Peaceful Uses of Outer Space Space Weather Working Team Steering Board of ESA Swiss representative on the Council of the Committee on Space Research (COSPAR) Federal Commission for Space Affairs (CFAS) Swiss Management Committee delegate to the COST action ES01005 (ECF) President of the national Committee on Space Research, Commission of SCNAT Member of the Commission for Astronomy, SCNAT GAW-CH Working Group (MeteoSwiss)
Wolfgang Finsterle	Member of: CIMO ET Standardization Member of EURAMET TC-PR Chairman of: ISO/TC180 SC1 (Solar Energy, Climate-Measurement and Data)
Julian Gröbner	Lecture course in Solar Ultraviolet Radiation WS 2013, ETH-ZH GAW-CH Working Group (Meteoswiss) NEWRAD Scientific committee member – chair elect Chairman of Infrared Working group of Baseline Surface Radiation Network (BSRN) Member IAMAS International Radiation Commission Member of the CIMO expert team on New In-Situ Technologies Swiss delegate to the Management Group of COST ES1207 "A EUropean BREWer NETwork – EUBREWNET", and Working Group Leader of WG1 "Instrument characterisation and calibration"
Margit Haberreiter	Co-Investigator of EUI and SPICE onboard Solar Orbiter Member of the SPICE Science Steering Committee Member of the Programme Committee of the ESA Alpbach Summer School, 2013 Swiss Substitute Delegate of the Management Committee of the COST Action ES1005, Leader of WP1.1 Co-Convenor of the EGU 2013 Session: ST5.2 Contribution of Solar and Geomagnetic indices to Space Climate and Space Weather Member of the Inter-Division IAU Working Group "Impact of Magnetic Activity on Solar and Stellar Environments"
Eugene Rozanov	International Comission on the Middle Atmosphere (ICMA, IAMAS) Swiss Management Committee delegate to the COST action ES01005 (ECF)
Christoph Wehrli	GAW-CH Working Group (Meteo Swiss) Scientific Advisory Group Aerosol (WMO/GAW)

Modernisation and Renovation: Controlling Environmental Conditions in Laboratories and Rooms

Werner Schmutz and Philipp Brückmann

An important pre-requisite for calibration, measurement and manufacturing activities at PMOD/WRC is that environmental conditions in laboratories and rooms are stable. However, after renovation work on the PMOD/WRC building had finished in 2013, it was discovered that this was not the case in certain key areas, mainly as a consequence of heat being given off by equipment, and the necessity of closing doors due to fire regulations. Only the optics laboratories and clean-room were being air-conditioned at that time. A separate ventilation unit had also been installed in the computer server room but was unable to keep it at an optimum temperature. Room temperatures during the summer rose above permitted values while air at temperatures as low as -10°C was ventilating the room in winter.

It was therefore decided to extend the existing air-conditioning/cooling-system to five other rooms. The existing cooling-system consists of an air-cooled cold-water aggregate with a capacity of 35 kW. Due to the exacting requirements and reliability placed on the cooling-system, a second cold water source was integrated. The geothermal heating system functions as an ideal heat-sink that always lies in the 4 – 11°C temperature range through use of ethylene glycol as a circulating liquid, even if heat from the solar panels is being stored in the bedrock. A refrigeration unit is therefore unnecessary, as a simple heat-exchanger is adequate (see picture).

The following additional rooms are now being air-conditioned as of September 2013: 1) The vacuum and black-body laboratories in the cellar, 2) the clean-bench room on the ground floor, 3) the server room on the 2nd floor (since March 2014), and 4) the data acquisition room on the 4th floor.

The heat transferred to the underlying bed-rock is about 55,000 kWh per year, where the computer server room is responsible for about half this amount. By not using the refrigerator, the consumption of electricity can be cut by about 23,000 kWh per year. The cold-water aggregate mainly functions as a backup to maintain the necessary high reliability.

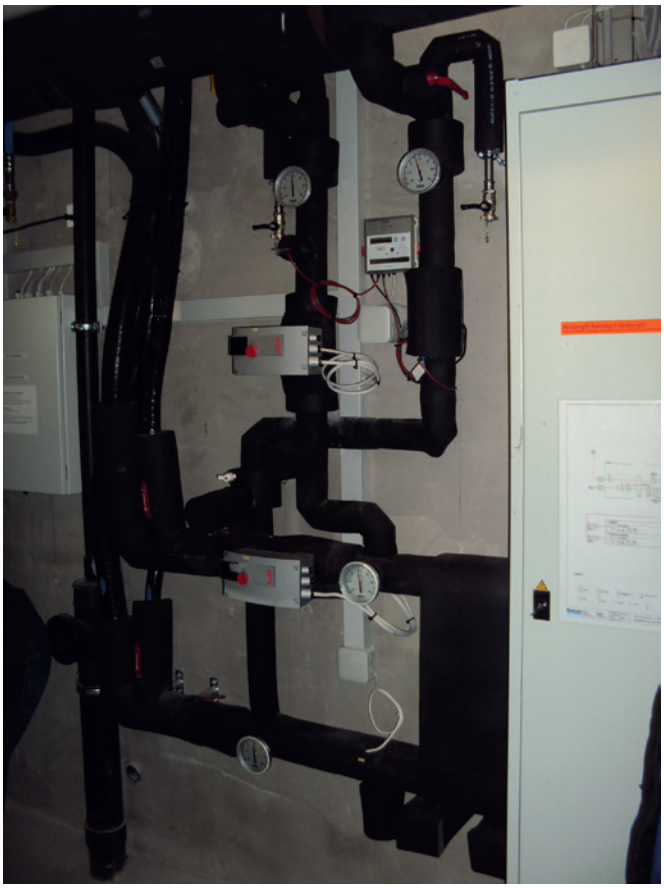

Figure 1. Part of the new heat-exchange system in the PMOD/WRC basement.

Initial operation during 2013 has shown that the above-mentioned laboratories and rooms can be operated under very stable environmental conditions.

Bilanz 2013 (inklusive Drittmittel) mit Vorjahresvergleich

Aktiven	31.12.2013 CHF	31.12.2012 CHF
Flüssige Mittel	1'086'503.14	2'772'234.19
Wertschriften	0.00	278'528.00
Forderungen	170'680.24	102'970.72
Aktive Rechnungsabgrenzungen	651'012.56	494'379.77
	1'908'195.94	3'648'112.68
Passiven		
Verbindlichkeiten	264'049.85	155'213.40
Kontokorrent Stiftung	40'441.25	9'567.60
Passive Rechnungsabgrenzungen	445'748.84	2'052'116.58
Rückstellungen	1'113'394.74	1'213'394.74
Eigenkapital	44'561.26	217'820.36
	1'908'195.94	3'648'112.68

Erfolgsrechnung 2013 (inklusive Drittmittel) mit Vorjahresvergleich

Ertrag	CHF	CHF
Beitrag Bund Betrieb WRC	1'366'896.00	1'366'896.00
Beitrag Bund (BBL), Umbau PMOD/WRC	656'000.00	2'195'467.00
Beitrag Kanton Graubünden	452'088.00	452'088.00
Beitrag Gemeinde Davos	589'555.00	589'555.00
Beitrag Gemeinde Davos, Mieterlass	160'000.00	154'614.00
Overhead SNF	114'742.55	151'413.95
Instrumentenverkäufe	110'924.90	150'560.00
Kalibrationen	183'344.62	192'290.15
Übriger Ertrag	26'816.85	83'095.70
Finanzertrag	21'512.10	19'003.70
Kongressertrag (DACA–13)	573'870.80	0.00
Ausserordentlicher Ertrag	10'149.30	3'788.28
Auflösung Rückstellungen	100'000.00	46'933.45
Drittmittel	2'080'388.22	2'323'820.71
	6'446'288.34	7'729'525.94
Aufwand		
Personalaufwand	3'914'619.84	3'716'962.50
Investitionen Observatorium	131'432.26	274'103.68
Investitionen Drittmittel	453'112.25	687'375.20
Unterhalt	55'672.10	77'828.64
Verbrauchsmaterial	118'775.59	57'727.90
Verbrauch Commercial	123'849.16	110'038.45
Reisen, Kurse	187'335.29	186'108.50
Kongressaufwand ohne Personalaufwand (DACA–13)	521'082.08	0.00
Raumaufwand/Energieaufwand	214'853.90	225'060.30
Versicherungen, Verwaltungsaufwand	127'156.17	144'858.05
Finanzaufwand	5'883.01	7'501.70
Übriger Betriebsaufwand	109'775.79	47'156.72
BBL, Umbau PMOD/WRC	656'000.00	2'195'467.00
	6'619'547.44	7'730'188.64
Jahresergebnis	–173'259.10	– 662.70
	6'446'288.34	7'729'525.94

Abbreviations

AERONET	Aerosol Robotic Network, GSFC, USA
AOCCM	Atmosphere-Ocean-Chemistry-Climate Model
AOD	Aerosol Optical Depth
BIPM	Bureau International des Poids et Mesures, Paris, France
BOLD	Blind to Optical Light Detector
BSRN	Baseline Surface Radiation Network of the WCRP
CCM	Chemistry-Climate Model
CAS	Commission for Atmospheric Sciences, Commission of WMO
CCPR	Comité Consultatif de Photométrie et Radiométrie, BIPM
CIE	Commission Internationale de l'Eclairage
CIPM	Comité International des Poids et Mesures
CIMO	Commission for Instruments and Methods of Observation of WMO, Geneva, Switzerland
CLARA	Compact Light-weight Absolute Radiometer
CMC	Calibration and Measurement Capabilities
CNES	Centre National d'Etudes Spatiales, Paris, F
CNRS	Centre National de la Recherche Scientifique, Service d'Aéronomie Paris, France
COCOSIS	Combination of COSI Spectra
COSI	Code for Solar Irradiance, solar atmosphere radiation transport code developed at PMOD/WRC
COSPAR	Commission of Space Application and Research of ICSU, Paris, France
COST	European Cooperation in Science and Technology
CSAR	Cyrogenic Solar Absolute Radiometer
CSL	Centre Spatial de Liège, Belgium
CTM	Chemical Transport Model
CUCF	Central UV Calibration Facility, NOAA, Boulder, USA
DARA	Digital Absolute Radiometer
DIARAD	Dual Irradiance Absolute Radiometer of IRMB
DLR	Deutsche Luft und Raumfahrt, Germany
EIT	Extreme UV Imaging Telescope
ESA	European Space Agency
ESF	European Science Foundation
ESTEC	European Space Research and Technology Centre, Noordwijk, Netherlands
ETH	Eidgenössische Technische Hochschule (Z: Zürich, L: Lausanne)
EUI	Extrem Ultraviolet Imager, Experiment on Solar Orbiter, to be launched 2017
EUV	Extreme Ultraviolet
FMI	Finnish Meteorological Institute, Finland
FUV	Far Ultraviolet
FP7	European Framework Programme of the European Commission
FSI	Full Sun Imager
GAW	Global Atmosphere Watch, an Observational Programme of WMO
GAWTEX	GAW Training and Education Centre
GCM	General Circulation Model
GHG	Greenhouse Gases
GSFC	Goddard Space Flight Center, Greenbelt, MD, USA
HRI	High Resolution Imagers
IACETH	Institute for Climate Research of the ETHZ., Switzerland
IAMAS	International Association of Meteorology and Atmospheric Sciences of IUGG
IAPS	Intensified Active Pixel Sensor
IAS	Institut d'Astrophysique Spatiale
IAU	International Astronomical Union of ICSU, Paris, France
ICSU	International Council of Scientific Unions, Paris, France
IO	Institut d'Optique
IPC	International Pyrheliometer Comparisons
IR	Infrared
IRC	International Radiation Commission, Commission of IAMAS
IRIS	Infrared Integrating Sphere Radiometer
IRMB	Institut Royal Météorologique de Belgique, Brussel, Belgium
IRS	International Radiation Symposium of the Radiation Commission of IAMAS
ISO/IEC	International Oranisation for Standardization/International Electrotechnical Commission
ISS	International Space Station
IUGG	International Union of Geodesy and Geophysics of ISCU
KIS	Kiepenheuer-Institut für Sonnenphysik, Freiburg i.Br., Germany
LATMOS	Laboratoire Atmosphères, Milieux, Observations Spatiales, French research institution
LVPS	Low Voltage Power Supply
LYRA	Lyman-alpha Radiometer, Experiment on PROBA 2, built by PMOD/WRC
METAS	Federal Office of Metrology
MITRA	Monitor to Determine the Integrated Transmittance
MPS	Max Planck Institute for Solar System Research
MRR	Manufacturing Readiness Review
MSSL	UCL Mullard Space Science Laboratory, London, UK
NASA	National Aeronautics and Space Administration, Washington DC, USA

NEWRAD	New Developments and Applications in Optical Radiometry
NILU	Norwegian Institute for Air Research, Norway
NIST	National Institute of Standards and Technology, Gaithersburg, MD, USA
NOAA	National Oceanographic and Atmospheric Administration, Washington DC, USA
NPL	National Physical Laboratory, Teddington, UK
NRI	Near Infrared
NRL	Naval Research Laboratory, Washington DC, USA
NREL	National Renewable Energy Lab, Golden, CO, USA
ODS	Ozone Destroying Substances
PFR	Precision Filter Radiometer
PI	Principle Investigator, Leader of an Experiment/Instrument/Project
PICARD	French Space Experiment to Measure the Solar Diameter, launched 2010
PMOD	Physikalisch-Meteorologisches Observatorium Davos, Switzerland
PMO6	PMO6 Type Radiometer
PREMOS	Precision Monitoring of Solar Variability, PMOD/WRC Experiment on PICARD
PROBA 2	ESA Technology Demonstration Space Mission, launched 2 December 2009
PRODEX	Programme for the Development of Experiments, ESA
PTB	Physikalisch-Technische Bundesanstalt, Braunschweig and Berlin, Germany
QASUME	Quality Assurance of Spectral Ultraviolet Measurements in Europe
QMS	Quality Management System
RA	Regional Association of WMO
RBCC-E	Regional Brewer Calibration Centre for Europe, Izaña Observatory, Spain
RMO	Regional Metrology Organisation
ROB	Royal Observatory of Belgium, Belgium
SCNAT	Swiss Academy of Sciences
SLF	Schnee und Lawinenforschungsinstitut, Davos, Switzerland
SFI	Schweiz. Forschungsinstitut für Hochgebirgsklima und Medizin, Davos, Switzerland
SI	International System of Units
SIAF	Schweiz. Institut für Allergie- und Asthma-Forschung, Davos, Switzerland
SMHI	Swedish Meteorological and Hydrological Institute, Sweden
SNSF	Swiss National Science Foundation, Switzerland
SOCOL	Combined GCM and CTM Computer Model, developed at PMOD/WRC
SOHO	Solar and Heliospheric Observatory, Space Mission of ESA/NASA
SOLAR	Experiment Platform on the ISS
SOLID	Solar Irradiance Data Exploitation
SORCE	NASA Space Mission
SOTERIA	Solar–Terrestrial Investigations and Archives
SOVAC	Solar Variability and Climate Change
SOVIM	Solar Variability and Irradiance Monitoring, PMOD/WRC Experiment on the International Space Station Alpha, 2008
SPICE	Spectral Imaging of the Coronal Environment, Experiment on Solar Orbiter, to be launched 2017
SSI	Solar Spectral Irradiance
STEP	Solar Terrestrial Energy Programme of SCOSTEP/ICSU
STM	Structural Model
SUSIM	Solar Ultraviolet Spectral Irradiance Monitor on Board UARS
TSI	Total Solar Irradiance
UARS	Upper Atmosphere Research Satellite of NASA
UCL	University College London, UK
UV	Ultraviolet
UVA	UV Radiation in the 315–400 nm range
UVB	UV Radiation in the 280–315 nm range
VIRGO	Variability of Solar Irradiance and Gravity Oscillations, PMOD/WRC Experiment on SOHO, launched December 1995
WCRP	World Climate Research Program
WDCA	World Data Centre for Aerosols
WIGOS	WMO Integrated Global Observing System
WIS	WMO Information System
WISG	World Infrared Standard Group of Pyrgeometer, maintained by WRC-IRS
WMO	World Meteorological Organisation, a United Nations Specialised Agency, Geneva, Switzerland
WRC	World Radiation Centre, Davos, Switzerland
WRC-IRS	Infrared Radiometry Section of the WRC
WRC-SRS	Solar Radiometry Section of the WRC
WRC-WORCC	World Optical Depth Research and Calibration Centre of the WRC
WRC-WCC-UV	World Calibration Centre for Ultraviolet of the WRC
WRDC	World Radiation Data Centre, St. Petersburg, Russia
WRR	World Radiometric Reference
WSG	World Standard Group, realising the WRR, maintained by WRC
WWW	World Weather Watch, an Observational Programme of WMO

Annual Report 2013

Editors: Werner Schmutz and Stephan Nyeki
Layout by Stephan Nyeki
Publication by PMOD/WRC

Edition: 700, printed 2014

PMOD/WRC, Davos, Switzerland

Dorfstrasse 33, 7260 Davos Dorf, Switzerland
Phone +41 81 417 51 11, Fax +41 81 417 51 00
www.pmodwrc.ch